TAMPEREEN TEKNILLINEN YLIOPISTO
TAMPERE UNIVERSITY OF TECHNOLOGY

Minna Haavisto

Studies on the Time-Dependent Demagnetization of Sintered NdFeB Permanent Magnets

Julkaisu 1180 • Publication 1180

Tampere 2013

Tampereen teknillinen yliopisto. Julkaisu 1180
Tampere University of Technology. Publication 1180

Minna Haavisto

Studies on the Time-Dependent Demagnetization of Sintered NdFeB Permanent Magnets

Thesis for the degree of Doctor of Science in Technology to be presented with due permission for public examination and criticism in Konetalo Building, Auditorium K1702, at Tampere University of Technology, on the 22nd of November 2013, at 12 noon.

Tampereen teknillinen yliopisto - Tampere University of Technology
Tampere 2013

ISBN 978-952-15-3191-0 (printed)
ISBN 978-952-15-3196-5 (PDF)
ISSN 1459-2045

Abstract

Increasing utilization of sintered NdFeB permanent magnets in large electrical machines has raised the question about the thermal stability and possible polarization losses occurring during the long-term operation of the machines. Knowledge of the evolution of the magnetic properties of NdFeB compounds over time at elevated temperatures has been limited. This causes difficulties in the optimization of the magnetic material selection.

In this work the polarization losses occurring in commercial sintered NdFeB magnets during long-term thermal exposures are studied. The influence of different parameters such as temperature, permeance coefficient of the sample, coercivity and *JH* curve squareness of the material, are examined. Also the influence of a stabilization heat treatment is studied. The losses detected in open- and closed-circuit exposures are compared. The demagnetization process is analyzed with the help of finite element modeling.

The detected polarization losses were found to follow the logarithmic decay law in the time scale from 1 hour to 10 000 hours. By assuming the behavior to continue also over the next decade of the logarithmic time scale, the losses can be extrapolated even to 30 years. For each material and each P_c it is possible to determine a temperature at which the total loss is expected to be less than 1 % even after 30 years of exposure. Above this critical temperature, the time-dependent losses start to increase. In open-circuit exposures also the initial loss after 1 hour exposure increases rapidly with increasing temperature or decreasing P_c. In open-circuit exposures, the total loss estimated to occur after 30 years was roughly twice the loss detected after 1 hour. However, in closed-circuit exposure this was not the case. The time-dependent demagnetization was found to be more severe in the close-circuit condition. This is likely to result from the acceleration of a chain reaction type demagnetization process. In open-circuit exposures the time-dependent demagnetization process is likely to be damped, since the demagnetizing self-field is reduced during the process.

The results show that the best way to control the time-dependent demagnetization is to use materials with a square *JH* curve. For this type of a material, the critical temperatures are easy to determine. The stabilization heat treatment is found to stabilize the magnets, but for a limited period of time only. An FEM analysis shows that the partial demagnetization applied to the magnets during the stabilization heat treatment is not homogenously distributed. The treatment needs to be performed in closed-circuit conditions to get a homogeneous stabilization.

The detected time-dependent demagnetizations are due to the material characteristics as well as to the magnetostatic field effects. It is difficult to distinguish the proportion of these two. The comparison between the open- and closed-circuit test results suggests that the open-circuit results can be used to estimate the long-term behavior of the material. However, more studies are needed to confirm this.

Preface

This work was carried out in the Magnet Technology Centre (MTC) at Prizztech Oy together with the Department of Materials Science (DMS) at Tampere University of Technology (TUT). I'd like to thank my supervisors Dr. Martti Paju at MTC and Prof. Veli-Tapani Kuokkala at DMS for the opportunity to study this fascinating topic. I'm grateful for their encouragement, advice and trust in my visions of the research.

Neorem Magnets Oy provided most of the samples and I appreciate all the support I got from the company. Special thanks belong to Kari Aittoniemi, Dr. Harri Kankaanpää and Juha Järvi who have helped me by endorsing my research plans and arranging the samples and *BH* curve measurements I needed.

I also want to thank my colleagues at MTC, Sampo Tuominen, Timo Santa-Nokki, Mika Svedberg and Dr. Ilkka Laitinen for their great help in the design and operation of the measurement systems and for performing the FEM analyses. This is an excellent team to work with! Prof. Pekka Ruuskanen at TUT Pori deserves thanks as well. He provided me a chance to continue the stability studies as a part time researcher at TUT Pori. His encouragement has been valuable.

This work was financially supported by the European Regional Development Fund, the Finnish Cultural Foundation, the Emil Aaltonen Foundation, the Ulla Tuominen Foundation, the High Technology Foundation of Satakunta, the Finnish Funding Agency for Technology and Innovation TEKES and several Finnish companies.

Finally I'd like to thank my family, my husband Markus and our children Vilma, Jaakko and Taneli for your understanding as I have occupied a corner in the living room with my desk and sometimes have concentrated more on the research than the household.

Pori, Finland, 6.11.2013

Minna Haavisto

List of included publications

I Haavisto, M. and Paju, M., Temperature Stability and Flux Losses Over Time in Sintered Nd–Fe–B Permanent Magnets, *IEEE Transactions on Magnetics*, **45** (2009) pp. 3114 – 3120

II Haavisto, M., Tuominen, S., Kankaanpää H. and Paju, M., Time Dependence of Demagnetization and Flux Losses Occurring in Sintered Nd-Fe-B Permanent Magnets, *IEEE Transactions on Magnetics*, **46** (2010) pp. 3582 – 3584

III Haavisto, M. and Paju, M., Time-dependent demagnetization in sintered NdFeB magnets, *Proceedings of 20th International Workshop on Rare Earth Permanent Magnets and Their Applications*, Bled (2010) pp. 224-226

IV Haavisto, M., Tuominen, S., Kankaanpää, H. and Paju, M., Estimation of Time-Dependent Polarization Losses in Sintered Nd-Fe-B Permanent Magnets, *IEEE Transactions on Magnetics*, **47** (2011) pp. 170 – 174

V Haavisto, M., Kankaanpää, H., Santa-Nokki, T., Tuominen, S. and Paju, M., Effect of Stabilization Heat Treatment on Time-Dependent Polarization Losses in Sintered Nd-Fe-B Permanent Magnets, *EPJ Web of Conferences*, **40** (2013) article no. 06001

Author's contribution

The author planned the experiments, conducted or supervised the experimental tests, interpreted the results and was responsible for the preparation of the manuscripts. All the included papers were commented by the other co-authors. In addition to the results published in the included Publications I-V, this thesis contains also previously unpublished results.

List of symbols, abbreviations and terms

3D	Three-dimensional
BH curve	Measured changes in magnetic flux density of a permanent magnet material in a constantly increasing reversal magnetic field. A second quadrant of a hysteresis loop of magnetic flux density.
B_r	Remanence of a permanent magnet material [T]
Co	Cobalt
crystalline anisotropy	Material characteristics change with changing lattice direction
Cu	Copper
Curie temperature	Temperature at which ferromagnetic material loses its magnetic properties and becomes paramagnetic.
demagnetization	Process which leads to polarization losses in a permanent magnet.
dM_{irr}	Irreversible change in the magnetization
Dy	Dysprosium
easy axis	Lattice direction which is favorable for magnetization
exchange interaction	Magnetic moment of an atom in a crystal lattice interact with moments of neighboring atoms trying to align its moment to the same direction
fcc	Face-centered cubic
FE	Finite Element
FEM	Finite Element Method
flux loss	Decrease in the magnetic flux that permanent magnet is producing to the surrounding space
Gd	Gadolinium
h	Height of a magnet, dimension parallel to the direction of magnetization

H_{ci}	Intrinsic coercivity of a permanent magnet material [A/m]
hcp	Hexagonal closed-packed
H_k	The value of the magnetic field strength at which the magnetic polarization of a permanent magnet has 90 % of its saturated value [A/m]
IEC	International Electrotechnical Commission
J	Magnetic polarization [T]
JH curve	Measured changes in magnetic polarization of a permanent magnet material in a constantly increasing reversal magnetic field
l	Length of a magnet
load line	Line drawn to the second quadrant of the hysteresis curve describing the geometry of the magnetic circuit
M	Magnetization [A/m]
magnetization reversal	A process which results in the reversed direction of magnetization
MH curve	Changes in magnetization of a permanent magnet in a constantly increasing reversal magnetic field
M_s	Spontaneous magnetization
Nd	Neodymium
$Nd_2Fe_{14}B$	Hard magnetic phase of NdFeB magnets
Nd_2O_3	Neodymium oxide with hexagonal close-packed crystal structure
NdFeB	Neodymium Iron Boron permanent magnet material
NdO	Neodymium oxide with face-centered cubic crystal structure
O	Oxygen
operating point	Intersection of a load line and a *BH* curve of a material
partial demagnetization	A process which results in magnetization reversal in some parts of the magnet. Partial demagnetization reduces the polarization of the magnet.
P_c	Permeance coefficient

PLP	Pressless production
polarization loss	Decrease in the magnetic polarization of a permanent magnet
PT100	Standardized platinum resistance thermometer
recoil curve	A new *BH* curve for the material after partial demagnetization
S	Magnetic viscosity coefficient
self-field	Reversal magnetic field that the polarization of a permanent magnet generates inside the magnet itself
SEM	Scanning Electron Microscope
SF	Squareness factor
SmCo	Samarium cobalt permanent magnet material
squareness	Term describing the rectangularity of the *JH* curve of a permanent magnet material.
stabilization	A procedure performed to a permanet magnet before starting the operation of the application. Aim of the stabilization is to prevent polarization losses occurring during the operation by introducing a slight demagnetization in advance.
S_v	Material specific magnetic viscosity coefficient
twin boundary	A symmetrical interface which separates two parts of a grain with different crystal orientations. Typically crystal orientation is mirrored at the twin boundary.
T_0	Temperature below which the estimated irreversible polarization loss after 30 years exposure is less than 1 %
w	Width of a magnet
α	Temperature coefficient of remanence [1/°C]
α-Fe	Soft magnetic phase of iron
β	Temperature coefficient of coercivity [1/°C]
χ_{irr}	Irreversible susceptibility
μ_0	Permeability of free space

Contents

Abstract 3
Preface 4
List of included publications 5
Author's contribution 5
List of symbols, abbreviations and terms 6
Contents 9
1. Introduction 11
1.1 Aim of the work 12
1.2 Structure of the thesis 13
2. Polarization losses in sintered NdFeB magnets 14
2.1 Analysis of hysteresis in NdFeB type materials 14
2.1.1 Hysteresis loop 14
2.1.2 Domain structure and energy profiles 16
2.1.3 Magnetization reversal 18
2.1.4 Magnetic viscosity 19
2.2 Sintered NdFeB 21
2.2.1 Microstructure 22
2.2.1.1 Hard magnetic phase 22
2.2.1.2 Grain boundary phases 24
2.2.1.3 Alloying elements 26
2.2.1.4 Domain structure 26
2.2.2 Production process of sintered NdFeB magnets 29
2.2.3 Recent developments in NdFeB magnets 31
2.3 Characteristics of sintered NdFeB magnets in motor and generator applications 31
2.3.1 Reversible, irreversible and permanent losses 32
2.3.2 Thermal stability 33
2.3.2.1 Maximum operating temperature 34
2.3.2.2 Stabilization heat treatment 35
2.3.3 Operating point 35
2.3.4 Specifications and quality control 37

3. Methods for testing the magnetic properties of permanent magnets 39
3.1 Helmholtz coil measurement 39
3.2 The demagnetization curve measurement 40
3.3 Magnetic field scanning 42
3.4 Long-term stabilization determination 42
3.4.1 Open-circuit measurements 43
3.4.2 Closed-circuit measurements 44
4. Experimental Procedure 46
4.1 Samples 46
4.2 Determination of the magnetic properties 46
4.3 Thermal exposures 48
4.4 Squareness of *JH* curves 48
4.5 Stabilization heat treatment 49
4.6 Study of the demagnetization process 49
4.7 Closed-circuit exposures 50
5. Results and discussion 51
5.1 Open-circuit exposure tests 51
5.1.1 Effect of temperature 53
5.1.2 Effect of the coercivity of the material 55
5.1.3 Effect of permeance coefficient 58
5.1.4 Accuracy of the estimations 60
5.1.5 Effect of *JH* loop squareness 61
5.1.6 Stabilization heat treatment 63
5.2 Analysis of the demagnetization process 67
5.3 Closed-circuit exposure tests 70
6. Summary and conclusions 74
7. References 77

1. Introduction

In the past fifteen years the utilization of permanent magnets in large electrical machines has increased rapidly. By replacing the conventional electromagnets in the rotor with permanent magnets, many benefits can be obtained. Driving forces towards the permanent magnet technology are the higher achievable power densities and higher efficiencies [1]. Other advantages of the permanent magnet technology are the size reduction of the devices and a possibility to construct gearless direct drive motors and generators.

The development of sintered NdFeB magnets has been intense since their discovery in 1984. Nowadays, the production method is well established and magnets of uniform quality can be produced in large quantities. The remanence of the mass produced magnets approaches the theoretical maximum of the NdFeB compound, and the essential increase in coercivity has been achieved by various alloying elements and advanced production methods.

There are a few weaknesses in NdFeB materials that have to be considered in the application design: their thermal stability and corrosion resistance are limited. Curie temperature, the temperature at which the material changes from ferromagnetic to paramagnetic and loses all its magnetization, is only about 300-400°C for NdFeB magnets depending on the composition [2]. The maximum operating temperatures for commercial magnets are reported to vary between 60°C and 200°C depending on the grade. The problem is that there is neither a consistent definition for “maximum operating temperature” nor international standard grades for NdFeB magnets [3]. It depends completely on the magnet producer, how they define those quantities.

In motors and generators the temperatures may rise even up to 200°C. The machine design and magnet material selection have to be performed with care to assure that the magnets are not destroyed at the operating conditions. The development of computer assisted simulation systems allows designers to optimize the structures of the devices. Optimization of the magnet material is also needed in order to control the costs, since the alloying for better temperature resistance increases also the price of the magnet.

In a typical design process, only rapid changes in the material characteristics are considered and long-term changes are ignored. The end users of permanent magnet motors and generators are sometimes skeptic about the permanence of the magnetization in the magnets. Expected lifetimes of these machines vary from 20 to 30 years, and no permanent polarization losses are allowed for magnets during that period of time. Consistent information about the demagnetization behavior over time is needed to be able to

guarantee the lifetime requirements. There are not many published studies on the time-dependent flux losses in commercial sintered NdFeB magnets. Clegg et al. [4] and Mildrum et al. [5] have shown that temperature, permeance coefficient (P_c), and coercivity of a magnet affect its time-dependent losses.

Demagnetization in constant conditions (temperature and field) is due to the effect termed magnetic viscosity. The physics of this phenomenon has been studied since 1940's. The verification of the theories is still questionable, since the measurement methods for magnetization are limited. Published theoretical studies or magnetic measurements in a time-scale of seconds do not give enough data for engineers to deduce reliable estimates for the lifetime of the applied magnets. In this thesis, the time-dependent demagnetization behavior of sintered NdFeB magnets is studied in the time-scales of hours and years.

1.1 Aim of the work

This work deals with the polarization losses occurring over time in commercial sintered NdFeB magnets. The effects of different parameters such as temperature, coercivity of the magnet, and the magnetic environment are studied. The first goal of the work is to evaluate the significance of the phenomenon from the application design point of view. The significance is expected to vary depending on the actual values of the above mentioned parameters.

For the end users of the applications it is important to verify the diminishing time-dependent losses under controlled conditions. The second goal of this work is to determine the limits of these conditions. The study concentrates to reveal the external conditions at which the time-dependent losses start to occur, and to connect these limiting conditions to the measured magnetic *BH* curves of the material.

Permanent magnet motor and generator designers need design guidelines: how to assure the long-term stability of the magnets in their applications. These guidelines should include rules how to take the time-dependent losses into account in materials selection and in the quality control of the magnets. Also the effectiveness of a stabilizing heat treatment needs to be verified. This work aims at producing essential information for the basis of the work towards practical material selection guidelines.

1.2 Structure of the thesis

The research work consists of five independently published parts and a previously unpublished part. Fig. 1 presents the structure of the work. The first study was a screening type analysis with many different magnet types, geometries and temperatures to get an overview of the phenomenon. This was followed by three studies focused on different parameters affecting the phenomenon. These four studies gave a good understanding about the phenomenon, and confirmed its significance. The results of these studies also demonstrated the fact that below some material specific limiting conditions the magnets were extremely stable.

The further studies concentrated more in applying the results. In these studies the effect of the squareness of the *BH* curve, sometimes considered as a quality of the magnet material, on the long-term behavior of the material was examined. Also the influence of the stabilization heat treatment of the magnets was analyzed. The results of these studies help to understand the possibilities to control the long-term losses.

In the final part of the work, an analysis of the applied measurement method is performed and the open and closed-circuit measurements are compared. This gives new information about the demagnetization process to be used in the formulation of the material specifications.

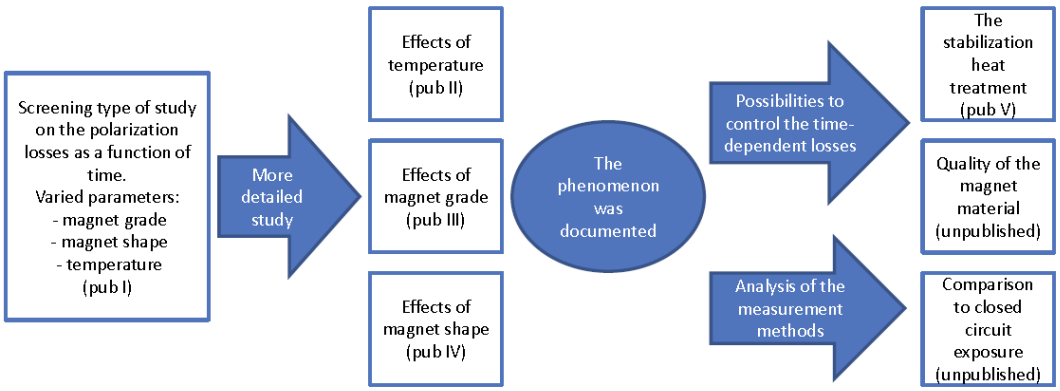

Figure 1. Structure of the work.

2. Polarization losses in sintered NdFeB magnets

During the manufacturing process the sintered NdFeB magnets are not externally magnetic. The magnetization is the last step in the production process. During the magnetization the magnetic moments of small magnetic domains inside the magnet are oriented with assistance of an external magnetic field to obtain a macroscopic polarized state. After the magnetization, the magnet consists of two magnetic poles, which generate an external magnetic field between them. This magnetized state is a metastable state and demagnetization occurs if certain amount of energy is introduced to the magnet. Partial demagnetization causes polarization losses and decreases the external magnetic field generated by the magnet.

This metastable polarization is based on the magnetic hysteresis of the material. The hysteresis phenomenon is discussed in more detail in Section 2.1. The hysteresis behavior of the NdFeB material, however, depends on the microstructure of the material. In Section 2.2, the microstructure and the production process to obtain the microstructure of sintered NdFeB magnets are briefly presented. In the last chapter of the theoretical background, Section 2.3, the aspects of the application of sintered NdFeB magnets affecting the polarization losses and some design issues are discussed.

2.1 Analysis of hysteresis in NdFeB type materials

Hysteresis is the dependence of a system not only on its current environment but also on its past. The state of the magnetization in magnetic materials is thus dependent on the magnetizing history. Changing external magnetic field forms metastable magnetic states in the material. Return of the material to the original state requires energy input.

The hysteresis phenomenon in this chapter is discussed from the permanent magnet point of view and especially considering the behavior of sintered NdFeB based magnet materials. The special characteristics of soft magnetic materials are excluded from the discussion.

2.1.1 Hysteresis loop

Fig. 2 illustrates the hysteresis behavior of a permanent magnet material. The vertical axis shows the magnetization state of the material and the horizontal axis represents the external magnetic field. At location 1 (hereafter loc. 1), the material is non-magnetized in zero external field. As the external magnetic field is increased, the magnetization of the material is also increased (loc. 2), but not linearly. Magnetization increases until the

saturation state is reached (loc. 3). After that, the magnetization is not increasing anymore. If the external field is then decreased, the magnetization remains close to the saturation level. Even at the point where the external field has disappeared (loc. 4), the remanent magnetization of the material is close to the saturation level. This magnetization state at zero external magnetic field (after saturation) is called the remanence (B_r) of the material.

In NdFeB materials the magnetization state remains close to the remanence even when the external magnetic field is increased in the reverse direction. At location 5, demagnetization of the magnet begins. As the reverse field is increased to the coercivity (H_{ci}) level (loc. 6), the macroscopic magnetization of the material has disappeared. Magnetization in the reverse direction starts to increase as the reverse field is further increased. At location 7, the saturation is achieved in the reverse direction.

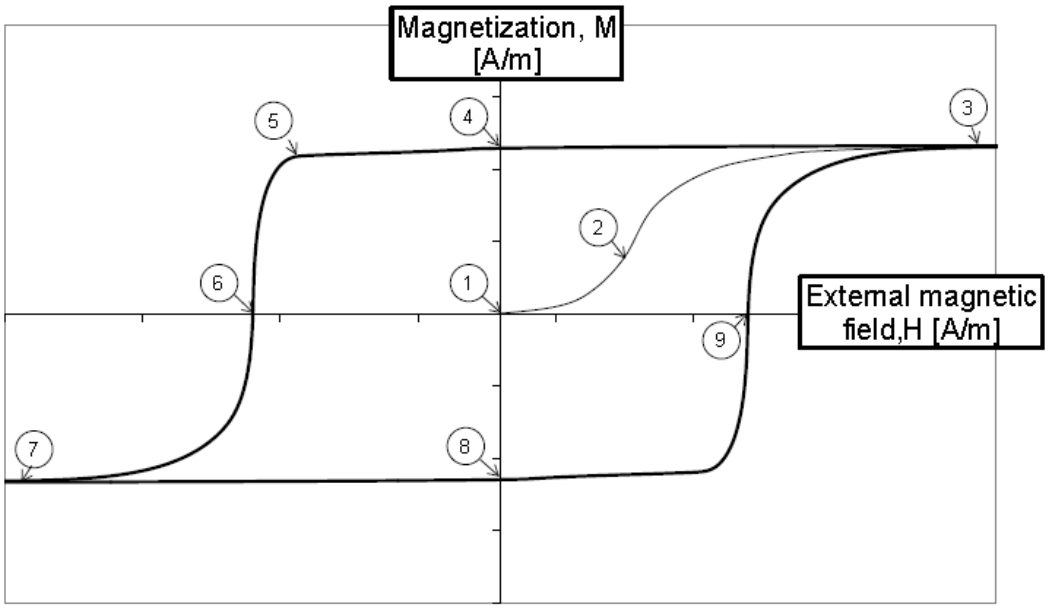

Figure 2. Schematic presentation of a hysteresis loop of a permanent magnet material.

The key properties of permanent magnets are thus the remanence, B_r, which determines the magnetic field produced by a given volume of magnetic material, and the intrinsic coercivity, H_{ci}, the material's resistance to demagnetization [6].

The theory of the hysteresis phenomenon is divided into three classes: rate-independent hysteresis, rate-dependent hysteresis, and thermal relaxation [2]. The rate-independent hysteresis does not include any time-dependent effects and it assumes that every *B/H* point describes the equilibrium state. Thermal effects are ignored in the rate-independent

hysteresis model, and it is therefore a zero temperature approximation. The rate-dependent hysteresis includes some dissipation mechanisms, such as eddy currents, which limit the rate at which the system can respond to the external field. Hysteresis loops increase in area with increasing field rate of change [7]. This is due to the shift of coercivity (loc. 6) to the left.

Thermal relaxation causes the system to approach thermodynamic equilibrium by thermal fluctuations. The thermal relaxation will shift the coercivity (loc. 6) of the rate-independent hysteresis to the right. Magnetic viscosity results from the thermal relaxation, and the phenomenon is discussed in more detail in Section 2.1.4.

Permanent magnet design usually relies on the rate-independent hysteresis theory even though it is precise only at 0 K. Thermal effects are considered only by measuring the M vs. H curves at different temperatures. Measured curves are assumed to present the equilibrium states at these temperatures. Permanent magnets are usually operated between loc. 4 and 5 in Fig. 2, and this part of the hysteresis is expected to be independent of the field rate of change. Magnetic viscosity is often considered to be so small that the approximation of rate-independent hysteresis can be safely adopted [7].

Hysteresis loops are measured by hysteresis-graphs, which are presented in more detail in Section 3.2.

2.1.2 Domain structure and energy profiles

Hysteresis behavior of permanent magnet materials is due to the changes in the magnetic domain structure. Domains are small volumes of the material in which the magnetic moments of atoms are aligned. Domains are separated by a domain wall. What type of domain structure is formed depends on four different factors: exchange interaction between neighboring atoms, crystalline anisotropy, magnetostatic effects, and external field [7]. Systems tend to approach an energy minimum state, and this is also a tendency in the domain structure formation. However, the domain structure realized in practice depends more on the external field history than the total energy minimum.

In NdFeB magnets, the uniaxial crystalline anisotropy is very strong, which favors the orientation of magnetization in the direction of easy axis only. It favors also narrow domain walls. In a domain wall, the direction of magnetization rotates from one direction to another. The width of the domain wall depends on the exchange and anisotropy energies.

In the non-magnetized state (loc. 1), one grain of sintered NdFeB material includes two or more domains that are equally distributed in opposite directions. This type of domain structure is illustrated in Fig. 3a. The net field outside the sample is zero. This type of domain structure is formed only by demagnetization of the material above the Curie temperature, which is like resetting the history of the external magnetic field. This is the energy minimum state of the material.

As the external field is increased (in the direction of the easy axis, i.e., the vertical direction in Fig. 3), the domains parallel to the field start to increase in volume by the movement of the domain walls. The reverse domains decrease in size accordingly. When the saturation has been achieved, the domain walls have disappeared and each grain contains only one domain. All the domains have the direction of the magnetization parallel to the external field (Fig. 3b).

After the saturation, each grain can be considered as a bistable system, which has two possible states of magnetization: magnetization upwards or magnetization downwards. The domain structure remains as in Fig. 3b even when the external field is removed. The energy profile of a single grain at this state (loc. 4) can be described as in Fig. 4a. There are two equal energy minima in the profile, corresponding to the two directions of magnetization. The energy barrier between the minima prevents the occupation of the other state. The energy barrier describes the energy needed to form a new domain wall or to release an existing wall from a pinning site.

As the reversed external magnetic field is increased, the occupied energy minimum starts to rise (Fig. 4b). The occupied energy minimum is not a total minimum of the system anymore, and the state becomes metastable. At the coercive field the occupied minimum has disappeared (Fig. 4c) and the reversal of the magnetization occurs. The external field energy has reached the energy needed to form a domain wall. As the domain wall is formed, the external field causes the wall to move fast across the grain, leading to the magnetization reversal of the grain.

In a multigrain material, this coercive field is slightly different for different grains. Some grains have reached their coercive field at loc. 5, and half of the grains have reversed the magnetization at loc. 6. Fig. 3c shows the domain structure at loc. 6. All the domains have reversed the magnetization at loc. 7, and the corresponding domain structure is presented in Fig. 3d. At the saturation conditions, there is only one energy minimum in the energy profile. As the external magnetic field is again removed (loc. 8), the magnetization state of the material remains (Fig. 3d). The energy profile of a single grain is shown in Fig. 4d. There are again two possible energy minima, but now the occupied minimum is the state of the reversed magnetization. This minimum is occupied until the coercive field is again

reached (loc. 9). The reversal field, equal to the coercive field, causes the minimum to vanish (Fig. 4e).

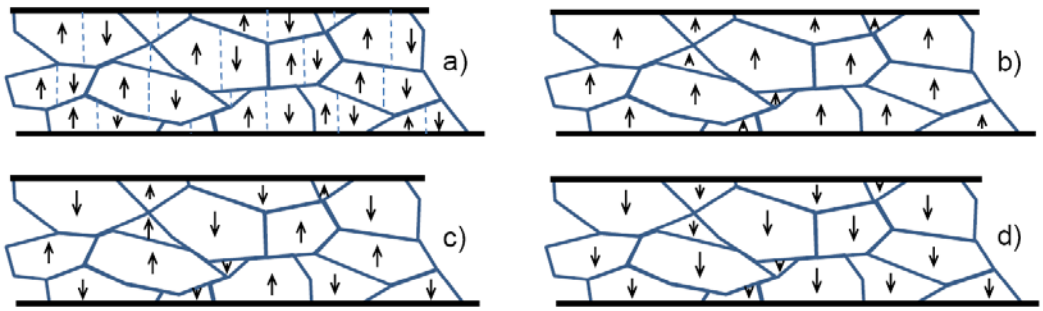

Figure 3. Domain structure of a sintered NdFeB permanent magnet material at different locations of the hysteresis curve.

Figure 4. Energy profiles of a bistable system. After saturation the single domain grains of sintered NdFeB magnets can be considered as bistable systems.

2.1.3 Magnetization reversal

The magnetization reversal occurs by the movement of domain walls. The reversal process is divided into two types: nucleation and pinning types. In the structure, where there are no domain walls present after saturation, the reverse domains need to be nucleated. In the pinning type of reversal, the domain walls are present but pinned for example on the grain boundaries or inclusions inside the grains.

In the NdFeB magnets, the reversal mechanism is found to be of the nucleation type [8]. As the nucleation field has been reached, the reverse domain nucleates and expands very fast by the movement of the domain wall [9], since the movement of the domain wall needs less energy than the nucleation. This is, however, not agreed entirely, and for example Durst and Kronmüller [10] suggest that the relevant magnetic hardening mechanism in NdFeB magnets is the nucleation process at lower temperatures, whereas at higher temperatures the pinning of domain walls at grain boundaries predominates.

In the theoretical studies, the reversal of the magnetization in NdFeB grains is in most cases discussed with a coherent rotation model, where the magnetization of a single grain is described by a single magnetization vector [7]. As the reversal takes place, the magnetization is considered to reverse simultaneously inside the whole volume of the grain as the direction of the magnetization vector is reversed.

As the grains in sintered NdFeB magnets are isolated by a grain boundary phase, the grains can be considered as independent small magnets. The behavior of the magnet material can then be determined as a sum of the behaviors of each grain. This Stoner-Wohlfarth model [11] is generally used to describe the formation of the magnetic hysteresis in sintered NdFeB magnets. However, the coercivity of the sintered NdFeB magnet materials produced today is only about 20 % of the theoretical maximum calculated according to the Stoner-Wohlfarth model [12]. Hrkac et al. [13] have shown that this is due to two effects: one is the magnetostatic field from the neighboring grains, and the second is the reduced anisotropy at the surface region of the grain.

2.1.4 Magnetic viscosity

The demagnetization process is found to be time-dependent, magnetic viscosity being the phenomenon delaying the process. During the demagnetization process, metastable states in magnetic materials transform to stable ones by a combination of field induced transitions and thermal activation [14]. At constant field conditions, the evolution of demagnetization is a result of thermal activation. The hysteresis curves describe the field induced process but neglect the time-depended effects caused by thermal activation. It follows that the representation of the magnetic behavior of a material by M vs. H data (like in Fig. 2) is incomplete [15].

This time dependence of extrinsic magnetic properties due to magnetic viscosity is also known as thermal after-effect or ageing [16]. Magnetic viscosity is known to be a statistical relaxation phenomenon. In constant field conditions, the magnet system approaches its thermodynamic equilibrium due to thermal fluctuations. The probability of energy peaks exceeding the energy barriers between the two magnetization states (Fig. 4b) determines the magnetization reversal of each domain.

Experimentally it has been found that the time dependence of magnetization (M) as a function of time (t) and magnetic field (H) can be described by a logarithmic law [16]:

$$M(t,H) = M(t_0,H) - S(H)\ln\frac{t}{t_0} \qquad (1)$$

where S is a phenomenological magnetic viscosity constant and t_0 is a reference time. This function is an approximation and valid only in a limited time interval.

Many magnetic viscosity studies beginning from Néel (1948), and Street and Woolley (1949) [17], have tried to connect the magnetic viscosity coefficient to the activation energy of the magnetization reversal. Néel's theory is based on thermally induced random fluctuations of spontaneous magnetization (fluctuation field) and Street's theory on thermally activated rate processes involving metastable states with a distribution of activation energies [14].

Wohlfarth et al. [18] have determined the magnetic viscosity constant as:

$$S = \frac{kT}{\upsilon K} f(H,T) M_S \qquad (2)$$

where kT represents the temperature dependence (k is the Bolzmann's constant, T is temperature), υK (υ is the activation volume, K is the anisotropy constant) depends on the material and its microstructure, and $f(H,T)$ is a complex function, which describes the precise nature of the magnetization process. Thus, magnetization losses over time in permanent magnets depend on the magnetic field, temperature, magnet material and its microstructure and the magnetization history.

The viscosity coefficient S is constant only at a constant demagnetizing field and constant temperature. To get a material characteristic, independent of the field, theories suggest to divide the magnetic viscosity coefficient S by the irreversible susceptibility χ_{irr} $(= dM_{irr}/dH)$ of the material [17]:

$$S_v = \frac{S}{\chi_{irr}} \qquad (3)$$

In many publications S_v (or H_f) for NdFeB magnets has been found to be independent of the magnetic field and constant at a constant temperature [19-23]. However, some studies show that it varies with the magnetic field [24]. The comparison of the results of the S_v measurements found in the literature is difficult due to many different experimental and theoretical procedures [25, 26]. There is no consistent understanding how χ_{irr} should be determined. For example, Estrin [27] claims that the susceptibilities in the previous studies have not been precisely defined. He sees that there is an analogy between the reversible and irreversible changes in the intensity of magnetization and the elastic and plastic components of strain. This means that appropriate values of the susceptibilities are those

obtained from magnetization vs. magnetic field curves taken at constant $\dot{M}_{irr}$. In most of the studies χ_{irr} are determined from the traditionally measured *MH* curves.

Independent of the experimental procedure, the measurements of S and χ_{irr} are performed in the time-scale of seconds. The fact that χ_{irr} is actually time-dependent [28] is mostly ignored in these studies. S_v might thus also become time-dependent. S_v is very important in the magnetic recording as the particle size reaches the nanometer range and the time-scales for magnetization and demagnetization processes are less than a second. These research results are not necessarily applicable to the demagnetization process of bulk magnets in the time-scale of years.

Usually the measurement equipment does not allow accurate measurements over long periods of time. The logarithmic law (Eqn. 1) is shown to hold for NdFeB magnets within different time intervals between 1 s and 30 min [21-23, 25, 29].

As a general rule, the time-dependent behavior is more pronounced in higher coercivity materials [15]. This indicates that also in high coercivity NdFeB magnets the magnetic viscosity might be significant in certain conditions.

2.2 Sintered NdFeB

The NdFeB permanent magnet material was discovered in the beginning of the 1980's, and the first results were published in 1984 by two different research groups independently. Croat et al. [30] produced the material by so-called melt-spinning process, while Sagawa et al. [31] used a sintering process. The magnetic phase is the same but the microstructure of these two differently produced NdFeB magnets is different. Melt-spinning leads to a nanocrystalline structure, whereas the sintering process forms a microcrystalline structure [32]. The sintering process is nowadays adopted as the production process for bulk NdFeB magnets, since it is more effective in mass production. The melt-spinning process is used mainly to produce NdFeB powders for plastic bonded magnets.

The properties of sintered NdFeB magnets depend on the intrinsic properties of the hard magnetic phase as well as the microstructure of the material. The microstructure of the material is dependent on the complex production process. In section 2.2.1 the microstructural features of sintered NdFeB magnets are discussed, and the production process of sintered NdFeB magnets is presented in Section 2.2.2.

2.2.1 Microstructure

Sintered NdFeB magnets compose of a hard magnetic $Nd_2Fe_{14}B$ matrix, an intergranular Nd-rich phase, and a small amount of a B-rich phase [33]. Fig. 5 shows a SEM image of the microstructure of a NdFeB based sintered magnet. The grains (gray) consist of the hard magnetic phase. Between the grains, there are very thin Nd-rich grain boundary phase regions with some small agglomerates consisting of neodymium oxides at the triple points of the grain boundaries (white).

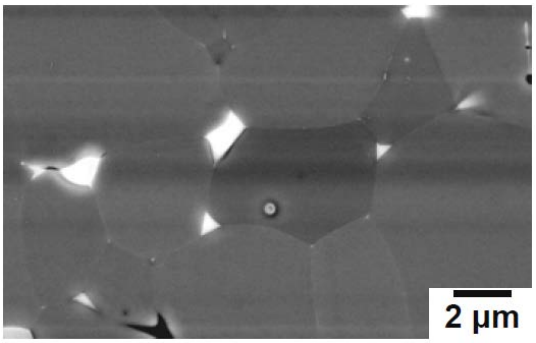

Figure 5. SEM image of the microstructure of sintered NdFeB magnet material [34].

Basically the hard magnetic phase is responsible for the magnetic properties of the material, but the grain boundary phase has also a major effect on the coercivity of the material. These phases are discussed in more detail in Sections 2.2.1.1 and 2.2.1.2., respectively.

2.2.1.1 Hard magnetic phase

The magnetization of a material arises from the quantum mechanics, which determines the magnetic states of an atom. Fe and rare-earth atoms are known to form binary compounds with high saturation magnetization due to the ferromagnetic coupling of the magnetic moments [31]. The search for a new stable phase with uniaxial anisotropy gained lot of efforts in the beginning of the 80's, and finally the ternary $Nd_2Fe_{14}B$ phase was discovered. The production of the compound requires rapid solidification. If the solidification is too slow, iron tends to solidify as α-Fe.

The $Nd_2Fe_{14}B$ phase has a tetragonal crystal structure [4] with a uniaxial anisotropy. It's easy direction of magnetization lies on the *c*-axis. The unit cell of a $Nd_2Fe_{14}B$ crystal is shown in Fig. 6.

The uniaxial crystalline anisotropy in the $Nd_2Fe_{14}B$ crystal means that all the magnetic moments of the ferromagnetic atoms will spontaneously point in the *c*-direction. In one grain there are thus two possible magnetization directions: along the *c*-axis upwards or downwards.

Sintered NdFeB magnets are produced from powder that consists of only single grain particles. As the grains are oriented during the pressing by an external magnetic field, the *c*-axis of all grains is pointing in the same direction. The obtained magnets are therefore anisotropic, meaning that there are only two possible magnetization directions.

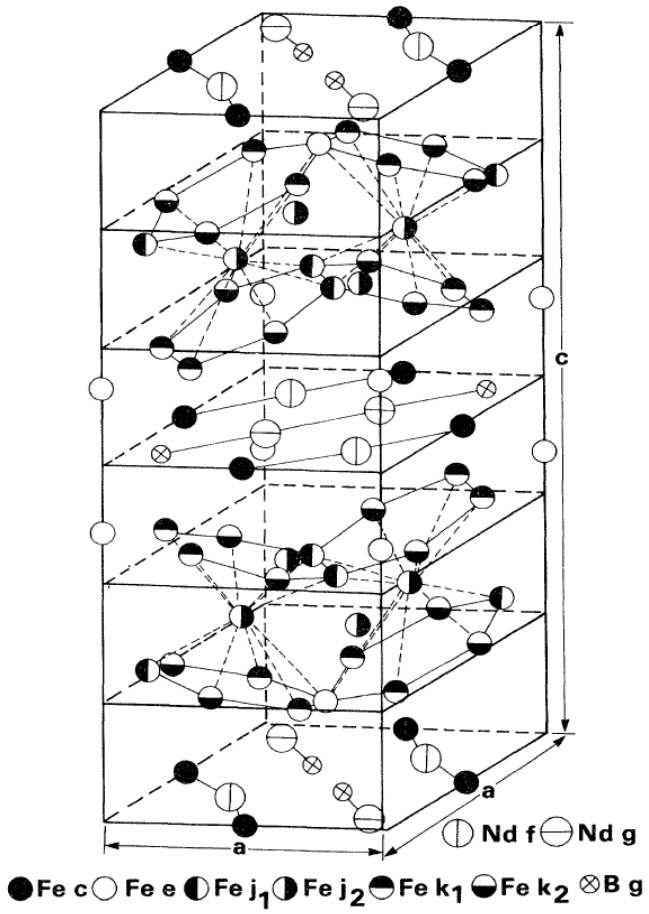

Figure 6. Crystal structure of $Nd_2Fe_{14}B$ [35].

The remanence of the material originates from the spontaneous magnetization *(M_s)* of the hard magnetic phase ($\mu_0 M_s$ = 1.6 T at 300 K in $Nd_2Fe_{14}B$) [12]. The remanence of the final magnet can be increased by increasing the volume fraction of the hard magnetic phase and by enhancing the alignment of the grains [36].

2.2.1.2 Grain boundary phases

The structure of the grain boundaries in sintered NdFeB magnets has a significant effect on the coercivity of the material. The function of the grain boundary phase is to isolate the hard magnetic grains and to prevent the magnetic interaction between them. In well isolated grains, the magnetic reversal process does not proceed from one grain to another. Instead, the magnetization reversal needs a nucleation of a reversal domain in each grain.

The key to the magnetic isolation is the paramagnetic Nd-rich phase. Also some Nd-oxides are present at the grain boundaries, since neodymium is a very active material and oxidizes easily. Fig. 7 shows a SEM image of some $Nd_2Fe_{14}B$ crystallites with a thin Nd-rich intergranular phase separating the individual grains. This type of microstructure should be very effective in preventing the nucleation of reverse domains [34]. The structure, formation and role of the grain boundary phase have been topics for many research works recently [37-40].

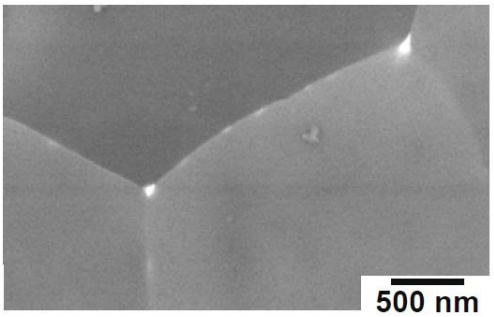

Figure 7. SEM image in the backscattered electron contrast of the NdFeB-type sintered magnet showing a very thin and homogeneous coating of the $Nd_2Fe_{14}B$ grains with Nd-rich intergranular phase [34].

Li et al. [37, 38] have found that the continuous thin layer of a Nd-rich phase along the grain boundaries has a chemical composition of $Nd_{30}Fe_{45}Cu_{24.1}B_{0.9}$. Cu addition enhances the formation of the Nd-rich thin layers along the grain boundaries. A fine Cu-enriched shell was also detected, suggesting that the $Nd_2Fe_{14}B$ grains are completely enveloped by the Cu- and Nd-enriched layers. 3D atom probe analysis showed that a thin Cu-rich layer

with a thickness of approximately 2 nm is present at the interface between the $Nd_2Fe_{14}B$ and Nd-rich phases. The result of this analysis is presented in Fig. 8. On the right is the $Nd_2Fe_{14}B$ grain and on the left the grain boundary.

The crystal structure of the Nd-rich phase mainly depends on its O content. As the O content increases, the structure of the Nd-rich phase changes as follows: double close-packed hexagonal (solid solution) → face-centered cubic (NdO) → close-packed hexagonal (Nd_2O_3) [41]. The wettability of the grain boundary phase decreases as the O content increases. Nd-oxides tend to form precipitates at the grain boundaries. Degradation of the coercivity of a NdFeB magnet with the grain size less than 3 μm was found to result from the inhomogeneous distribution of the fcc-Nd oxide. The volume fraction of fcc-Nd oxide increased when the grain size of the material was decreased [42]. The wettability of the grain boundary phase becomes even more important as the grain size decreases, since the total surface area of the grains increases.

The coercivity of high-performance sintered NdFeB magnets is still about 20% of the theoretical Stoner–Wohlfarth limit. This can be explained by a distorted region of $Nd_2Fe_{14}B$ at the grain boundaries, which leads to a reduced local magnetic anisotropy [13]. Depending on the boundary composition of fcc-NdO and hcp-Nd_2O_3, the thickness of this region of reduced anisotropy varies between 0.4 nm for fcc and 1.6 nm for the hcp phase. Simulations show that this distorted region on the grain surface together with magnetostatic fields from the neighboring grains give the coercivity levels found in commercial sintered NdFeB magnets today.

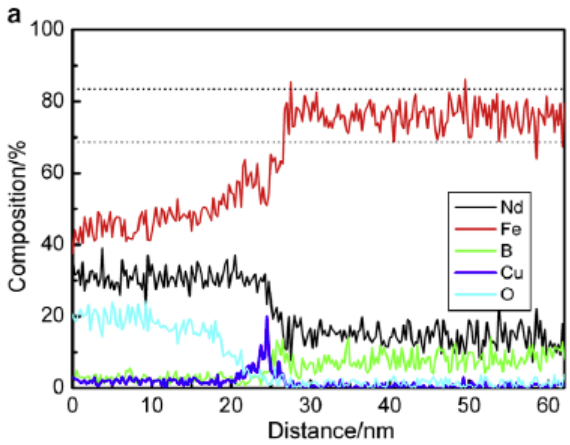

Figure 8. Concentration depth profiles for Nd, Fe, B and Cu, determined from a 3D atom probe analysis. The dotted lines mark the statistical errors of Fe [38].

2.2.1.3 Alloying elements

Different types of alloying elements are used in NdFeB magnets for various reasons. Basically there are two types of additional elements: substitution elements and dopants. Fidler et al. [43] have divided the elements into four categories according to their tendency to substitute either Nd or Fe atoms in the hard magnetic phase (substituents S1 and S2) or to form grain boundary phases with Nd or B (M1 and M2). The structure of the material will be (Nd,S1)-(Fe,S2)–B:(M1,M2). Selected S1 substituent elements (Dy,Tb) replace the Nd atoms and S2 atoms (Co,Ni,Cr) the Fe atoms in the hard magnetic phase and considerably change the intrinsic properties, such as the spontaneous magnetization, the Curie temperature, and the magnetocrystalline anisotropy.

If dopant elements M1 or M2 are added to Nd–Fe–B, in some cases the coercivity is increased and the corrosion resistance is improved. Type M1 dopants (M1=Al, Cu, Zn, Ga, Ge, Sn) form binary M1-Nd or ternary M1-Fe–Nd phases, whereas M2 dopants (M2=Ti, Zr, V, Mo, Nb, W) form binary M2-B or ternary M2-Fe–B phases. M1 dopants influence the wetting behavior of the liquid phase during the sintering. This leads to a more homogeneous distribution of the grain boundary phase, which enhances the coercivity.

The most important and widely used substitutions are dysprosium and cobalt. By substitution of Nd with Dy, a rise in coercivity is achieved. In the magnet grades intended for high temperature applications Dy additions are essential. However, while the Dy addition increases the coercivity it also decreases the remanence, which is an unfavorable effect.

Partial replacement of Fe by Co raises the Curie temperature of the $Nd_2Fe_{14}B$ compound, which improves the temperature coefficient of remanence, but the coercivity is decreased [33]. Co segregations at the grain boundaries improve the corrosion resistance of the material.

2.2.1.4 Domain structure

The grains in the NdFeB magnet material are split into domains in the pre-magnetized state. The domains are separated by domain walls. Magnetization is realized by the movement of these domain walls. The macroscopic magnetic properties of the material are due to the magnetic microstructure, i.e., the domain structure. Fig. 9 presents a Kerr microscopy image of a NdFeB crystal around a twin boundary, meaning that the upper part has a different magnetization direction than the lower part. The image represents the domain structure of a thermally demagnetized NdFeB material.

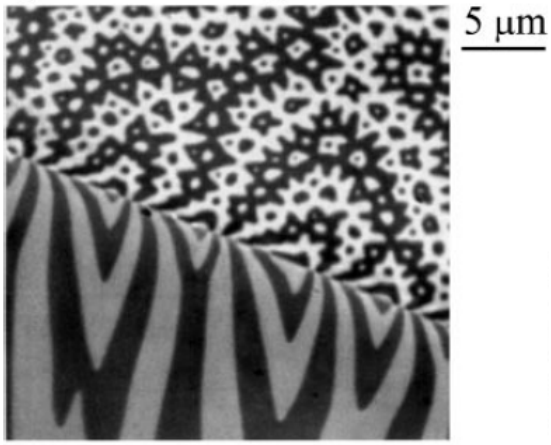

Figure 9. Kerr image obtained around a twin boundary in a NdFeB crystal [44].

In the thermally demagnetized state there exist multi-domain grains in sintered NdFeB magnets, but after magnetization to saturation the domain walls are either disappeared or pinned to the grain boundaries. According to the theory presented in Section 2.1.2, NdFeB grains can be considered as single domains all the time after the saturation magnetization. The multi-domain structure can be returned only by heating the material above the Curie temperature.

The domain structure of magnetized sintered NdFeB magnets is difficult to detect. Takezawa et al. [45-47] have recently studied the magnetization reversal of NdFeB magnets by Kerr microscopy. Fig. 10 reveals that there occur multi-domain grains during the reversal process at room temperature. Only at the saturation state all the grains are single domains. Conclusions are difficult to draw, since the image is only representing the magnetic microstructure of the surface of the sample. During the sample preparation, some deterioration on the surface occurs and it has an effect on the magnetic properties of the surface layer [48].

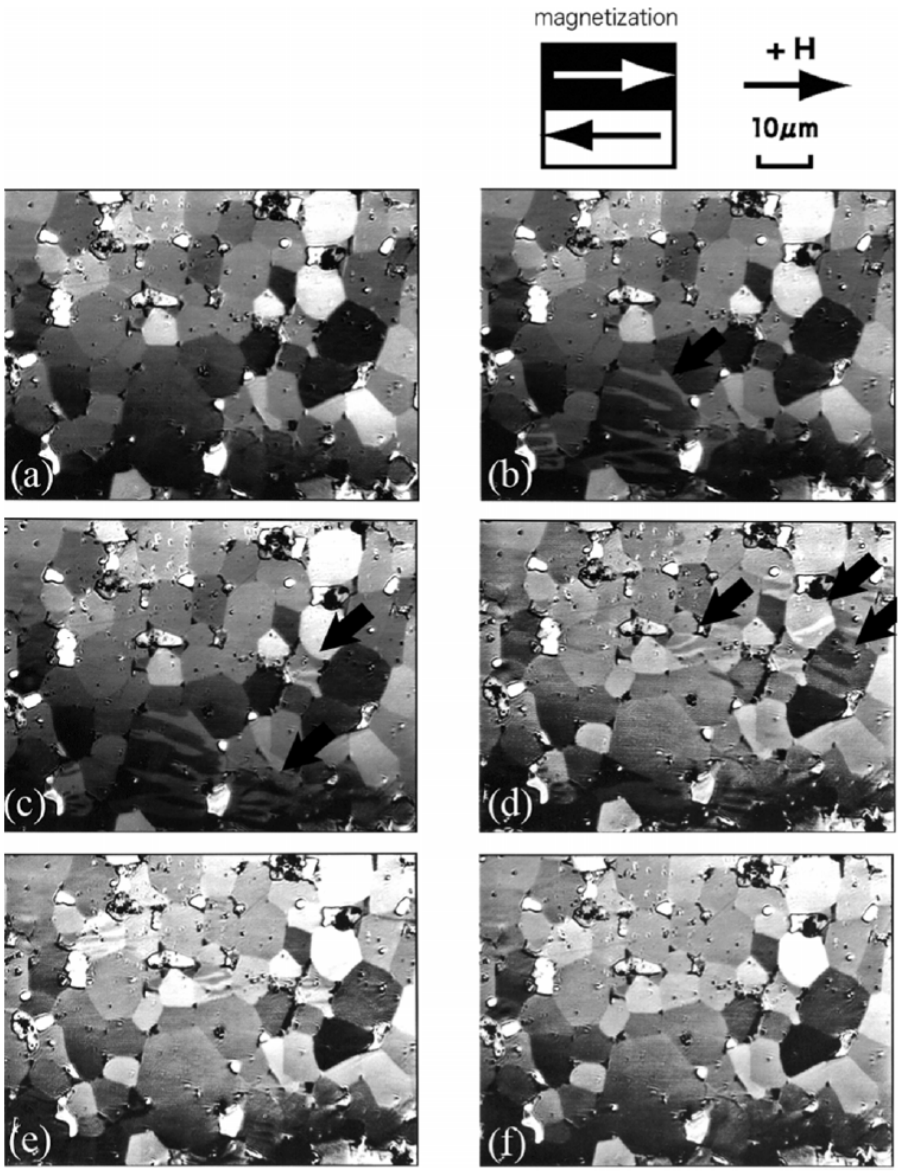

Figure 10. Magnetization process of sintered NdFeB magnet at 20°C: (a) + 14 kOe (1114 kA/m), (b) + 1.1 kOe (87 kA/m), (c) + 0.8 kOe (64 kA/m), (d) 0 kOe, (e) - 1.4 kOe (-111 kA/m), and (f) - 7.2 kOe (-573 kA/m) [47].

2.2.2 Production process of sintered NdFeB magnets

The production process of sintered NdFeB magnets starts from the casting of the alloy. Cast ingots are crushed and further processed by the hydrogen decrepitation (HD) process to a fine powder. The powder is further milled by jet milling until the particle size is about 5 µm. After milling, the powder consists of only single grain particles. A green compact is then pressed from the powder in the presence of an external magnetic field. The magnetic field aligns the particles and results in anisotropic magnets. The green compacts are then densified by sintering at a temperature over 1000°C. A post sintering heat treatment at about 600°C is also necessary to enhance the coercivity of the magnet. For finishing the magnet, some machining and surface treatments are typically performed. The last step in the production process is the magnetization. The process is presented in Fig. 11. Each step of the process, until machining, will have an effect on the microstructure and magnetic properties of the magnet.

Cooling rate is a critical parameter in the casting. In traditional ingot casting, there is a risk of α-Fe formation if the Nd content is reduced close to the stoichiometric level of the $Nd_2Fe_{14}B$ compound [49]. The formation of a soft magnetic α-Fe phase will deteriorate the magnetic properties of the final magnet. The formation of dendritic α-Fe in cast alloys can be reduced by additives as well as by optimizing the casting technique [50, 51]. Strip casting is an improved casting technique that provides a finer and more homogenous microstructure. Effects of this casting method on the properties of the magnet have been studied actively [52-54].

In the milling and compaction steps it is important to avoid oxidation. The coercivity of the magnet can be increased by decreasing the grain size [55]. This requires milling to a smaller particle size. The reduction in the particle size, however, increases the risk of oxidation which, in turn, leads to the reduction in coercivity, as explained in Section 2.2.1.2.

Sintering will solidify the magnets. The sintering temperature has to be high enough to allow the grain boundary phase to liquefy, but not too high, since the grain growth is easily activated at high temperatures. The optimal sintering temperature varies slightly with the composition of the magnet. Post-sintering heat-treatment enhances the coercivity by forming a continuous thin Nd-rich grain boundary phase with a thin Cu-enriched layer along the Nd-rich/$Nd_2Fe_{14}B$ interface. The formation of such a Cu-rich layer is expected to decouple the exchange interaction between the $Nd_2Fe_{14}B$ hard magnetic grains and thereby increase the coercivity.

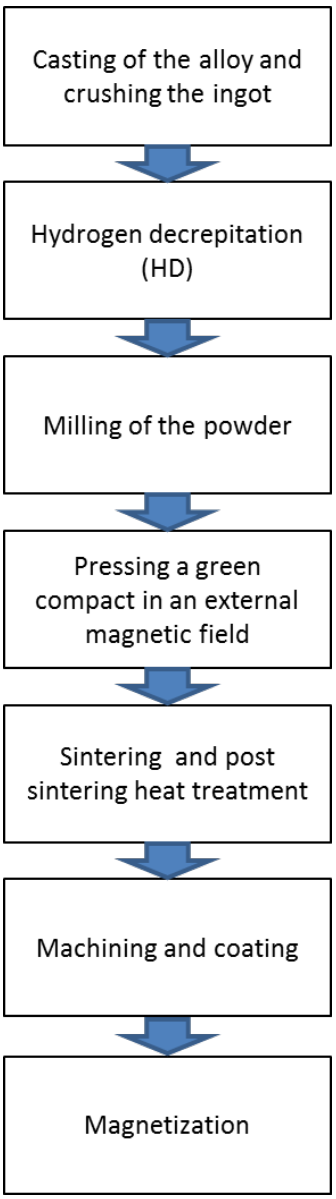

Figure 11. Production process of sintered NdFeB magnets.

The production process of sintered NdFeB magnets is well established and many industrial magnet producers have adjusted the parameters of each production step to optimize the properties of their products.

2.2.3 Recent developments in NdFeB magnets

The dominant application of sintered NdFeB magnets has been changed from the hard disc drives to the motors [56], which means that thermal stability properties have become more important. The production of high coercivity grades that contain large amounts of dysprosium is common nowadays. Dysprosium is, however, not as abundant as Nd in ores and thus it is much more expensive. There is a strong attempt today to find new ways to increase the coercivity of sintered NdFeB magnets without Dy additions [57-59].

There are two main ways to reduce the Dy content in high coercivity grades. The first one is the refining of the grain size. The Japanese have developed a production process called PLP (pressless production), which allows to compact fine powders [60]. Magnetic properties can be enhanced also with a narrow particle size distribution [61].

The second one is the introduction of Dy only on the surface layer of the NdFeB hard magnetic grains. This is done by diffusion of Dy along the grain boundaries from the surface of the magnet [62, 63]. This method is limited to very thin magnets only.

One of the goals of this thesis is to examine the possibility to save Dy by optimizing the selection of the magnet material, i.e., to avoid any excess Dy additions in the used material due to too high safety factors.

2.3 Characteristics of sintered NdFeB magnets in motor and generator applications

Motor and generator applications are one of the high-tech applications of sintered NdFeB magnets. This means that the properties of the magnets need to be modified carefully to match the design of the application. Magnetic properties of permanent magnet materials are typically determined by measuring the magnetic flux density, B, as a function of external field strength, H. This BH curve characterizes the behavior of the material in a changing external field.

The most important parameter of NdFeB magnets used in a motor or generator application is the remanent flux density. The flux density should be also fairly stable over the operating conditions of the application. It is important to control the operating conditions to avoid any permanent changes in the polarization. IEC has published a technical report [64], which describes the temperature behavior of rare earth sintered magnets. Changes in the magnetic properties due to the changing temperature are explained well, but the knowledge on the time-dependent effects at constant conditions is admitted to be inadequate.

Three different types of losses might occur in the remanent polarization of the magnet: reversible, irreversible, and permanent losses. These are discussed in Section 2.3.1. Thermal stability and maximum operating temperature are discussed in Section 2.3.2. The magnet material selection based on the operating point method is discussed in Section 2.3.3. The last Section, 2.3.4, deals with the specifications and quality control of the magnets.

2.3.1 Reversible, irreversible and permanent losses

The possible losses occurring in permanent magnets are divided into three categories according to the nature of the loss. Reversible polarization losses occur as the temperature rises, but the polarization increases back to the original level as the temperature is decreased again. This is a material property and can be affected only slightly by the alloying elements. The temperature dependence of the remanent polarization is described by a temperature coefficient of remanence, α. The temperature dependence is not actually linear, but in a short temperature range it can be approximated by a linear coefficient. Typically the coefficient is determined for the temperature range from 20°C to 100°C.

Irreversible polarization losses are not recovered as the temperature is decreased. Fig. 12 illustrates the differences of the reversible loss (R) and the irreversible loss (I). The original magnetic moment in the Figure decreases from about 120 to about 60 (arb. units) as the temperature is increased from room temperature to 200°C. As the temperature is returned back to room temperature, the magnetic moment of about 80 is achieved. This means that the total loss occurring due to the temperature rise can be divided into the reversible and irreversible parts. The irreversible part can be further divided into recoverable and permanent losses. Permanent losses result from the structural changes in the microstructure. Mainly these are due to oxidation in the sintered NdFeB magnets. Recoverable irreversible losses can be recovered by remagnetization. This part of the total loss is only caused by the demagnetization of the magnet.

The reversible loss has to be taken into account in the application design, since it cannot be avoided. The permanent loss can be controlled by careful corrosion protection. Even though the losses due to demagnetization are recoverable by remagnetization, they need to be avoided in the applications, as the remagnetization of the assembled magnets is nearly impossible.

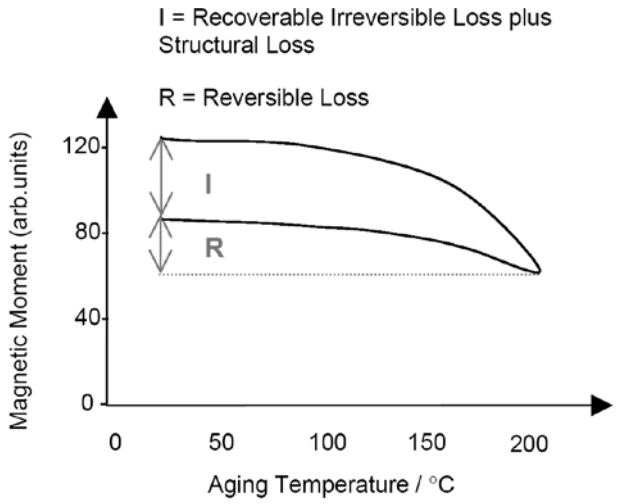

Figure 12. Illustration of the flux losses experienced by a NdFeB magnet at elevated temperatures [32].

2.3.2 Thermal stability

There is no consistent definition for the term “thermal stability”, even though it is a very important issue in the design of NdFeB magnet applications. The thermal stability of different types of NdFeB materials is being studied actively [65-74], but it is difficult to compare these results since the authors determine the concept of thermal stability differently.

In some cases, such as in [74], the thermal stability of a permanent magnet material is considered to be described only by the temperature coefficient of remanence, α. This description is valid only if the demagnetization and oxidation are totally avoided. In this particular paper, the increase of thermal stability of the NdFeB material is considered as the decrease of the temperature coefficient α gained by Gd substitution. However, the intrinsic coercivity H_{ci} is at the same time decreased, and the risk of partial demagnetization of the magnet is thus increased. Anyway, this is not considered to affect the thermal stability of the material.

In most cases also the partial demagnetization due to temperature rise is considered. The coercivity of NdFeB material typically decreases radically as the temperature raises, and thus, the control of the demagnetization is challenging. The partial demagnetization is typically defined as the amount of irreversible flux loss detected after a certain exposure. This gives, however, only one loss value after a fixed exposure. For example, Zhang et al.

[66, 67] have used a two hour exposure time, Kim et al. [70] an exposure time of one hour, and Cheng et al. [72] only a half-our exposure time. Some studies do not mention the exposure times at all. Also the dimensions of the samples vary in these studies, leading to different types of field conditions.

Even though these studies do not give applicable information to machine design, they reveal the potential methods to manipulate the properties of NdFeB compounds. For example Ma et al. [68] showed that Dy and Nb additions clearly reduce the irreversible flux loss at elevated temperatures, and Chen et al. [69] showed the same effect with MgO and ZnO additions. Also Ga [72] and Ti+C [67] additions are found to decrease the flux loss at elevated temperatures.

2.3.2.1 Maximum operating temperature

In the application industry, the thermal stability is frequently defined by setting a maximum operating temperature for a magnet [3]. The maximum operating temperature should be defined as the maximum temperature to which the magnet may be exposed with no significant long-term instability [75]. However, this temperature is strongly dependent on the dimensions of the magnet and as assembled, on the magnetic field conditions the magnet is facing during the operation. So, the maximum operating temperature is not just a material characteristic but also depends on the operating point.

Another issue in the definition of the maximum operating temperature is the question of 'significant instability'. Machine designers use a term of critical temperature [76-78], but in FEM design it means a limiting temperature with no irreversible losses at all. Many times it is determined theoretically from the measured *BH* curves of the material. This theoretical method ignores the time-dependent effects and is thus not accurate. The operating point method is discussed in more detail in Section 2.3.3.

A more practical way of defining the critical temperature is to set a maximum allowable loss to the polarization. Kato et al. [79] have determined the thermal stability by a critical temperature of 3 % irreversible flux loss under thermal cycles. According to Trout [3], it is a common way to specify the maximum operating temperature as the temperature, where the total flux loss reaches 5 %. For the applications these limitations to the total loss are clear and are expected to represent the total loss during the expected lifetime of the application. Tests are, however, performed with much shorter time periods. There is a lack of a consistent and well known theory for how to convert these short-period thermal stability test results to applicable information for the assurance of the long-term stability.

2.3.2.2 Stabilization heat treatment

The stabilization heat treatment, also known as the pre-aging heat treatment, is a method used in order to improve the thermal stability of permanent magnets. This means that the magnets are exposed to a higher temperature than their intended operating temperature, before being installed. However, there are not many published papers about the effects of such heat treatments on the subsequent loss behavior of sintered NdFeB magnets. Radiation-induced demagnetization is claimed to decrease due to the thermal stabilization [80]. A pre-ageing heat treatment that caused a 0.69 % decrease in the polarization was found to be sufficient to decrease the subsequent demagnetization in the electron beam exposure close to zero.

The effects of stabilization heat treatment on SmCo based magnets have been studied previously [81, 82]. As long as the stabilization treatment is performed at moderate temperatures, the effects are purely due to the domain wall motion and a stabilizing effect is attained [81]. Remanence of the magnets was reduced proportionally during the stabilization treatment. In [82], the time-dependent demagnetization of SmCo magnets within a three-year measurement period was found to decrease to about 0.3 % after a two-hour pre-ageing treatment.

The principal idea of thermal stabilization is to demagnetize the weakest domains in the magnet. The domains that maintain their original magnetization state despite the thermal exposure are assumed to be stable at temperatures below the stabilization temperature. Based on this assumption, stabilization heat treatment is introduced as a part of the production process in some companies utilizing sintered NdFeB magnets. The exposure temperature and the duration of the heat treatment are more or less chosen on the basis of rough estimates, or the treatments are combined with other processing steps like curing or potting, and the parameters of the heat treatments are optimized for these processes. Also stabilization treatments using magnetic field pulses are used, since they are easier to carry out.

2.3.3 Operating point

The permeance coefficient *(P_c)*, the load line, and the operating point of a magnet are many times considered to be the same measure. These are related to the dimensions of the magnet and its associated magnetic circuit [75]. The operating point is also related to the material's *BH* curves, and it is defined as the intersection point of the load line and the material's *BH* curve. This is a way to describe the magnetic field conditions inside the magnet during the operation. There are two things affecting the magnetic field conditions:

the self-field produced by the magnet itself and the external magnetic field produced elsewhere in the application.

For individual magnets, the only source of magnetic field is the self-field. The permeance coefficient of a single magnet can be determined according to its dimensions. The permeance coefficient of a rectangular magnet is calculated according to the following formula [83]:

$$P_C = 1.77 \frac{h}{lw} \sqrt{h(l+w)+lw} \quad (4)$$

where h is the height (the direction of the magnetization), l is the length, and w is the width of the magnet. The calculated P_c gives an average value for the load line $-B/\mu_0 H$ (μ_0 is used to change the units of H from kA/m to T [84]) for the magnet. In reality, the value of $-B/\mu_0 H$ is not constant but varies inside the magnet.

The operating point is typically considered as a point on the measured BH curve of the material. It is an intersection of the BH curve and the load line representing the magnetic field conditions ($-B/\mu_0 H$). Fig. 13 shows the measured JH and BH curves of one magnet grade produced by Neorem Magnets Oy. J is the magnetic polarization of the material, and it is connected to the magnetic flux density by:

$$J = B - \mu_0 H \quad (5)$$

There are six different curves in the Fig. 13 measured at different temperatures. Load lines $-B/\mu_0 H$ = 0.4 and 0.75 starting from the origin are also added to the Figure. These load lines represent the magnetic conditions of magnets with different dimensions. If there exits an external magnetic field, the load line will be moved to start from the external field strength value.

The operating point is expected to reveal the demagnetization behavior of the magnet. It is also used to determine the limiting operating conditions for the material. As long as the operating point is on the linear part of the BH curve, no irreversible losses are expected. For example for a material, whose BH curves are presented in Fig. 13, the maximum operating temperature at the operating point of 0.4 is 100°C, while at the operating point of 0.75 it is 120°C. However, the determination of the maximum operating temperature only by the measured BH curves does not guarantee zero losses, since time-dependent losses are ignored.

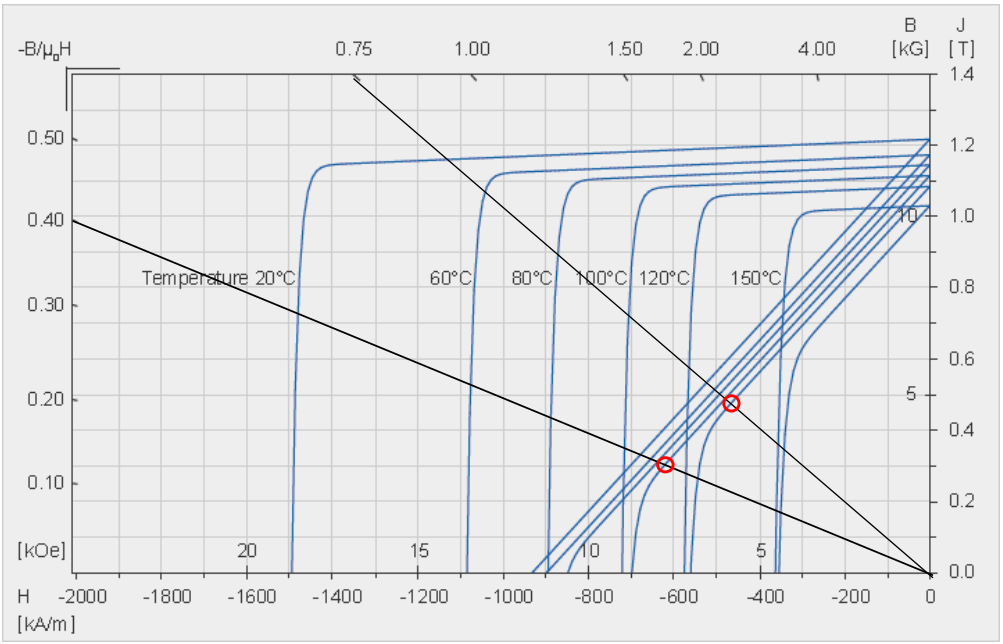

Figure 13. Nominal *JH* and *BH* curves for Neorem Magnets grade 453a. Load lines $-B/\mu_0 H$ = 0.4 and 0.75 are also presented. The intersection of the load line and the *BH* curve need to be in the linear part of the *BH* curve to avoid irreversible losses.

2.3.4 Specifications and quality control

FE-modeling is nowadays an efficient way of designing the applications. The optimization of the magnetic circuits is thus much easier today than a few decades ago. There are many papers published recently about the studies of the demagnetization risks of permanent magnets in different types of machines [85-91].

In addition to the FEM calculations, it is important to understand how to convert the used magnetic behavior optimally to the real material properties and especially to the specifications when ordering magnets. The magnetic behavior of a commercial permanent magnet material is not necessarily close to ideal, which is in many cases assumed in design. Usually the *BH* curves are measured only for one sample in the production lot, but there is always some variation in the properties from sample to sample. There also might be some inhomogeneities inside the magnet, and the measured *BH* curve only represents the average behavior of the material. Locally the response to a reverse magnetic field can differ from the measured one.

The magnetic behavior of the NdFeB magnet material is not defined completely by its remanence and coercivity values. Also the shape of the *JH* curve is important. A common way to quantify the shape of the curve is to use a parameter termed squareness factor (*SF*) (or in some papers squareness ratio *SR*).

$$SF = \frac{H_k}{H_{ci}} \tag{6}$$

where H_k refers to the field at which 10 % of the remanence is lost (= field at 90 % of B_r) [92]. A squareness factor of 1 describes an ideal magnet material in which the magnetization of all domains is reversed at the same opposing field, the coercive field. In real materials this is almost impossible to achieve, but the closer the *SF* gets to unity the better is the homogeneity of the material. Consequently, *SF* is considered as a quality measure of a magnet material.

The shape of the *JH* curve depends on the microstructure of the magnet material [92, 93], and the microstructure depends on the production process. Factors affecting the squareness are at least the mean grain size and its standard deviation and the grain shape homogeneity [93]. In addition, all kinds of defects in the microstructure, especially in the soft magnetic phases, deteriorate the squareness easily [92]. If there exists roundness in the material's *JH* and *BH* curves, it can be treated by a partial demagnetization (stabilization or pre-ageing) by a heat treatment or a reverse field pulse. If the slight demagnetization is done in a closed circuit, the recoil curve, i.e., the new *BH* curve for the material after partial demagnetization, will be close to linear [94].

3. Methods for testing the magnetic properties of permanent magnets

The magnetic properties of permanent magnets are determined by measuring the external magnetic field they induce to the surrounding space. The easiest way to determine the polarization or flux density of a magnet is to measure the total induction with a Helmholtz coil and divide it with the volume of the sample. This reveals only the state of the magnet at the moment of the measurement. The method is introduced in Section 3.1.

To characterize the magnetic behavior of a material in an external magnetic field, its hysteresis loop has to be measured. The full hysteresis loops are difficult to measure for sintered NdFeB magnets, and in many cases they are also unnecessary. The demagnetization curve, i.e., the second quadrant of the whole loop, provides enough information for the utilization. The demagnetization curves are measured typically by Hysteresis-graphs, and the obtained curve represents an average response of the material to the changes in external field. More about the demagnetization curve measurement is presented in Section 3.2.

The demagnetization curve measurements do not give information about the local variations of flux density inside the magnet. The homogeneity of the flux density, however, can be detected by scanning the surface of the sample with a Hall probe. This method is described in Section 3.3.

The above methods are commonly used in the magnetic material characterization. However, they do not reveal the time-dependence of the magnetic properties. In general, it is difficult to get reliable data on the long-term performance of permanent magnets because of the limitations of the testing methods. This problem is discussed in Section 3.4.

3.1 Helmholtz coil measurement

Helmholtz coil consists of two identical coils that are separated from each other by a distance that equals the radius of the coils. They form an area of homogeneous field between them. This can be reversed to use the coils as a flux sensing devise instead of a flux generating one [95]. By measuring the current induced to the coils when a magnet is brought to the center of the system, a magnetic flux generated by the magnet can be determined. The current is usually detected by a fluxmeter, which integrates the signals from the coils. Helmholtz coil used in this study is presented in Fig. 14.

There are two possible ways of performing the measurements. First, after zeroing the integrator the sample is brought to the center of the coils from a long distance, or the other way around by placing the magnet in the center of the coils and then zeroing the integrator and moving the magnet away from the coils far enough so that it is no longer affecting the reading. The second practice is to turn the sample around inside the coils. If the integrator is zeroed before inserting the magnet, the result will be an average of the two readings without signs. If the integrator is zeroed after inserting the magnet, the result will be half of the reading.

In this research the proportional changes in flux densities of the samples were studied and so the samples were brought to the Helmholtz coil always from the same distance.

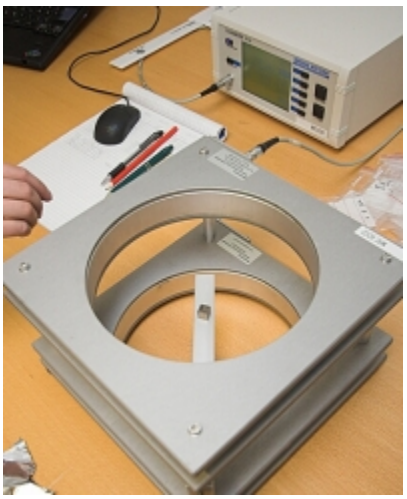

Figure 14. A Helmholtz coil and fluxmeter used in this study.

The flux density of a magnet can be calculated by dividing the measured total flux by the measured volume of the magnet.

3.2 The demagnetization curve measurement

Demagnetization curves are obtained by measuring the changes in magnetic flux inside the magnet while the external reverse magnetic field is increased continuously. Samples are attached to an iron yoke that provides a closed magnetic circuit. The change in the flux density in the magnet is measured by pick-up coils attached around the sample and the

signal is integrated by a fluxmeter. Fig. 15 shows a commercial hysteresis-graph (Permagraph) used in most of the *BH* curve measurements of this work.

There is a limitation in this method, since the iron poles saturate at about 2 T. High coercive magnets cannot therefore be measured by a hysteresis-graph at room temperature.

Heating of the sample is done by heating the poles of the Permagraph. Conduction of the heat from the poles to the sample has to be taken into account during the measurement, and a few seconds waiting times are needed before starting the measurement.

Figure 15. Permagraph C 300 from Magnet Physik used in the BH curve measurements.

There is also a more advanced method for *BH* curve measurement utilizing a pulsed magnetic field. It is developed by Metis Instruments & Equipment N.V., and it is called HyMPulse. This method allows to measure *BH* curves also from magnets with irregular shape, since the measurements are performed in open circuit. As the maximum magnetic field density produced by the coils of the pulse equipment is not limited to the saturation magnetization of iron poles, as in the traditional hysteresis-graphs, the full hysteresis loops of NdFeB magnets can be measured.

Independent of the measurement method, the obtained *BH* curves give a good approximation of the behavior of the material in an external magnetic field. Temperature dependences of the magnetic properties are obtained by measuring the *BH* curves at different temperatures.

3.3 Magnetic field scanning

The homogeneity of the magnetization inside the magnet can be studied by scanning the surface of the magnet with a Hall probe. The Hall sensor detects the axial component of the magnetic flux density in the vicinity of the surface. In the homogeneity study, the Hall probe is fixed to measure the flux density component perpendicular to the sample surface at a very short distance from the surface. The resulting flux density profile depends on the sample shape and the homogeneity of the magnetization. Results of identically shaped samples can be compared if the scans are performed along the same line section.

The scanning system is presented in Fig. 16. It includes a step motor (Lego NXT) moving the sample under the fixed Hall probe in 0.3 mm steps. The signal from the Hall sensor is read by a gaussmeter. The system is operated by LabView.

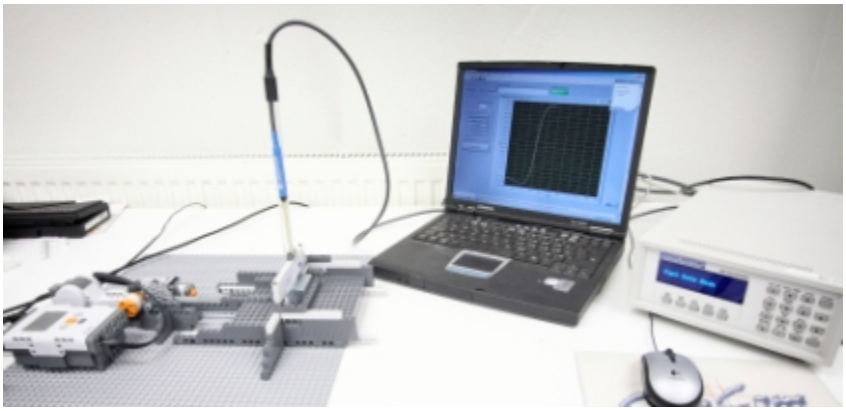

Figure 16. Magnetic field scanning system with Lakeshore MNA-1904-VH Hall sensor and Model 450 gaussmeter.

3.4 Long-term stabilization determination

Long-term changes in the magnetic properties of sintered NdFeB magnets in static conditions are fairly difficult to measure. In the magnetic viscosity studies from the 1980's and 1990's, the measurements were mostly performed with hysteresis-graphs. Measurement of the demagnetization curve was interrupted at a chosen field, and the subsequent change in the magnetic field density of the sample was detected as a function of time. The integrator analyzing the signal of the pick-up coil can give accurate results only within a limited period of time. The creep in the measurement electronics due to the

induced electric currents distorts the readings in the long run. Also the influence of the change in the field conditions prior to the magnetic viscosity measurement on the results is not known.

Another way of performing long-term stability measurements is the Helmholtz-coil measurements that are applied before and after the sample is exposed to an elevated temperature. The thermal exposure can be performed in open-circuit or closed-circuit conditions. Open-circuit measurements are mostly used, since it is difficult to accomplish long-lasting static closed-circuit conditions. The demagnetizing field in open-circuit measurements is only the self-field of the magnet. Magnet Technology Centre has developed a device for closed-circuit tests. Open-circuit measurements are presented in Section 3.4.1 and closed-circuit measurements in Section 3.4.2.

3.4.1 Open-circuit measurements

In open-circuit tests the magnets are exposed to an elevated temperature freely without any ferromagnetic material close to it. The demagnetizing field is formed purely by the self-field of the magnet. The procedure is as follows:

Immediately after magnetization, the magnetic flux produced by the sample is measured with a Helmholtz coil. The sample is placed into an oven with an aluminum foil wrapped around it as a corrosion protection. The sample is taken out of the oven at logarithmic time intervals, cooled down to room temperature, and measured again with a Helmholtz coil. The relative loss is calculated as:

$$Loss = -\frac{\Phi_{initial} - \Phi_{after}}{\Phi_{initial}} - \left(T_{initial} - T_{after}\right) \cdot 0{,}0013 \frac{1}{^{\circ}C} \qquad (7)$$

where $\Phi_{initial}$ is the flux measured after magnetization and Φ_{after} the flux measured after the thermal exposure. $T_{initial}$ is the temperature during the initial flux measurement and T_{after} the temperature during the measurement after the exposure. The latter term is the temperature correction, which aims at compensating the variations in the measurement temperature. The magnetic flux density of NdFeB magnets depends strongly on the temperature, typically B_r varies between 20°C and 100°C about 0,13 %/°C. Room temperature is not usually stable in the laboratory and it can easily vary between 20°C and 24°C. The variation in measurement temperature can cause a ±0,5 % variation to the result if the correction is not done.

After each measurement the exposure is continued. The exposure is defined to start when the oven with samples inside has reached the exposure temperature and to stop when the samples are taken out of the oven. All the prior exposure periods are summed to get the total exposure time. Results are presented as the total flux or polarization loss as a function of time for each sample type and each exposure temperature.

The problem in the open-circuit measurement is that the self-field is dependent on the shape of the magnet and is not homogenously distributed inside the magnet. This limits the applicability of the results to equally shaped magnets only. Also during the partial demagnetization of the samples, the local self-field conditions can vary significantly.

3.4.2 Closed-circuit measurements

To overcome the problems in open-circuit measurements, Magnet Technology Centre has designed a system, which can be used to expose the magnets to elevated temperatures at constant and homogenous field conditions. The system consists of an iron yoke, a bias magnet, and coils to adjust the field conditions. The system is presented in Fig. 17. The upper pole of the system moves and it can be screwed tightly to the sample. The yoke is manufactured from lamellar electric steel, welded together from the outer edges. The lamellas are tightened together with aluminum plates on both sides of the system. In the middle of the yoke, there is a bias magnet made from NdFeB with high coercivity, producing a bias field of about 400 kA/m in the air gap.

There are two coils wound on the yoke to produce an adjustable field. These coils are connected in series with a precision resistor. The current is fed by a bipolar power source, Kepco 20-20M. The magnetic field strength in the air gap is measured by a transversal Hall sensor, which is fixed to the pole with silicone. The sensor was calibrated against a calibration coil. Temperature of the yoke is measured by a PT100 resistance thermometer fixed to the pole.

The yoke is placed in an oven to get the desired elevated temperature exposure. At the same time, the field is adjusted to the desired level by feeding current to the coils. The exposure time is considered to start when the field has reached the set level. After the exposure, the coils are disconnected from the power source and the yoke is taken out of the oven to cool down. The sample is detached from the yoke, when it has cooled down close to room temperature. When the sample has reached room temperature, the magnetic state is measured with a Helmholtz coil. The exposure is continued by placing the yoke in the oven to heat up, and the sample is attached to the yoke again after it has reached the target temperature.

Figure 17. The iron yoke for testing materials in homogenous magnetic field conditions.

4. Experimental Procedure

This Chapter describes the samples and the procedures used in this work. The thermal stability of different sintered NdFeB magnet samples was studied first in different conditions. The studies were then focused on certain materials and certain conditions to understand the long-term stability phenomenon in more detail. As the knowledge increased, also the limitations of the measurement procedure became apparent. To be able to distinguish the field-induced effects caused by the shape of the sample and the thermal relaxation of the material, a method for closed-circuit measurements was developed. Closed-circuit measurements are very time-consuming and only the first results obtained are included in this thesis.

4.1 Samples

The samples were commercial sintered NdFeB magnets produced mainly by Neorem Magnets Oy. For a reference, one set of samples was from an unspecified Chinese magnet producer. Samples were cut from bigger blocks picked up from normal production lots. The materials contained different amounts of dysprosium and they had different magnetic properties. The higher the dysprosium content, the higher is the coercivity of the material and the higher the coercivity, the higher is the maximum operating temperature of the material. Room temperature coercivities and Dy contents of the test materials are listed in Table 1. The last column in Table 1 lists the publications, in which the materials are presented. In the brackets, there is the label of the material used in the publication. The labels listed in the last column are used as material labels in this thesis. In unpublished research results, material labels UP (1) and UP (2) are used. Table 1 lists also the permeance coefficients calculated according to Eqn. (4) for the samples produced from each material.

The production processes for each material were optimized by the magnet producer. The magnetic properties of the materials were optimized for different types of applications. One material included also recycled material, which means higher total oxygen content of the product. This resulted in a more rounded *JH* curve than for the other materials. One material was produced from a strip cast material, which resulted in a squarer *JH* curve.

4.2 Determination of the magnetic properties

The magnetic properties of the materials were determined using a Magnet Physik Permagraph C-300, and in the case of material V, a HyMPulse magnetic property tester at

Metis Instruments & Equipment N.V. Fig. 18 shows an example of the *BH* and *JH* curves measured at different temperatures for two different materials.

Table 1. Materials tested in this study.

H_{ci} at room temperature [kA/m]	Dy-content [%]	Permeance coefficients of the samples	Special	Publication (material no.)
1240	1	0.33 1.1 3.3		I (1), II, III (1)
1540	4	0.33 1.1 3.3		III (2, A), V (A)
1600	4	0.33 1.1 3.3	Contained recycled material	I (2), III (B)
1900	7,5	0.33 1.1 3.3		I (3), III (3)
>3000	11,5	0.33 1.1 3.3		I (4), III (4)
1670	NA	0.5 0.66 0.78 0.93 1.15 1.3	Chinese 38SH	IV
1680	4	1.0 1.2 1.4		V (B), UP (2)
1700	3	1.0 1.2 1.4	Produced from strip cast material	UP (1)

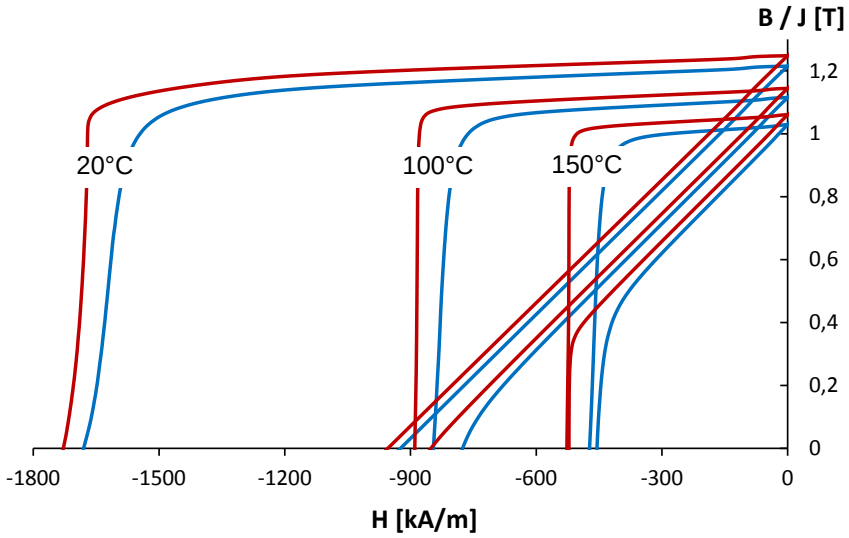

Figure 18. *JH* and *BH* curves measured at room temperature, 100°C and 150°C for materials UP (1) (red) and UP (2) (blue).

4.3 Thermal exposures

At the beginning, the thermal exposures were applied to all samples at room temperature, 60°C, 80°C, 120°C, and 150°C. In further studies, the exposures were focused on the temperature ranges, where the time-dependent losses were expected to start. The first tests were continued until 10 000 hours of exposure to get reliable loss trends.

The oxidation protection was performed by wrapping the samples in an aluminum foil. The possibility of oxidation or any diffusion induced processes was checked by remagnetization of the samples after the long-term thermal exposure. The magnetic flux density of the samples reached the original level after the remagnetization even when the samples were previously exposed to elevated temperatures for more than 10 000 hours and had suffered significant flux losses. This proves that the flux losses detected were purely resulted from demagnetization due to thermal relaxation.

The interaction between samples was prevented by placing the magnets far apart (> 65 mm) in the sample holders made from aluminum. To minimize the heating-up and cooling-down times, the samples were placed in aluminum holders that were already in the oven at the set-up temperature, and when the samples were taken out of the oven, they were placed in aluminum holders that were at room temperature.

4.4 Squareness of *JH* curves

Squareness factors *(SF)* of the *JH* curves of materials UP (1 and 2) measured at 100°C were determined according to Eqn. (6). Fig. 19 shows the principle of the *SF* determination. The parameters determined from Fig. 19 are summarized in Table 2.

Table 2. Properties of the materials UP (1 and 2) at 100°C

Material	**Coercivity H_{ci} [kA/m]**	**Remanence B_r [T]**	**H_k [kA/m]**	**Squareness factor *SF***
1	889	1.14	875	0.98
2	845	1.12	758	0.90

The *JH* curves measured at room temperature (see Fig. 18) were not suitable for *SF* determination, since the saturation of the hysteresis-graph poles distorted the curves in the vicinity of the coercive field.

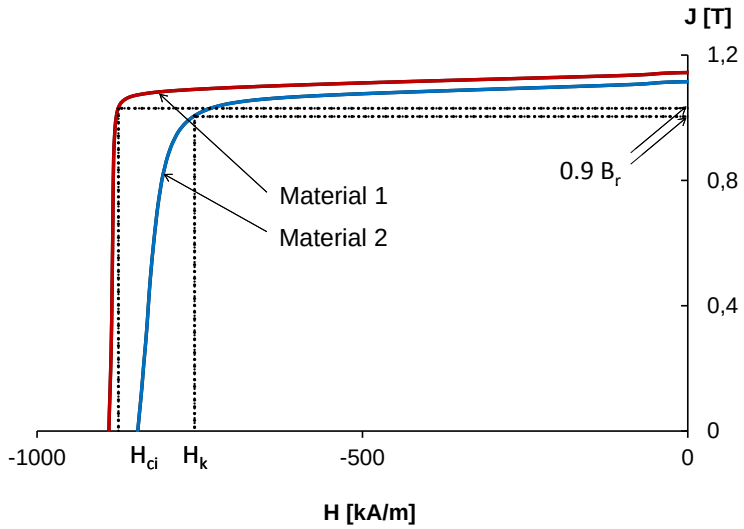

Figure 19. *JH* curves measured at 100°C for materials UP (1 and 2) with elucidation of the parameters needed for the squareness factor determination.

4.5 Stabilization heat treatment

The stabilization heat treatment was first tested with material I (2) samples, but the accuracy of the measurements was not good enough to draw any clear conclusions. The stabilization tests were then repeated for materials V (A and B).

Temperatures of the used stabilization heat treatments were 10°C higher than the subsequent exposure temperature. The duration of the treatments was one hour. For material I (2), the stabilization heat treatment temperature was 90°C and for materials V (A and B) 130°C. The further exposures were performed at 90°C and 120°C respectively. In the latter case the exposure was continued almost 10 000 hours.

4.6 Study of the demagnetization process

The interpretation of the results requires understanding of the demagnetization process occurring in the samples. Local changes in the magnetization were studied by magnetic field scanning and computer simulations. These scanning measurements were performed on material V (B), and these samples were also modeled by FEM using Vector Fields Opera software. The measured *BH* curves were used in the FE models to describe the magnetic behavior of the samples.

4.7 Closed-circuit exposures

The closed-circuit exposures were performed for material V (B) samples (= UP (2)), since there was enough open-circuit results to be compared with. All closed-circuit experiments were performed at 120°C, and the field conditions were varied from 400 kA/m (equals to P_c = 1) to 540 kA/m (P_c = 0.5).

5. Results and discussion

The flux or polarization losses mainly presented in this Chapter are averages of three to six identically tested samples. In the case of material IV, the results are only for single samples. Also the results of closed-circuit tests are for single samples only. When showing the results as average losses of multiple samples, the possible sample specific anomalous behaviour of individual samples does not disturb the results too much.

5.1 Open-circuit exposure tests

At room temperature no losses were detected in any of the samples during the 10 000 hour test period. Fig. 20 shows the measured losses for material I (1) at room temperature, 60°C, 80°C and 120°C. The measured losses follow well the logarithmic decay law introduced in Equation (1). The logarithmic trend curves for the losses are extended to reach 250 000 hours, which corresponds to the 30-year life-time expected for the application. The measured losses show similar trends as reported in [64, 96].

There is a small time-dependent demagnetization phenomenon detected with the smallest samples at 60°C. At 80°C, this time-dependent loss trend is more apparent with notable initial demagnetization. At 120°C, the time-dependent demagnetization can be observed also in the largest samples.

The loss trends seem to be fairly similar regardless of the varying parameter, i.e., temperature, permeance coefficient, or coercivity of the material (Figs. 20-22). At certain conditions the losses are minimal and the trend line is horizontal. When the conditions exceed some critical limits, time-dependent demagnetization starts to occur. As the conditions get more severe, also the initial loss detected after one hour starts to increase.

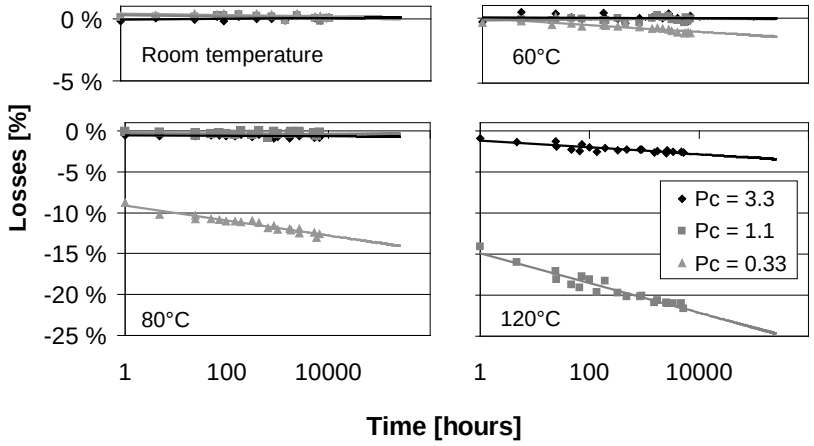

Figure 20. Flux losses as a function of time at room temperature, 60°C, 80°C and 120°C for material I (1) with a room temperature coercivity of 1240 kA/m. *(Publication I, © 2009 IEEE)*

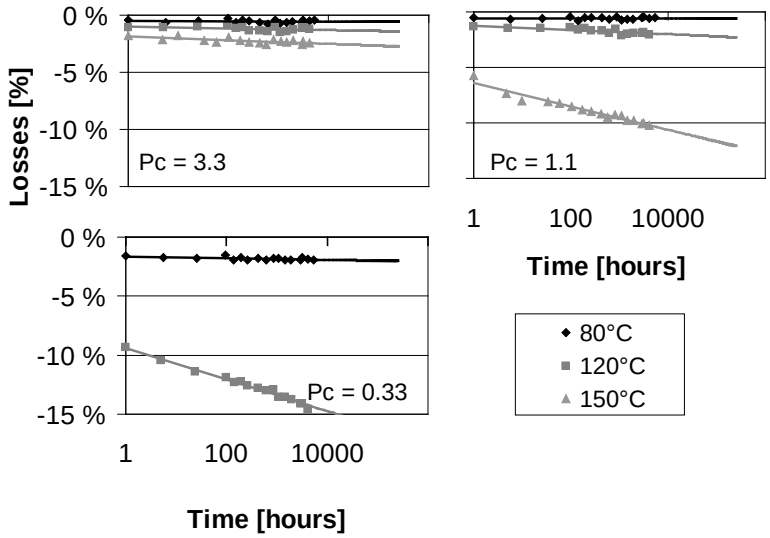

Figure 21. Flux losses as a function of time for material I (2) with a room temperature coercivity of 1600 kA/m in samples with P_c = 3.3, 1.1 and 0.33. *(Publication I, © 2009 IEEE)*

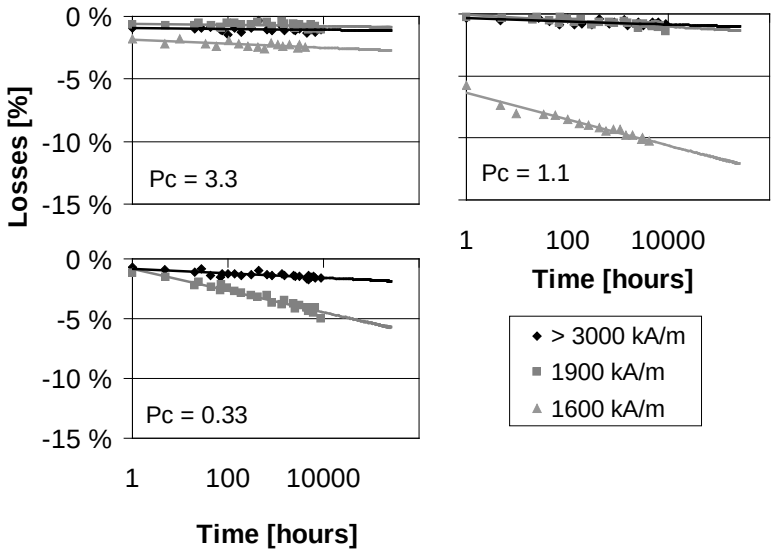

Figure 22. Flux losses at 150°C as a function of time for materials I (2, 3 and 4) in samples with P_c = 3.3, 1.1 and 0.33. *(Publication I, © 2009 IEEE)*

5.1.1 Effect of temperature

Material I (1) was further tested at 90°C, 100°C and 110°C to get more detailed information about the effect of temperature on the time-dependent losses. In Fig. 23, loss trends at five different exposure temperatures are presented. Fig. 24 shows the development of the initial loss and the magnetic viscosity coefficient *S* according to Equation (1) as a function of temperature. The Figure reveals that the time-dependent losses start at a lower temperature than the immediately occurring losses. Coefficient *S* grows fast as the temperature rises but seems to saturate to a certain level at higher temperatures.

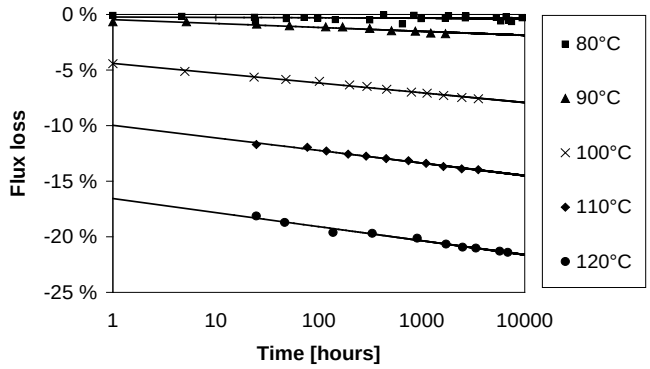

Figure 23. Flux losses as a function of time at different temperatures. Material II, P_c of the samples is 1.1. *(Publication II, © 2010 IEEE)*

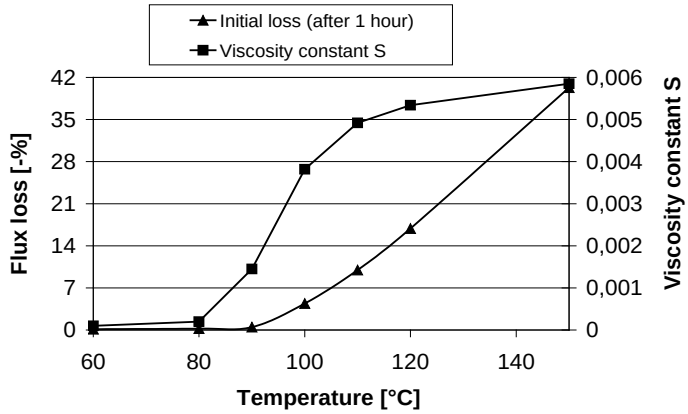

Figure 24. Comparison of the changes in the immediate loss and the viscosity coefficient *S* as a function of temperature. *(Publication II, © 2010 IEEE)*

The estimated losses after different exposure times can be calculated from the trend curves shown in Fig. 23. In Fig. 25, the estimated losses after 30 years, after 1 hour, after 1 second, and after 10 milliseconds are presented as a function of temperature. At 100°C there are losses of about 5 % after 1 hour exposure, and after 30 years these losses can be estimated to be almost 10 %. If the same trend is expected to continue also to the time scale of seconds or even milliseconds, one can notice that after 10 ms the losses would be negligible.

The magnetic properties of permanent magnet materials are measured typically by a hysteresis-graph, in which the reverse field is increased and the measurements are

performed at about 10 ms time intervals. This suggests that even though there is no demagnetization detected at certain conditions in the *BH* curve measurement, there might occur significant time-dependent demagnetization in the magnet in the long run. If the expected losses at a certain temperature are calculated only according to the measured *BH* curves as in [97], it includes an assumption that the duration of the fault condition of the application is limited to a millisecond range. The calculations are not valid for longer exposures.

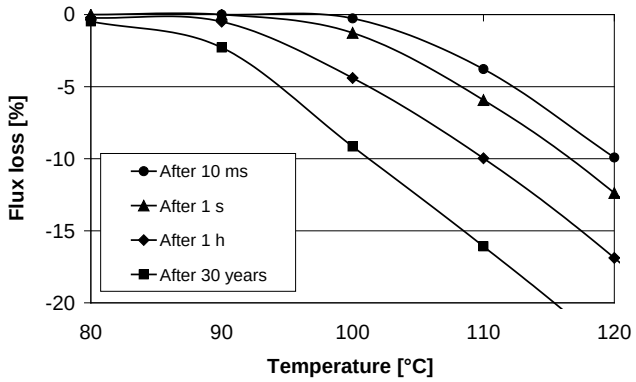

Figure 25. Estimated flux losses as a function of temperature in material II magnets with a room temperature coercivity of 1240 kA/m and permeance coefficient of 1.1. *(Publication II, © 2010 IEEE)*

5.1.2 Effect of the coercivity of the material

The previous Section describes the behavior of one material with one sample shape at different temperatures. To find out whether this type of behavior is typical for other NdFeB materials as well, similar exposure tests were performed for three materials having different coercivities. The trend curves of the detected losses are presented in Fig. 26. For each material there is a maximum temperature at which the total loss even after 30 years is expected to be negligible. This temperature is here denoted by T_0. The T_0 temperatures for the tested materials are listed in Table 3.

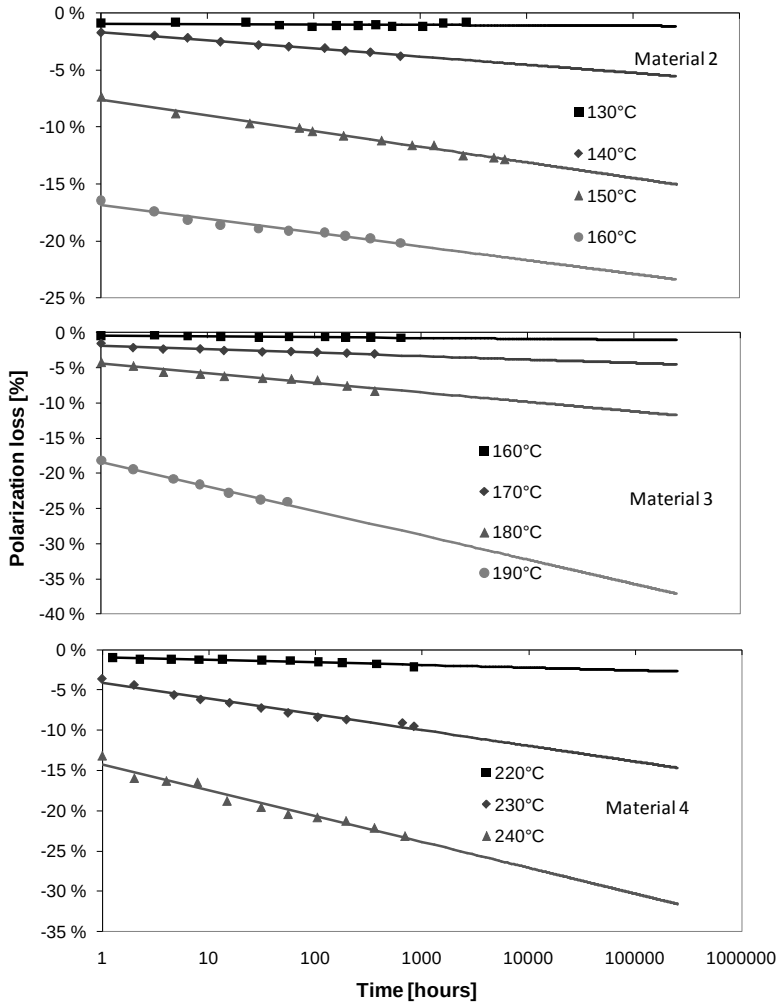

Figure 26. Polarization losses measured as a function of time in magnets with a permeance coefficient of 1.1 produced from materials III (2, 3, and 4). *(Publication III, © 2010 IEEE)*

In Fig. 27, the estimated losses after 1 hour and after 30 years of exposure are presented for each material as a function of temperature at T_0 and above. In the low coercivity material, moderate losses occur at a quite large temperature range, unlike in the high coercivity material, where the losses are massive when the temperature exceeds the critical T_0. This is visible also in the values presented in Tables 3 and 4. The magnetic viscosity coefficients (in Table 3) as well as the estimated losses after 1 hour and 30 years (in Table 4) increase faster with temperature for the high coercivity materials. This is consistent with the argument presented in Section 2.1.4 that the time-dependent behavior is more pronounced in higher coercivity materials.

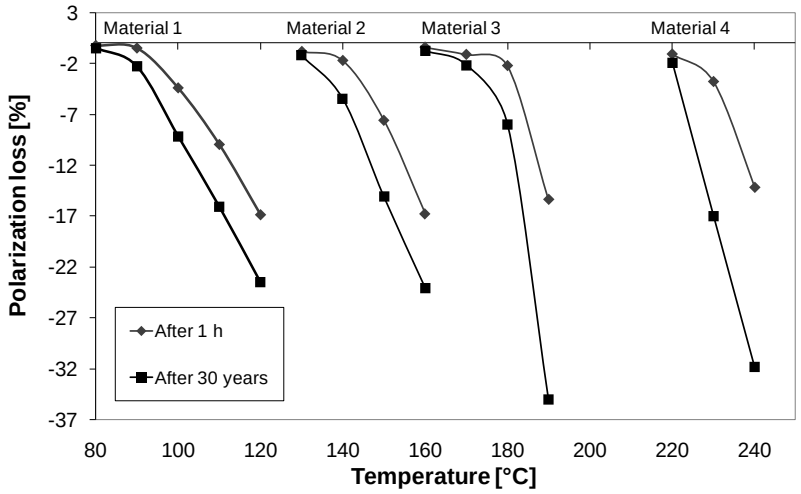

Figure 27. Estimated polarization losses as a function of temperature in magnets produced from materials III (1, 2, 3 and 4) with a P_c of 1.1. *(Publication III, © 2010 IEEE)*

Table 3. Viscosity coefficients of the samples from materials III (1, 2, 3 and 4) at different temperatures. P_c of the samples is 1.1. *(Publication III, © 2010 IEEE)*

Material	Coercivity at room temperature [kA/m]	T_0 [°C]	Viscosity coefficient S at temperature T [10^{-3}]				
			$T = T_0$	$T = T_0$ + 10°C	$T = T_0$ + 20°C	$T = T_0$ + 30°C	$T = T_0$ + 40°C
1	1240	80	0.2	1.5	3.8	4.9	5.3
2	1540	130	0.3	3.0	6.1	5.9	
3	1900	160	0.3	0.8	4.6	15.8	
4	>3000	220	0.7	10.6	14.2		

Table 4. Estimated losses of the samples from materials III (1, 2, 3 and 4) at different temperatures. P_c of the samples is 1.1. *(Publication III, © 2010 IEEE)*

Material	T_0 [°C]	Estimated polarization loss after 1 h at temperature T [%]					Estimated polarization loss after 30 years at temperature T [%]				
		$T = T_0$	$T = T_0$ + 10°C	$T = T_0$ + 20°C	$T = T_0$ + 30°C	$T = T_0$ + 40°C	$T = T_0$	$T = T_0$ + 10°C	$T = T_0$ + 20°C	$T = T_0$ + 30°C	$T = T_0$ + 40°C
1	80	-0.2	-0.5	-4.4	-10	-17	-0.5	-2.3	-9.2	-16	-24
2	130	-0.8	-1.7	-7.6	-17		-1.2	-5.4	-15	-24	
3	160	-0.4	-1.1	-2.2	-15		-0.8	-2.2	-8.0	-35	
4	220	-1.1	-3.8	-14			-1.9	-17	-32		

The trend lines in Fig. 26 were extrapolated also to the time-scale of seconds, but as the coercivity of the material increased, the extrapolated loss after one second at T_0 + 10°C turned to the positive side of the y-axis. For material III (4), the extrapolated value for the loss after one second suggested a 5 % gain of magnetization, which is physically impossible. This suggests that the trends are not continuous to the time-scale of seconds.

5.1.3 Effect of permeance coefficient

The samples used in the tests described in the two previous Sections were identical in shape. Their permeance coefficient, calculated according to the dimensions of the samples, was 1.1. To study the effect of the sample shape on the time-dependent demagnetization, different sized samples were used. Fig. 28 shows the loss trends for six different sample sizes. In Fig. 29 the estimated losses after different exposure times according to the trends are presented as a function of the permeance coefficient, showing that when the permeance coefficient decreases, the total loss increases. However, it is mainly the initial loss that increases while the further time-dependent loss stays more or less constant. The interpretation of these results is difficult since the permeance coefficient calculated according to the dimensions of the magnet is not necessarily a relevant way of expressing the demagnetization conditions inside the sample. This problem is discussed in Section 5.2 in more detail.

There exists again one extrapolated point, which is located on the positive side of the loss axis in Fig. 29. It is, however, physically impossible that the samples could increase their magnetization during the exposures. This suggests once again that the loss trends are not continuous down to the time-scale of seconds.

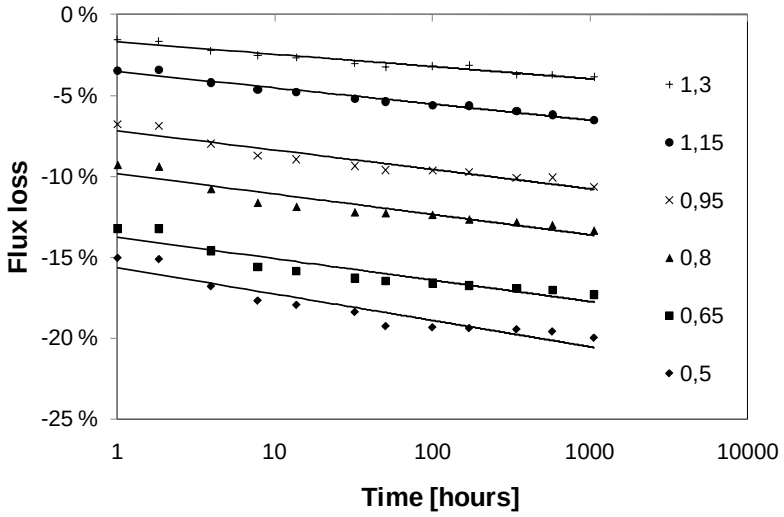

Figure 28. Flux losses as a function of time in material IV samples with different P_cs at 140°C. Losses will occur even in samples with P_c = 1.3. *(Publication IV)*

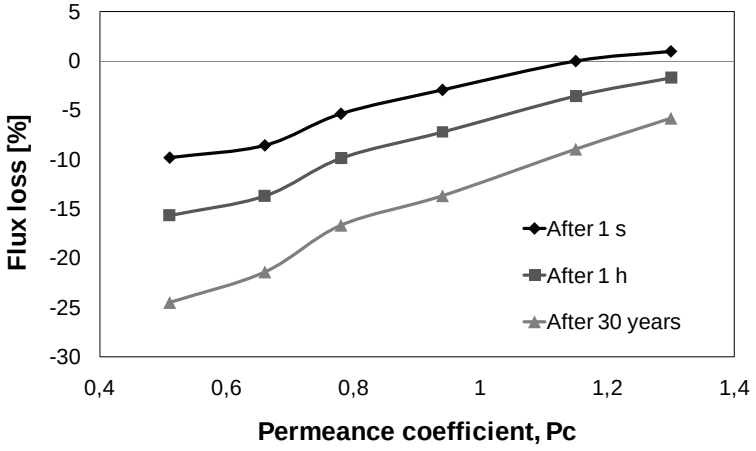

Figure 29. Estimated flux loss as a function of the permeance coefficient of the magnet after 1 second, after 1 hour, and after 30 years of exposure to the temperature of 140°C. Flux loss values are calculated according to the trend lines presented in Fig. 28. *(Publication IV)*

5.1.4 Accuracy of the estimations

In the first study, the exposures and loss measurements were continued until 10 000 hours. The experience showed that it is unnecessary to test the samples that long. As the measurements were carried out at fixed time intervals (like in Fig. 26 for materials 3 and 4), not more than 10 measurement points were needed to give a relatively accurate estimate for the loss after 30 years. In Fig. 30 this estimate is presented as a function of measurement points for material III (3) at three different temperatures. According to this Figure, it seems that after six measurement points, the estimate is not changing much anymore with increasing number of points. This suggests that a 100-hour exposure with at least six measurements would be enough to estimate the loss after 30 years.

The higher the temperature the more sensitive the losses are for small variations in the exposure temperature. This can be seen in the curve for the measurements conducted at 180°C (Fig. 30), which is not clearly saturating even after 10 measurement points. Anyway, the relative change in the loss estimate after seven measurement points can be considered small in the point of view of the application design.

The measurement points presented in Fig. 26 are average losses of six identically tested samples. By using an average value, small variations in the results of individual samples are eliminated. In the case of results based on the measurements with a single sample only, these variations are more visible, as seen in Fig. 28. In this case more measurement points are needed to get an appropriate accuracy for the estimates.

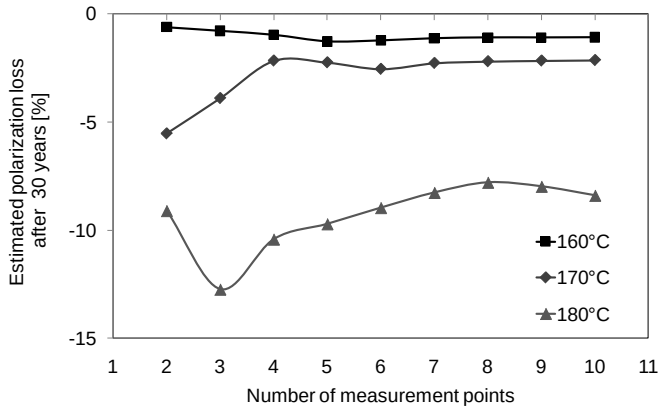

Figure 30. Estimated polarization loss after 30 years as the number of measurement points increases. Magnets made of material III (3). *(Publication III, © 2010 IEEE)*

5.1.5 Effect of *JH* loop squareness

In the previous Sections only the coercivity was considered to define the material and its demagnetization behavior. Since the shape of the demagnetization curve is also an important parameter, the effect of the *JH* loop squareness on the time-dependent demagnetization was studied. Figs. 31 and 32 present the losses as a function of time for two different materials. The *JH* and *BH* curves of these materials are presented in Fig. 18. and the squareness factors for the *JH* curves in Table 2. The plotted measurement points in Figs. 31 and 32 are the average losses of five tested samples. Error bars representing the variation of the results between samples are also included.

There are four different loss trend curves in Fig. 31, and two of these are overlapping. These horizontal trend lines indicate no time-dependent losses at all. Instead, in Fig. 32, there are loss trends at six different temperatures and all of them have a slope that differs from the horizontal. The variation of the results of similar samples is very small when the detected losses are small, but as the average losses are increasing also the deviation of the single results are increasing. The samples from the material with a rounder *JH* curve UP (2) show more homogeneous loss results than the material with squarer *JH* curve UP (1).

Fig. 33 presents the estimated losses after 1 hour and after 30 years as a function of temperature for both materials. The material with a squarer *JH* curve UP (1) shows almost zero losses until the temperature exceeds the critical value, in this case 140°C, and above that there occur both initial and time-dependent losses. The material with a rounder *JH* curve UP (2) shows small losses, both immediate and time-dependent, over a large temperature range.

The observed difference in the demagnetization behavior of these two materials results from the differences in the homogeneity of the materials. Material UP (1) was originally cast by the strip casting technique, which provides more homogeneous raw material for the magnet production. This includes a good dispersion of rare earth-rich phases in the strip cast alloys, which leads to an optimal distribution of the liquid phase during sintering [50]. The optimal distribution of the grain boundary phase prevents the interaction between the grains. Together with a narrow grain size distribution, the coercivities of individual grains are expected to be close to each other and the demagnetization occurs at similar conditions throughout the magnet. The traditional book mold raw material is not as homogeneous as the strip cast material, and therefore there might exist grains with lower coercivity and interaction between the grains. Low coercivity grains reverse their magnetization at lower temperatures, and the magnetic interaction between the grains increases the demagnetization risk of neighboring grains as well.

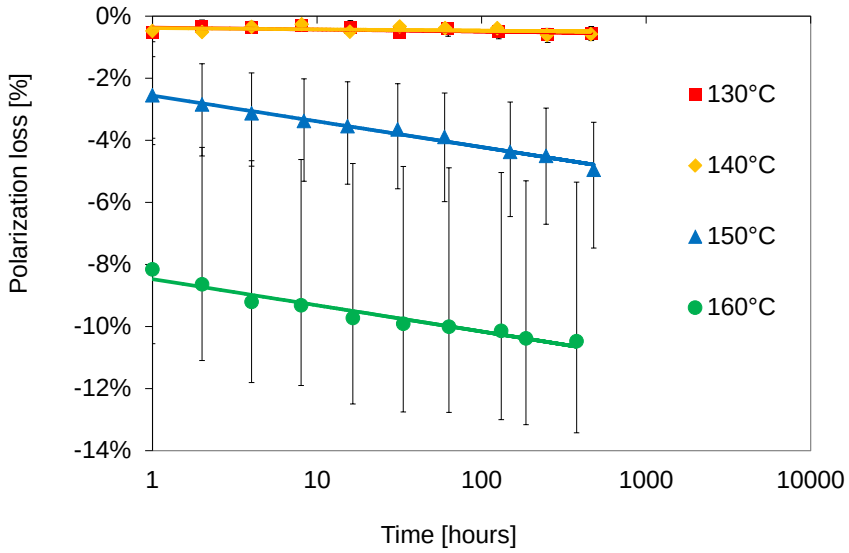

Figure 31. Polarization losses as a function of time at different temperatures in material UP (1) magnets.

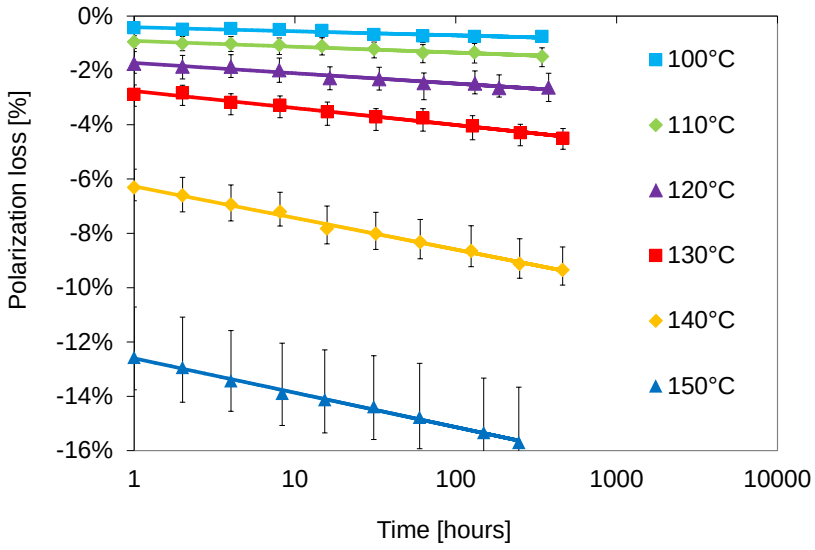

Figure 32. Polarization losses as a function of time at different temperatures in material UP (2) magnets.

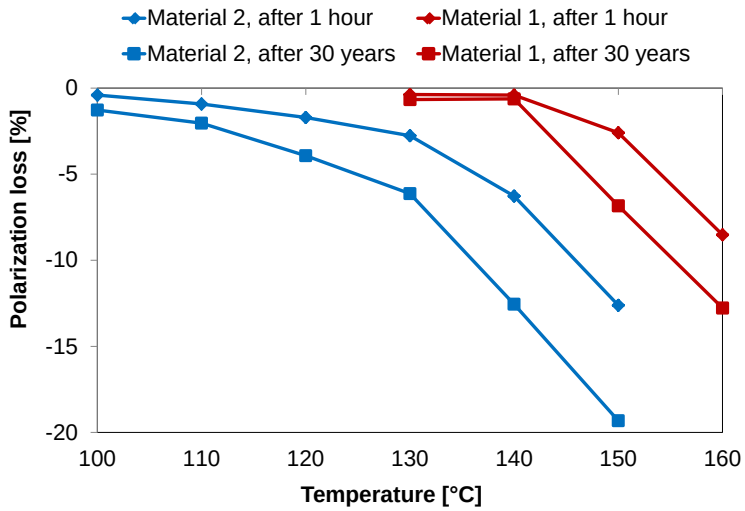

Figure 33. Estimated polarization losses after 1 hour and after 30 years as a function of exposure temperature. Curves on the left refer to material UP (2) and curves on the right to material UP (1).

The differences in the *JH* curve squareness could explain also the differences in the behaviors of the materials presented in Fig. 27. High coercivity materials typically show squarer *JH* curves than low coercivity materials. This leads to clearer critical temperatures for high coercivity materials.

From the point of view of the application design, it would be much easier to use a material with a squarer *JH* curve. With this type of material, the time-dependent demagnetization can be ignored as long as the operating temperature is below a certain critical temperature, which is typical for the material. This type of critical temperature is impossible to determine for a material with a rounder *JH* curve.

5.1.6 Stabilization heat treatment

All the previous results were obtained by raising the temperature of the samples from room temperature to the exposure temperature and then kept at constant conditions. A stabilization heat treatment before the static exposure changes the time-dependent demagnetization behavior of the magnet. In Fig. 34, the loss trends for the stabilized and non-stabilized samples are compared together for two different materials. Material V (A) shows a square *JH* curve (*SF* = 0.97), while material V (B) shows rounder *JH* curve (*SF* = 0.89) at 120°C and 130°C. These curves are presented in Fig. 35.

The stabilization heat treatment did not have an effect on the loss trends of material V (A) samples. Losses at 120°C are small anyway, and no changes in the slope of the trend curve were detected after the stabilization. Material V (B) samples showed a clear time-dependent loss trend at 120°C. The stabilization treatment at 130°C caused an initial loss of about 3 % in the samples. After the treatment the magnetization of the samples was stable until the trend line crossed the trend line of the non-stabilized samples. A clear stabilizing effect was detected, but it was limited to a certain period of time only.

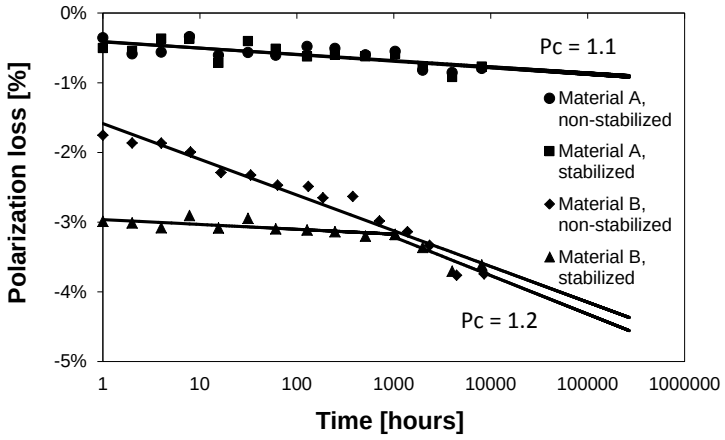

Figure 34. Polarization losses as a function of time for stabilized and non-stabilized magnets produced from materials V (A and B). The dimensions of the samples were 10 x 10 x 4.6 mm in material A samples and 10 x 10 x 4.9 mm in material B samples. *(Publication V)*

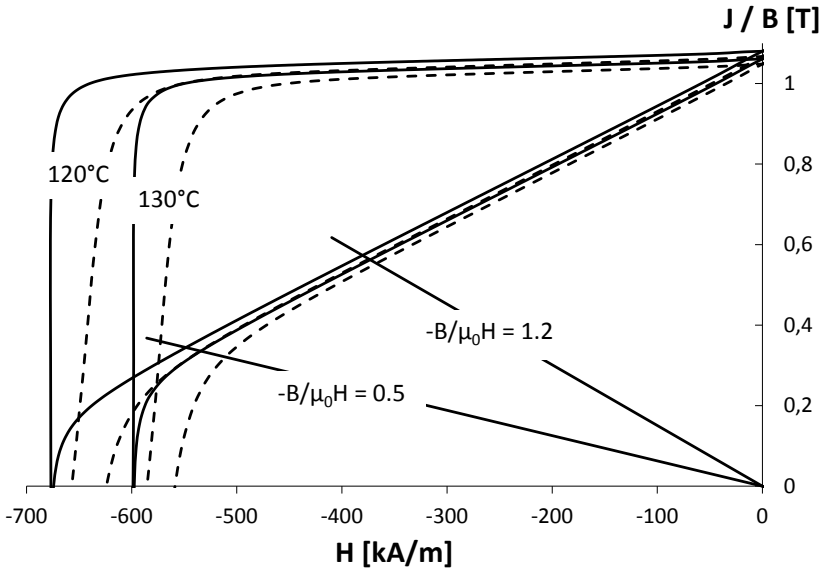

Figure 35. *BH* and *JH* curves at 120°C and 130°C for material V (A) (solid line) and for material V (B) (dashed line). Load lines 0.5 and 1.2 are also included. *(Publication V)*

To be sure that the stabilizing effect is independent of the size of the magnet, the results of different sized samples were compared. Figure 36 summarizes the results of three different sized samples from material V (B), showing that the trends are similar for all the samples.

Changes in the loss trends of the stabilized samples after a certain period of time raise a lot of questions. What happens at the point where the trend turns downwards? To understand this, it was necessary to study the demagnetization process of the magnet more in detail. This type of behavior indicates that even though the detected polarization of the magnet is stable, there probably occur changes in the magnetic microstructure during the long-term exposure. The demagnetization processes might proceed differently depending on the rate of the process. This is likely to be caused by the geometry of the sample and not to be any material characteristic.

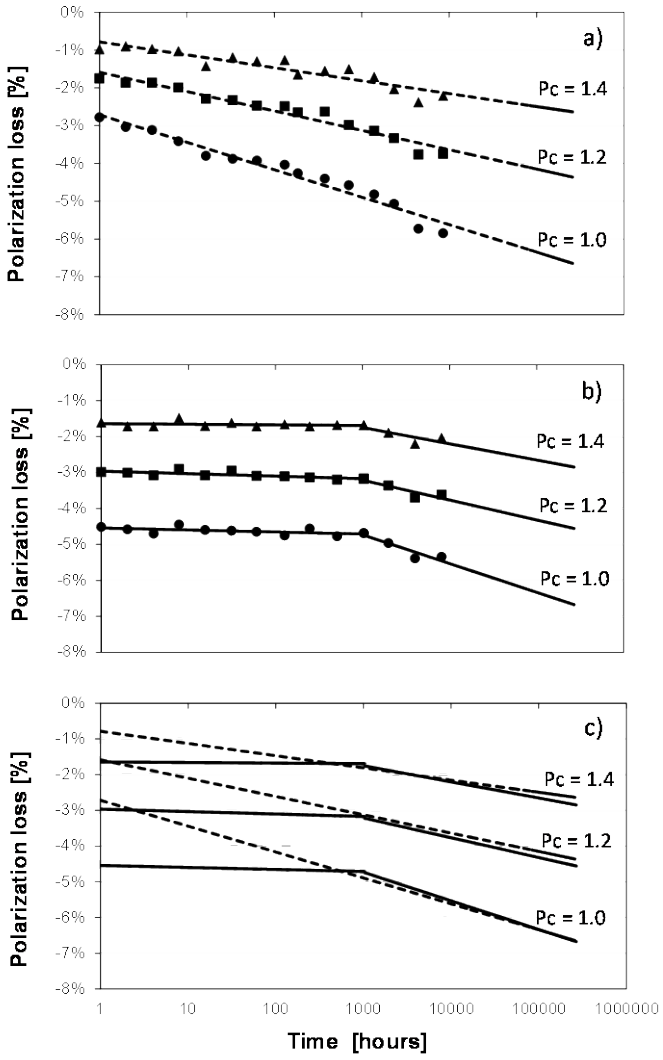

Figure 36. Polarization losses in non-stabilized (a) and stabilized samples (b), and the combined trends of these two (c). Material was V (B) and the exposure temperature 120°C. The stabilization heat treatment before the exposure was 1 hour at 130°C. *(Publication V)*

5.2 Analysis of the demagnetization process

In open-circuit conditions, the demagnetizing field is due to the self-field of the magnet. Each magnetized grain forms a unit magnetic field around itself. The total demagnetizing field is the sum of these unit fields. Each grain experiences a little bit different demagnetizing field depending on its location in the magnet. At the edges of the magnet, the self-field is lower, since there are neighboring grains only on one side. In the middle of the magnet there are also parallel field components from the grains above and below, affecting the total demagnetizing field. At the top and bottom surfaces, the parallel fields are at the minimum.

An FE-model of the sample reveals this inhomogeneity in the demagnetizing field inside the magnet. Fig. 37 shows FE-models of material V (B) samples used in the stabilization tests. The parameter shown is $-B_z/\mu_0 H_z$, which can be considered as P_c. The model includes one eighth of the sample. The upper right corner is the actual corner of the magnet, while the lower left corner is the center of the magnet. The model depicts a sample produced from material V (B) at room temperature.

The average P_c values of the samples according to Eqn. (4) are 1.0, 1.2 and 1.4. The FE models suggest that the minimum P_c is less than 0.5 in the two smallest samples, and only slightly above that in the biggest sample. The low P_c area is concentrated in the center of the top (and bottom) surface. There are contour lines for different P_c values illustrating the low P_c volumes in the samples. The lower the average P_c of the sample, the larger are the low P_c volumes.

The models indicate that the demagnetization of the samples initiate at the center of the top and bottom surfaces. To verify this, magnetic flux density line scans were performed on a sample with average P_c = 1.0 before and after a one-hour heat treatment at 130°C. The detected magnetic flux densities, perpendicular to the sample surface, are presented in Fig. 38. Before the heat treatment, the magnetic flux density was found to be fairly constant above the sample surface. This indicates that the magnetization inside the sample is homogeniously distributed. However, after the heat treatment the magnetic flux density has dropped most at the center of the surface. This is consistent with the results of the FE-model.

As the variation of P_c inside the samples is as large as shown in Fig. 37, it certainly has an effect on the long-term demagnetization process. As the demagnetization proceeds, changes in the P_c distribution inevitably appear. This raises the question, what is the influence of this phenomenon to the loss results of open-circuit measurements. The previously introduced results are sample specific, not material specific, since there are two

phenomena mixed affecting the results: the changes in the self-field distribution and the material specific magnetic viscosity.

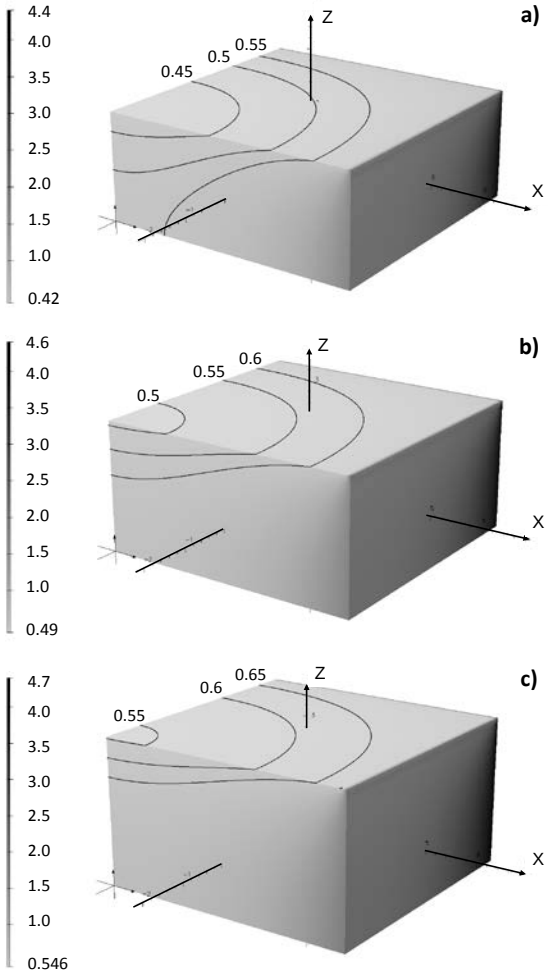

Figure 37. Variations of $-B_z/\mu_0 H_z$ inside the studied samples at room temperature before the exposure to elevated temperature. The heights of the modeled magnets are 4.1 mm (a), 4.9 mm (b) and 5.6 mm (c), corresponding to an average P_c of 1.0 (a), 1.2 (b) and 1.4 (c). The models include one eighth of the samples. The upper right corners are the actual corners of the magnets, and the lower left corners are the centres of the magnets. The models depict the samples produced from material V (B). *(Publication V)*

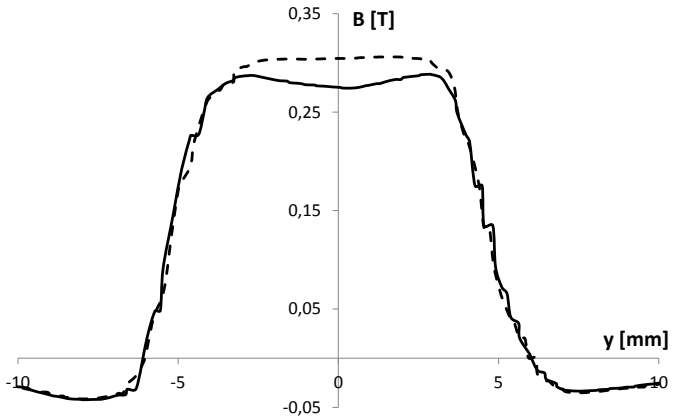

Figure 38. Scanned magnetic flux density on the surface perpendicular to the magnetization direction (Z) of a sample from material V (B) (P_c = 1.0): before the stabilization heat treatment (dashed line) and after the treatment (solid line). Scanning was performed about 0.2 mm from the magnet surface. *(Publication V)*

One possible explanation for the behavior of the stabilized samples shown in Fig. 36 is presented in Fig. 39. Initially the surface region of the magnet is fully magnetized and the magnetic moments of all domains are parallel (Fig. 39a). During the one-hour stabilization heat treatment, the magnetization reversal concentrates on the area where P_c is the lowest (Fig. 39b), i.e., on the center of the surface area. However, this new magnetic microstructure changes radically the field conditions in the area. This is likely to induce further changes in the domain structure.

Since the energy profiles of individual grains change during the magnetization reversal of neighboring grains, the probability of the reversal of these grains also changes. This is likely to cause a chain reaction type of effect.

There might thus occur changes in the magnetic microstructure also during the “stable” period after the stabilization heat treatment, even though the macroscopic polarization of the magnet remains constant. The magnetic microstructure might look like in Fig. 39c after 1 000 hours of exposure. It is likely that the magnetic microstructures are similar in the non-stabilized and stabilized samples after the 1 000-hour exposure independent of the thermal history. However, the evolution towards that structure is likely to be different.

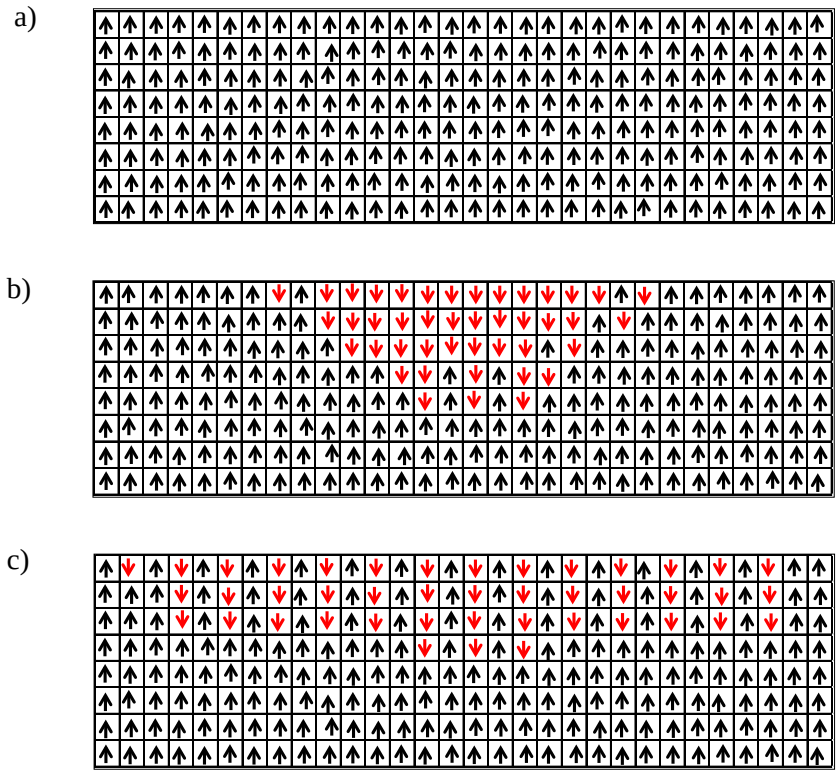

Figure 39. Schematic presentation of the suggested magnetic microstructure at the surface of the magnet used in the stabilization heat treatment studies (a) after magnetization, (b) after one hour stabilization heat treatment, and (c) after subsequent long-term exposure at a lower temperature.

5.3 Closed-circuit exposure tests

To eliminate the effects of the self-field distribution on the long-term loss behavior, closed-circuit exposure tests are required. Fig. 40 presents losses measured in samples exposed to different demagnetizing fields at 120°C. The sample material is the same as in the stabilization tests (V (B), UP (2)). Fig. 41 shows the measured *BH* curve for the material at 120°C. The studied field range was from 400 kA/m to 540 kA/m. This range is marked in Fig. 41. The maximum field strength used, 540 kA/m (P_c = 0.48), represents approximately the minimum P_c occurring in the open-circuit samples. The minimum field, 400 kA/m (P_c = 1.0), represents approximately the average P_c of the smallest samples in the open-circuit exposures.

The loss trends in Fig. 40 differ clearly from the loss trends in Figs. 32 and 28. In open-circuit exposures the initial loss after one hour dominates and subsequent time-dependent losses are fairly similar, independent of the magnitude of the exposure. In closed-circuit exposures the initial loss is not changing much, but the slope of the time-dependent demagnetization increases as the exposure field increases. This suggests that the saturation of the viscosity constant at higher temperatures found in the open-circuit tests (Fig. 24) might not occur in the closed-circuit tests. This saturation effect seems to result from the changes in the self-field distribution.

In Fig. 42, the estimated losses after one hour and after 30 years are presented as a function of P_c for open-circuit and closed-circuit tests of the same material. The P_c of the open-circuit tests are considered as the average P_c determined according to the dimensions of the samples. The open-circuit test gives a bigger loss-estimate than the closed-circuit test at P_c = 1. This means that the conclusions of the material's long-term loss behavior drawn based on the open-circuit measurements are actually conservative.

The closed-circuit exposure tests are very time-consuming, and only one sample at a time can be measured. The results presented in Figs. 40 and 42 are for individual samples only, and the variation of the properties between samples causes also variation in the loss results.

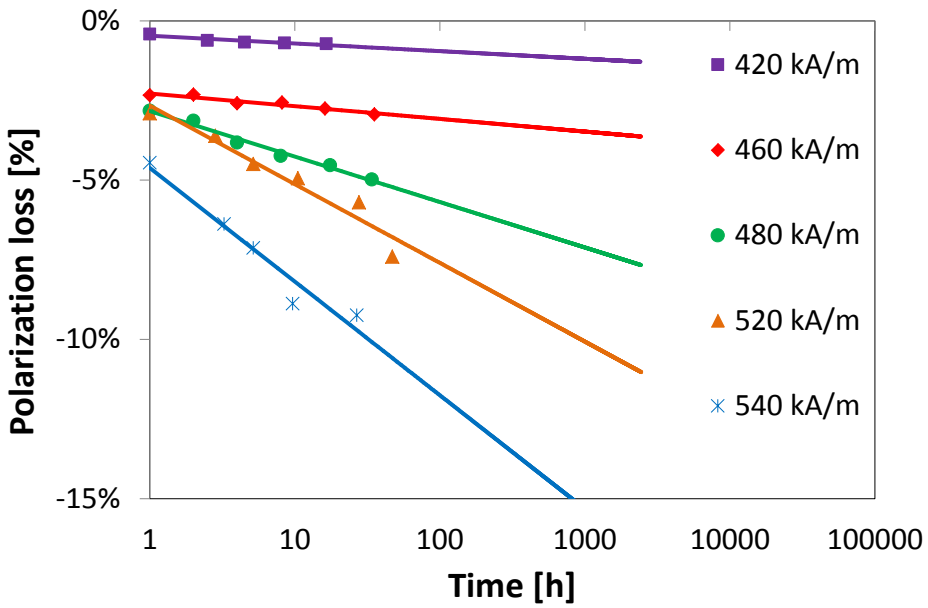

Figure 40. Polarization losses as a function of time at different demagnetizing fields in material UP (2) magnets at 120°C.

Fig. 42 reveals also that dramatic time-dependent demagnetization occurs at magnetic field strengths that can be considered to lie on the linear part of the demagnetization curve. The theoretical assumption in Section 2.1.1 that the effect of thermal relaxation is small and can be neglected in the design is clearly wrong. The results of this study suggest that time-dependent demagnetization has to be taken into consideration when designing the applications.

From a single measured *BH* curve, such as in Fig. 41, it is impossible to determine the operating point at which the time-dependent demagnetization starts to be significant. The *BH* curve is only a depiction of an average response of the magnet material to the changing field at a certain rate of change. Typically, hysteresis-graphs detect the response of the material in the time-scale of milliseconds. The deviation from the response detected in the time-scale of years is much bigger in the fields close to the knee-point of the *BH* curve.

The deviation between the measured *BH* curve and the long-term response of the material is expected to increase with increasing temperature. This is due to the fact that the magnetic viscosity is enhanced in high coercive materials at higher temperatures, as demonstrated in Section 5.1.2. At higher temperatures also the accuracy of the temperature determination is worse. In the permagraph that was used in the *BH* curve measurements in this work, the heat is introduced to the sample through the pole pieces. The temperature measurements are also performed from the pole piece. The sample between the pole pieces is not necessarily uniformly at the same temperature. Application designers should therefore take a critical attitude towards the *BH* curves measured at elevated temperatures.

Loss results from the closed-circuit tests can be considered to reveal the material specific, long-term loss behavior. Time-dependent demagnetization in open-circuit exposures can be considered as a sum of the behaviors of different permeance coefficients. The distribution of the permeance coefficients inside a magnet, however, changes during the demagnetization process. After the initial demagnetization, the distribution is not the same as at room temperature anymore. The algorithms of FEM software seem to be unable to solve the demagnetization occurring in open-circuit magnets. Two different softwares gave different types of results and neither of those matched with the detected magnetic field densities scanned above the partially demagnetized samples. This is no wonder if the magnetic microstructures differ depending on the rate of demagnetization process.

The problem would need micromagnetic simulation, which takes also the microstructure of the material into consideration. Micromagnetic simulation studies of NdFeB-based materials have so far concentrated on modeling the demagnetization process of a system

consisting of only a few grains [98]. Bulk magnets would be very challenging tasks for this type of simulations.

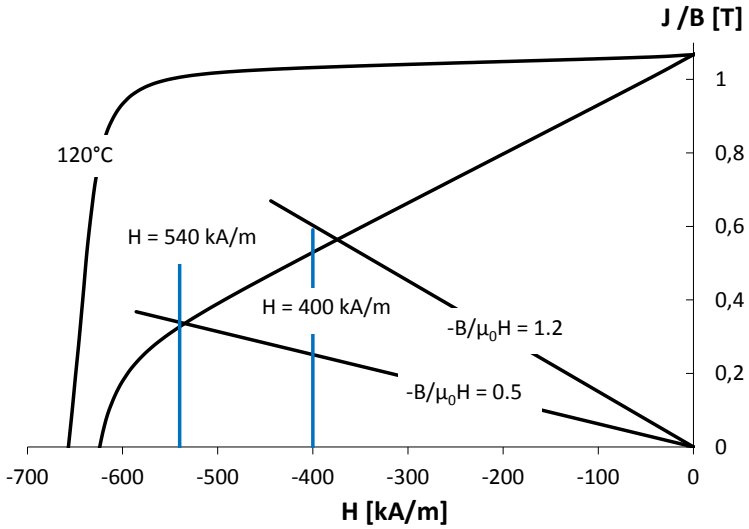

Figure 41. *JH* and *BH* curves measured for material UP (2) at 120°C. Load lines of 0.5 and 1.2 are also shown.

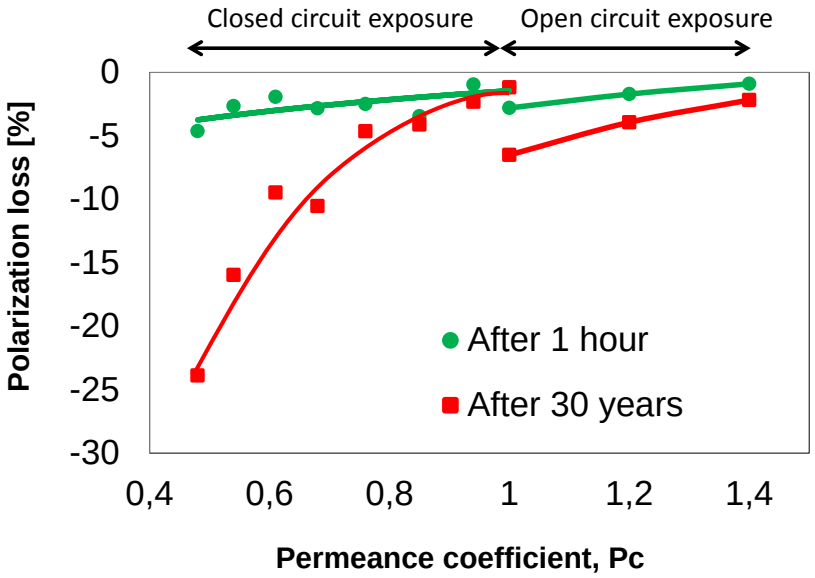

Figure 42. Estimated polarization losses as a function of P_c in closed and open-circuit exposures of material UP (2) magnets at 120°C.

6. Summary and conclusions

In this work, the time-dependent demagnetization of different types of commercial sintered NdFeB magnets was studied. The polarization losses occurring over time in permanent magnets are typically assumed to be small and the effect of magnetic viscosity is neglected in the application design. The main aim of this study was to increase the general understanding of the phenomenon. For the application designers it is important to know if there exist certain limiting conditions under which no polarization losses over time are expected.

NdFeB samples were exposed to elevated temperatures in some cases for more than 10 000 hours, which is almost 1.5 years. The detected polarization losses as a function of time were found to follow well the logarithmic decay law. The total loss after 30 years can be estimated from the trend curve, provided that the possibility of corrosion is prevented.

The observations suggest that it is possible to determine a critical temperature for each material and each P_c under which the estimated loss after 30 years is less than 1 %. This temperature is naturally higher for high coercive magnets and for high P_c samples. This temperature is higher also for materials showing a squarer *JH* curve than for materials with a rounder curve. The determination of this type of a critical temperature is not possible with only one measured loss level after a certain period of exposure. More measurements during the exposure and the determination of the demagnetization trend as a function of time are needed.

Above the critical temperature, the time-dependent demagnetization starts to occur. The time-dependent demagnetization seems to be more severe in high coercivity materials and to start at lower temperatures than the measured *BH* curves of the material indicate. This is an important thing to notice when selecting the material for an application. In the long-term stability tests, the loss results can be divided into the initial loss after one-hour of exposure and the subsequent time-dependent loss. In many cases the time-dependent loss starts to increase before there appears any initial loss. This makes the phenomenon significant in the application point of view.

In open-circuit exposures the estimated loss after 30 years was found to be approximately twice the loss detected after one hour of exposure. This is not valid, however, just above the critical temperature. About 10°C above the critical temperature the estimated loss after 30 years was found to be four or five times the loss after one hour. The total loss after 30 years cannot thus be estimated from the loss measurement after one hour exposure only. Again, more measurement points are needed.

The open-circuit exposures give sample specific results, which means that the results are affected by both the magnet material properties and the shape of the magnet. The permeance coefficient P_c is often considered to describe the demagnetization conditions originated from the shape of the magnet, since it is calculated according to the dimensions of the magnet. An FE-model of a rectangular sample showed that the P_c is actually varying considerably inside the magnet. The P_c calculated according to the dimensions of the magnet gives only an average value for all the P_cs in the magnet. There are large volumes in the centre of the top and bottom surfaces of the magnet that are well below the average P_c. It is possible that the minimum P_c of the magnet is below the knee-point of the *BH* curve even though the average P_c is well above it. This leads to the initial partial demagnetization of the sample at temperatures lower than the *BH* curves with an average P_c analysis indicate. Partial demagnetization also changes the local field conditions resulting in changes in the P_c distribution. So, in open-circuit tests the field conditions are not stable during the exposure. This leads to the fact that open circuit test results cannot be easily connected to the *BH* curves of the material.

Since the application designers are mainly interested in the material properties, a test method from which the effect of the geometry of the sample is eliminated was developed. It requires loss measurements in the closed-circuit condition. In close-circuit exposures, the external field is stable and homogenously distributed over the volume of the sample. The results of the closed-circuit exposure tests differ significantly from the open-circuit test results. In the open-circuit tests, the initial loss after one hour seems to dominate, but in the closed-circuit tests the time-dependent part of the loss dominates.

In the open-circuit tests, the change in the demagnetizing field condition during the exposure is likely to lead to a damping effect. The time-dependent demagnetization becomes slower than what the material specific magnetic viscosity would cause in the static field conditions. In the closed-circuit condition the external field was static and homogenously distributed, but the reversal of magnetization of individual grains causes also changes to the local field conditions and might increase the demagnetizing field locally. This will accelerate the demagnetization process. The condition in the motor and generator applications is closer to the situation in the closed-circuit tests, where the external field remains constant. To optimize the magnet material selection in motor and generator applications, closed-circuit loss measurements of the materials at operating conditions are needed.

Comparison of the open-circuit and closed-circuit results indicates that the critical temperature determinations according to the loss measurements in open-circuit conditions give conservative results. This assumption is based on the measurements with only one material and only a few P_c values. More measurements would be needed to verify the

universal validity of this conclusion. The schedule of this work did not allow a more comprehensive study on the subject.

Further studies are also needed to understand the demagnetization process locally and the effect of partial demagnetization on the demagnetizing field distribution. This would also help to understand the effect of stabilization treatments. The stabilization heat treatment was found to stabilize the magnets for a certain period of time. Even though the total polarization of the magnet is stable during the test period, there most likely occur local changes in the magnetic microstructure. Identification of these changes with magnetic field scanning or Kerr microscopy would also be important in the future. The results of this work suggest only that the stabilization heat treatment should be performed in magnetic conditions similar to those the magnets will face in the application. The stabilization treatment performed in the open-circuit condition does not stabilize the magnets uniformly.

A study on the magnetic microstructure of the magnets during the thermally activated time-dependent demagnetization process would be interesting in the future. Thermal demagnetization above the Curie temperature is known to result in a multi-domain structure, but the field induced demagnetization maintains the single domain structure in sintered NdFeB magnets. Fang et al. [99] have shown that a partial multi-domain structure is achieved in the heat treatment below the Curie temperature. This leaves the question whether the long-term demagnetization due to thermal relaxation can result in a multi-domain structure.

Based on the results obtained in this work, the time-dependent demagnetization of commercial sintered NdFeB magnets can be tested in the open-circuit conditions, even though the obtained loss data is not material specific. The open-circuit measurements are easier and faster to perform than the closed-circuit measurements. The received critical temperature data from the open-circuit tests, when P_c of the sample is calculated according to the dimensions of the magnet, can be used as guiding information even though it is conservative. Further studies are, however, recommended to optimize the magnet material selection with long-term stability considerations.

7. References

1. Haring, T., et al. “Direct drive-opening a new era in many applications” *Pulp and Paper Industry Technical Conference*, 2003, Charleston, USA

2. Rodewald, W. and Fernengel, W., “Properties of sintered Nd-Fe-TM-B magnets” *IEEE Transactions on Magnetics*, 1988, **24**(2): p. 1638-1640

3. Trout, S.R. “Material selection of permanent magnets, considering thermal properties correctly” *Electrical Insulation Conference and Electrical Manufacturing & Coil Winding Conference*, 2001, Cincinnati, USA.

4. Clegg, A.G., et al., “The temperature stability of NdFeB and NdFeBCo magnets” *IEEE Transactions on Magnetics*, 1990, **26**(5): p. 1942-1944

5. Mildrum, H.F. and Umana, G.M., “Elevated temperature behavior of sintered Nd-Fe-B type magnets” *IEEE Transactions on Magnetics*, 1988, **24**(2): p. 1623-1625

6. Davies, B.E., Mottram, R.S. and Harris, I.R., “Recent developments in the sintering of NdFeB” *Materials Chemistry and Physics*, 2001, **67**(1-3): p. 272-281

7. Bertotti, G., “Hysteresis in magnetism, for physicists, materials scientists and engineers”, ed. I. Mayergoyz, 1998, Academic Press

8. Kou, X.C., et al., “Coercivity mechanism of sintered $Pr_{17}Fe_{75}B_8$ and $Pr_{17}Fe_{53}B_{30}$ permanent magnets” *Physical Review B*, 1994, **50**(6): p. 3849-3860

9. Givord, D., Rossignol, M. and Barthem, V.M.T.S., “The physics of coercivity” *Journal of Magnetism and Magnetic Materials*, 2003, **258-259**: p. 1-5

10. Durst, K.-D. and Kronmuller, H., “The Coercive Field of Sintered and Melt-spun NdFeB Magnets” *Journal of Magnetism and Magnetic Materials*, 1987, **68**: p. 63-75

11. Stoner, E.C. and Wohlfarth, E.P., “A Mechanism of Magnetic Hysteresis in Heterogeneous Alloys” *Philosophical Transactions of the Royal Society of London. Series A, Mathematical and Physical Sciences*, 1948, **240**(826): p. 599-642

12. Woodcock, T.G., et al., “Understanding the microstructure and coercivity of high performance NdFeB-based magnets” *Scripta Materialia*, 2012, **67**(6): p. 536-541

13. Hrkac, G., et al., “The role of local anisotropy profiles at grain boundaries on the coercivity of $Nd_2Fe_{14}B$ magnets” *Applied Physics Letters*, 2010, **97**(23): p. 232511

14. Street, R. and Brown, S.D., “Magnetic viscosity, fluctuation fields, and activation energies (invited)” *The 6th joint magnetism and magnetic materials (MMM)-intermag conference*, 1994, Albuquerque, USA

15. Folks, L. and Street, R., “Analysis and interpretation of time dependent magnetic phenomena (invited)” *The 6th joint magnetism and magnetic materials (MMM)-intermag conference*, 1994, Albuquerque, USA

16. Skomski, R. and Coey, J.M.D., “Permanent Magnetism. Studies in Condensed Matter Physics” ed. J.M.D. Coey and D.R. Tilley, 1999, London, Institute of Physics Publishing

17. Street, R. and Woolley, J.C., “A Study of Magnetic Viscosity” *Proceedings of the Physical Society*, 1949, **62**: p. 562

18. Wohlfarth, E.P., “The coefficient of magnetic viscosity” *Journal of Physics F: Metal Physics*, 1984, **14**: p. L155

19. Givord, D., et al., “Magnetic viscosity in Nd-Fe-B sintered magnets” *Journal of Magnetism and Magnetic Materials*, 1987, **67**(3): p. L281-L285

20. Givord, D., et al., “Magnetic viscosity in different Nd-Fe-B magnets” *Journal of Applied Physics*, 1987, **61**(8): p. 3454-3456

21. Martinez, J.C. and Missell, F.P., “Magnetic viscosity and texture in NdFeB magnets” *Journal of Applied Physics*, 1988, **64**(10): p. 5726-5728

22. Ferguson, G.B., O'Grady, K., and Popplewell, J., “Magnetisation mechanisms and magnetic viscosity in NdFeB alloys” *IEEE Transactions on Magnetics*, 1989, **25**(5): p. 3449-3451

23. Liu, J., Luo, H. and Wan, J., “On the activation volumes of reversal in RE-TM-B-type sintered magnets” *Journal of Physics D: Applied Physics*, 1992, **25**(5): p. 838

24. Ferguson, G.B., et al. “The temperature relationship of the fluctuation field and coercivity in NdFeB alloys” *Journal of Applied Physics*, 1991, **69**(8): p. 5495 - 5497

25. Jahn, L., Schumann, R. and Rodewald, W., “Magnetic viscosity of modified neodymium iron boron magnets with high coercivities” *Journal of Magnetism and Magnetic Materials*, 1996, **153**(3): p. 302-310

26. Cammarano, R., McCormick, P.G. and Street, R., “The measurement of irreversible magnetization and activation volumes” *38th Annual Conference On Magnetism and Magnetic Materials*, 1994, Minneapolis, USA

27. Estrin, Y., McCormick, P.G. and Street, R., “A phenomenological model of magnetisation kinetics” *Journal of Physics: Condensed Matter*, 1989, **1**(29): p. 4845

28. Lyberatos, A. and Chantrell, R.W., “The fluctuation field of ferromagnetic materials” *Journal of Physics: Condensed Matter*, 1997, **9**(12): p. 2623

29. Tomka, G.J., et al., “Magnetic viscosity, susceptibility and fluctuation fields in sintered NdFeB” *IEEE Transactions on Magnetics*, 1990, **26**(5): p. 2655-2657

30. Croat, J.J., et al., “Pr-Fe and Nd-Fe-based materials: A new class of high-performance permanent magnets (invited)” *Journal of Applied Physics*, 1984, **55**(6): p. 2078-2082

31. Sagawa, M., et al., “New material for permanent magnets on a base of Nd and Fe (invited)” *Journal of Applied Physics*, 1984, **55**(6): p. 2083-2087

32. Brown, D., Ma, B.-M. and Chen, Z., “Developments in the processing and properties of NdFeb-type permanent magnets” *Journal of Magnetism and Magnetic Materials*, 2002, **248**(3): p. 432-440

33. Sagawa, M., et al., “Permanent magnet materials based on the rare earth-iron-boron tetragonal compounds” IEEE Transactions on Magnetics, 1984, **20**(5): p. 1584-1589

34. Gutfleisch, O., “Advanced Structural Characterisation for Magnetic Materials Development. in High Performance Magnets and their Applications. 2004. Annecy, France

35. Herbst, J.F., “$R_2Fe_{14}B$ materials: Intrinsic properties and technological aspects” *Reviews of Modern Physics*, 1991, **63**(4): p. 819

36. Matsuura, Y., “Recent development of Nd–Fe–B sintered magnets and their applications” *Journal of Magnetism and Magnetic Materials*, 2006, **303**(2): p. 344-347

37. Li, W.F., et al., “The role of Cu addition in the coercivity enhancement of sintered Nd-Fe-B permanent magnets” *Journal of Materials Research*, 2009, **20**(2): p. 413-420

38. Li, W.F., Ohkubo, T. and Hono, K., “Effect of post-sinter annealing on the coercivity and microstructure of Nd–Fe–B permanent magnets” *Acta Materialia*, 2009, **57**(5): p. 1337-1346

39. Sasaki, T.T., et al., “Correlative multi-scale characterization of a fine grained Nd–Fe–B sintered magnet” *Ultramicroscopy*, 2013, **132**: p. 222–226

40. Liu, Q., et al., “Increased coercivity in sintered Nd–Fe–B magnets with NdF_3 additions and the related grain boundary phase” *Scripta Materialia*, 2009, **61**(11): p. 1048-1051

41. Mo, W., et al., “Dependence of the crystal structure of the Nd-rich phase on oxygen content in an Nd–Fe–B sintered magnet” *Scripta Materialia*, 2008, **59**(2): p. 179-182

42. Li, W.F., et al., “The origin of coercivity decrease in fine grained Nd–Fe–B sintered magnets” *Journal of Magnetism and Magnetic Materials*, 2009, **321**(8): p. 1100-1105

43. Fidler, J. and Schrefl, T., “Overview of Nd-Fe-B magnets and coercivity (invited)” *Journal of Applied Physics*, 1996, 79(8): p. 5029

44. Zueco, E., et al., “Combined Kerr-/magnetic force microscopy on NdFeB crystals of different crystallographic orientation” *Journal of Magnetism and Magnetic Materials*, 1998, **190**(1–2): p. 42-47

45. Takezawa, M., et al., “Domain observation technique for Nd-Fe-B magnet in high magnetic field by image processing using liquid crystal modulator” *Journal of Applied Physics*, 2007, **101**(9): p. 09K106-09K106-3

46. Takezawa, M., et al., “Surface Domain Configuration of Nd-Fe-B Sintered Magnets Influenced by Underneath Magnetization” *IEEE Transactions on Magnetics*, 2009, **45**(10): p. 4439-4442

47. Takezawa, M., et al., “Magnetic Domain Observation of Nd-Fe-B Sintered Magnets at Elevated Temperatures by Using Kerr Microscope” *IEEE Transactions on Magnetics*, 2011, **47**(10): p. 3256-3258

48. Nakamura, H., et al., “Magnetic properties of extremely small Nd-Fe-B sintered magnets” *IEEE Transactions on Magnetics*, 2005. **41**(10): p. 3844-3846

49. Scott, D.W., et al., “Microstructural control of NdFeB cast ingots for achieving 50 MGOe sintered magnets” *The 40th annual conference on magnetism and magnetic materials*, 1996, Philadelphia, USA

50. Bernardi, J., et al., “Microstructural analysis of strip cast Nd-Fe-B alloys for high $(BH)_{max}$ magnets” *Journal of Applied Physics*, 1998, **83**(11): p. 6396-6398

51. Liu, W.L., et al., “Effects of Nb addition and/or casting method on the amount of precipitated Fe in NdFeB alloys” *IEEE Transactions on Magnetics*, 1992, **28**(5): p. 2154-2156

52. Yu, L.Q., et al., “On the cooling rate of strip cast ingots for sintered NdFeB magnets” *Physica B: Condensed Matter*, 2007, **393**(1-2): p. 1-5

53. Yan, G.H., et al., “The preparation of sintered NdFeB magnet with high-coercivity and high temperature-stability” *Journal of Physics: Conference Series*, 2011, **266**(1): p. 012052

54. Kaneko, Y., “Highest performance of Nd-Fe-B magnet over 55 MGOe” *IEEE Transactions on Magnetics*, 2000, **36**(5): p. 3275-3278

55. Uestuener, K., Katter, M. and Rodewald, W., “Dependence of the Mean Grain Size and Coercivity of Sintered Nd-Fe-B Magnets on the Initial Powder Particle Size” *IEEE Transactions on Magnetics*, 2006, **42**(10): p. 2897-2899

56. Sugimoto, S., “Current status and recent topics of rare-earth permanent magnets” *Journal of Physics D: Applied Physics*, 2011, **44**(6): p. 064001

57. Sepehri-Amin, H., et al., “Microstructure of fine-grained NdFeB sintered magnets with high coercivity” *Scripta Materialia*, 2011, **65**(5): p. 396-399

58. Goto, R., et al., “Microstructure evaluation for Dy-free Nd-Fe-B sintered magnets with high coercivity” *Journal of Applied Physics*, 2012, **111**(7): p. 07A739

59. Morimoto, K., et al., “Coercivity enhancement of anisotropic Dy-free NdFeB powders by conventional HDDR process” *Journal of Magnetism and Magnetic Materials*, 2012, **324**(22): p. 3723-3726

60. Sagawa, M., et al., “NdFeB sintered magnet production method and production device, and NdFeB sintered magnet produced with said production method” *Patent EP 2472535 A1*, 2012

61. Namkung, S., Kim, D.H. and Jang, T.S., “Effect of particle size distribution on the microstructure and magnetic properties of sintered NdFeB magnets” *Reviews on Advanced Materials Science*, 2011, **28**: p. 185-189

62. Komuro, M., Satsu, Y. and Suzuki, H., “Increase of Coercivity and Composition Distribution in Fluoride-Diffused NdFeB Sintered Magnets Treated by Fluoride Solutions” *IEEE Transactions on Magnetics*, 2010, **46**(11): p. 3831-3833

63. Sagawa, M., “NdFeB sintered magnet, and process for production thereof” *Patent EP 2453448 A1*, 2012

64. IEC/TR62518, “Rare earth sintered magnets - Stability of the magnetic properties at elevated temperatures” 2009

65. Li, L., et al., “The effect of compound addition Dy_2O_3 and Sn on the structure and properties of NdFeNbB magnets” *Journal of Magnetism and Magnetic Materials*, 2007, **308**(1): p. 80-84

66. Zhang, R., et al., “Effect of Nb substitution on the temperature characteristics and microstructures of rapid-quenched NdFeB alloy” *Journal of Alloys and Compounds*, 2007, **427**(1-2): p. 78-81

67. Zhang, R., et al., “Effect of Ti&C substitution on the magnetic properties and microstructures of rapidly-quenched NdFeB alloy” *Materials Characterization*, 2008, **59**(5): p. 642-646

68. Ma, B.M., et al., “Comparison of the improvement of thermal stability of NdFeB sintered magnets: Intrinsic and/or microstructural” *38th Annual Conference on Magnetism and Magnetic Materials*, 1994, Minneapolis, USA

69. Chen, Z., Yan, A. and Wang, X., “Effects of intergranular additions of oxides on the coercivity, thermal stability and microstructure of Nd-Fe-B magnets” *Journal of Magnetism and Magnetic Materials*, 1996, **162**(2-3): p. 307-313

70. Kim, A.S. and Camp, F.E., “The role of oxygen for improving magnetic properties and thermal stability of sintered (Nd,Dy)(Fe,Co)B magnets” *IEEE Transactions on Magnetics*, 1995, **31**(6): p. 3656-3658

71. Yan, A., et al., “Effect of MgO additive on coercivity, thermal stability and microstructure of Nd-Fe-B magnets” *Journal of Alloys and Compounds*, 1996, **239**(2): p. 172-174

72. Cheng, W.-H., et al., “The magnetic properties, thermal stability and microstructure of Nd-Fe-B/Ga sintered magnets prepared by blending method” *Journal of Magnetism and Magnetic Materials*, 2001, **234**(2): p. 274-278

73. Lewis, L.H., Gallagher, K. and Panchanathan, V., “The effect of Nb additions on the thermal stability of melt-spun $Nd_2Fe_{14}B$” *Journal of Applied Physics*, 1999, 85(8): p. 5926

74. Yu, L.Q., et al., “Production for high thermal stability NdFeB magnets” *Journal of Magnetism and Magnetic Materials*, 2008, **320**(8): p. 1427-1430

75. Liu, J. and Walmer, M., “Designing with High Performance Rare-Earth Permanent Magnets” *High Performance Magnets and their Applications*, 2004, Annecy, France

76. Yang, Y., et al., “Study on the performance sensitivity to ambient temperature for permanent magnet synchronous motor used in pump jack” *Sixth International Conference on Electrical Machines and Systems*, 2003, Beijing, China

77. Negrea, M. and Rosu, M., “Thermal analysis of a large permanent magnet synchronous motor for different permanent magnet rotor configurations” *Electric Machines and Drives Conference*, 2001, Cambridge, USA

78. Hwang, C.C., John, S.B. and Bor, S.S., “The analysis and design of a NdFeB permanent-magnet spindle motor for CD-ROM drive” *IEEE Transactions on Energy Conversion*, 1999, **14**(4): p. 1259-1264

79. Kato, Y., “Thermal stability of sintered and bonded rare-earth magnets” *Journal of Applied Physics*, 1999, **85**(8): p. 4868-4870

80. Bizen, T., et al., “Baking effect for NdFeB magnets against demagnetization induced by high-energy electrons” *Nuclear Instruments and Methods in Physics Research Section A: Accelerators, Spectrometers, Detectors and Associated Equipment*, 2003, **515**(3): p. 850-852

81. Mildrum, H., et al., “An investigation of the aging of thermally prestabilized sintered samarium-cobalt magnets” *IEEE Transactions on Magnetics*, 1974, **10**(3): p. 723-725

82. Liu, J.F. and Walmer, M.H., “Thermal stability and performance data for SmCo 2:17 high-temperature magnets on PPM focusing structures” *IEEE Transactions on Electron Devices*, 2005, **52**(5): p. 899-902

83. Parker, R.J., “Advances in Permanent Magnetism”, 1990, John Wiley & Sons

84. Cullity, B.D. and Graham, C.D., “Introduction to Magnetic Materials”, 2009, John Wiley & Sons

85. Kim, H.-K., et al., “Characteristic analysis of IPM type BLDC motor considering the demagnetization of PM by stator turn fault” *Energy Conversion Congress and Exposition*, 2010, Atlanta, USA

86. Kral, C., et al., “Modeling demagnetization effects in permanent magnet synchronous machines” *XIX International Conference on Electrical Machines*, 2010, Rome, Italy

87. McFarland, J.D. and Jahns, T.M., “Investigation of the rotor demagnetization characteristics of interior PM synchronous machines during fault conditions” *Energy Conversion Congress and Exposition*, 2012, Raleigh,USA

88. Guglielmi, P., et al., “Magnet minimization in IPM-PMASR motor design for wide speed range application” *Energy Conversion Congress and Exposition*, 2011, Phoenix, USA

89. Shin, H.-K., Kim, T.H. and Kim, C.-J., “A study on irreversible permanent magnet demagnetization in flux-reversal machines” *International Conference on Electrical Machines and Systems*, 2011, Beijing, China

90. Zhou, P., et al., “Temperature-Dependent Demagnetization Model of Permanent Magnets for Finite Element Analysis” *IEEE Transactions on Magnetics*, 2012, **48**(2): p. 1031-1034

91. Wang, J., Wang, W. and Atallah, K., “A Linear Permanent-Magnet Motor for Active Vehicle Suspension” *IEEE Transactions on Vehicular Technology*, 2011, **60**(1): p. 55-63

92. Branagan, D.J., et al., “Maximizing loop squareness by minimizing gradients in the microstructure” *Journal of Applied Physics*, 1999, **85**(8): p. 5923-5925

93. Perigo, E.A., et al., “Microstructure and squareness factor: A quantitative correlation in (Nd, Pr)FeB sintered magnets” *Journal of Applied Physics*, 2007, **102**(11): p. 113912-4

94. Ruoho, S., Dlala, E. and Arkkio, A., “Comparison of Demagnetization Models for Finite-Element Analysis of Permanent-Magnet Synchronous Machines” *IEEE Transactions on Magnetics*, 2007, **43**(11): p. 3964-3968

95. Trout, S.R., “Use of Helmholtz coils for magnetic measurements” *IEEE Transactions on Magnetics*, 1988, **24**(4): p. 2108-2111

96. Rodewald, W. and Katter, M., “Properties and applications of high performance magnets” *High Performance Magnets and their Applications*, 2004, Annecy, France

97. Ruoho, S., et al., “Demagnetization Testing for a Mixed-Grade Dovetail Permanent-Magnet Machine” *IEEE Transactions on Magnetics*, 2009, **45**(9): p. 3284-3289

98. Suss, D., Schrefl, T. and Fidler, J., “Micromagnetics simulation of high energy density permanent magnets” *IEEE Transactions on Magnetics*, 2000, **36**(5): p. 3282-3284

99. Fang, Y.-K., et al., “Magnetic microstructures of a high coercivity Nd–Fe–B sintered magnet in remanent and incomplete thermal demagnetization states” *Journal of Magnetism and Magnetic Materials*, 2010, **322**(22): p. 3720-3723

Publication I

Haavisto, M. and Paju M.

Temperature Stability and Flux Losses Over Time in Sintered Nd–Fe–B Permanent

Magnets, *IEEE Transactions on Magnetics*, **45** (2009) pp. 3114 – 3120

Temperature Stability and Flux Losses Over Time in Sintered Nd-Fe-B Permanent Magnets

Minna Haavisto, Martti Paju, *Member, IEEE*

Magnet Technology Centre, Prizztech Ltd., Pori, Finland

It is important to ensure that no permanent flux losses occur in permanent magnets during their use in industrial applications. Demagnetization occurring with time in a constant temperature is often assumed to be negligible, provided that the operating point of the magnet is above the knee of the BH curve. There is, however, a clear need to demonstrate these time dependent losses. In this study, losses over time were measured for four commercial sintered Nd-Fe-B magnet grades at five different temperatures (23°C - 150°C). Samples with three different permeance coefficient (Pc) values were tested for each material. The time-dependent losses measured fitted the logarithmic law of magnetic viscosity well. It was demonstrated that the total flux loss in a lifetime of 30 years can be estimated according to the temperature, coercivity of the material and the permeance coefficient of the magnet. With the proper selection of the magnet material, in accordance with the designed Pc of the application, the total flux loss in 30 years can be minimized almost to zero even at 150°C.

***Index Terms*— Permanent magnets, Losses, Neodymium compounds, Stability**

I. Introduction

The number of sintered Nd-Fe-B magnets used in industrial machine applications has increased in recent years. Driving forces towards the permanent magnet technology are the higher achievable power densities and higher efficiencies [1]. This technology requires however a fairly stable magnetic polarization in the permanent magnets through the whole lifetime of the application, typically 20 to 30 years. For this reason, it is important to control the operating environment of magnets.

In rotating machines, induced eddy currents cause a temperature rise, which could be detrimental to the commonly used Nd-Fe-B magnets. Studies of more precise eddy current calculations [2-3] and of the effects of overheating in fault conditions [4] are attempts towards a better understanding of the operation of these machines. An accurate simulation of the application is required to assist in the selection of the proper magnet material.

Demagnetization effects in Nd-Fe-B magnets occurring in temperature cycling are quite well studied [5-7] and documented [8]. In temperature cycling, magnets are at a maximum temperature only for a short time, which represents the overload condition. If the coercive force of the material decreases too much due to the temperature rise and the operating point of the magnet falls below the knee of the demagnetization curve, some permanent flux loss will appear. The term used by the machine designers for the temperature where irreversible losses start to occur is the "critical temperature of the magnet" [9-11]. Critical temperature is a characteristic of an application with a certain permeance coefficient (operating point).

Demagnetization curves measured for materials are commonly used in defining the critical temperature of a magnet system. Demagnetization curves, however, consider only the demagnetization occurring immediately. Losses over time are usually assumed to be negligible. The assumption is reasonable when the temperature rise is only temporary. However, continuous eddy currents maintain the operating temperature close to the critical temperature of the magnets, which causes a time-dependent demagnetization through the so-called magnetic viscosity effect.

There are not many published studies on the time-dependent flux losses in commercial sintered Nd-Fe-B magnets. Clegg et al. [12] and Mildrum et al. [13] have shown that temperature, permeance coefficient (Pc) and coercivity of a magnet affects its time dependent losses. However, in [12] only one temperature and two Pc values were tested for 200 hours and in [13], samples were exposed to elevated temperatures in air with a clear effect of oxidation. If proper corrosion protection is applied, the losses with time are only due to the magnetic viscosity.

Magnetic viscosity is known to be a statistical relaxation phenomenon due to thermal fluctuation in the non-equilibrium state of the material [14]. Time dependence of the magnetization (M) as a function of time (t) and magnetic field (H) is described by a logarithmic law [11]:

$$M(t,H) = M(t_0,H) - S(H)\ln\frac{t}{t_0} \quad (1)$$

Where S is a phenomenological magnetic viscosity constant and t_0 is a reference time. Wohlfarth et al. [15] have determined the magnetic viscosity constant as:

$$S = \frac{kT}{\upsilon K} f(H,T) M_S \quad (2)$$

Where kT represents the temperature dependency (k is Bolzmann constant, T is temperature), υK (υ is the activation volume, K is the anisotropy constant) depends on the material and its microstructure and $f(H,T)$ is a complicated function, which describes the precise nature of the magnetization process. Thus, magnetization losses over time in permanent

Digital Object Identifier inserted by IEEE

magnets depend on the magnetic field, temperature, magnet material and its microstructure and the magnetization history.

In this work, demagnetization losses in commercial sintered Nd-Fe-B magnets were studied. The main interest was in losses over time and the effects of temperature, coercivity and permeance coefficient on the loss behavior of a magnet. Additionally, a study was made into the effect of a stabilization heat treatment on the losses over time.

II. Method

A. Temperatures

Samples were kept at five different temperatures. The holding temperatures were room temperature (23°C), 60°C, 80°C, 120°C, and 150°C. The elevated temperatures were generated with StabiliTherm EU2 ovens with a temperature accuracy and homogeneity of ±0.5°C.

B. Material

Four different commercial Nd-Fe-B magnet materials were tested. Intrinsic coercivities at room temperature of these materials are listed in Table 1.

C. Permeance coefficients

All samples had a rectangular shape with a cross section of 10 mm x 10 mm. The heights of the samples varied according to the tested permeance coefficients Pc = 0.33, 1.1 and 3.3 (h = 1.6 mm, 4.6 mm and 10.5 mm respectively).

During the aging process, the samples were kept in aluminum sample holders, with a distance of 67 mm between the center points of individual samples. The effect of external magnetic fields on the permeance coefficient of each sample, caused by other samples, was evaluated and considered to be negligible.

D. Measurements

The samples were fully magnetized in a 3.5 T pulsed field. The reference value of the flux of each sample was measured with a Helmholtz coil immediately after the magnetization. To make the plotting of the results easier on a logarithmic time scale, t_0 in (1) was chosen to be 1 hour. So, the first loss measurement was carried out after a one-hour stay at the holding temperature. Samples were cooled down to room temperature before the measurements. Flux measurements were carried out at suitable time intervals, at the beginning once a day, and later less frequently, once a week or once a month. Totally, the measurements were carried out at least fifteen times during the 8 000-hour aging period. The number of identical samples measured at a time varied between 3 and 6.

To minimize oxidation, samples were wrapped in aluminum foil before heating. The foils were removed before the measurements were carried out. After the 8 000 hours period at 150°C, the surface area of the samples was checked by optical microscopy and no traces of significant oxidation were observed.

TABLE I
Room Temperature Coercivities of the Samples

Material	Remanent polarization [T]	Coercivity in room temperature [kA/m]
1	1.26	1240
2	1.19	1600
3	1.14	1900
4	1.02	>3000

E. Stabilization

A stabilization test was performed on a set of samples of material 2. The samples were heat treated at 90°C for 1 hour prior to placing them to the holding temperature of 80°C. The aim of the stabilization heat treatment is to demagnetize the most unstable domains in the magnet and thus reduce the following losses over time. This means that (1) is not necessarily valid anymore since the initial loss (first term on the right hand side) is achieved at a different temperature than the time dependent losses (second term).

III. Results

Average measured losses are presented as a function of time in Figs 1-4. Logarithmic trend curves are plotted in compliance with the measurement points. Trend curves are extended to over 250 000 hours, which represents a design life of 30 years.

A. Effect of Permeance Coefficient

The permeance coefficient had no effect on the losses at room temperature since no losses were detected in any of our samples during the 10 000 hours test period. Fig. 1 shows the measured losses for material 1 (see Table I) at room temperature, 60°C, 80°C and 120°C.

At 60°C the trend curve of samples with Pc = 0.33 has slightly bent downwards, but other curves are horizontal. The expected loss after 30 years for Pc = 0.33 samples is less than 2 %. At 80°C the trend curves for samples with Pc = 1.1 and Pc = 3.3 are still horizontal, but the curve for Pc = 0.33 has dropped and reaches as high as 14 % in 30 years. At 120°C all samples show a downward loss trend. Only in samples with Pc = 3.3 losses in 30 years time are less than 5 %. Losses in Pc = 1.1 are estimated to be approximately 25 % and Pc = 0.33 samples fall outside the scale.

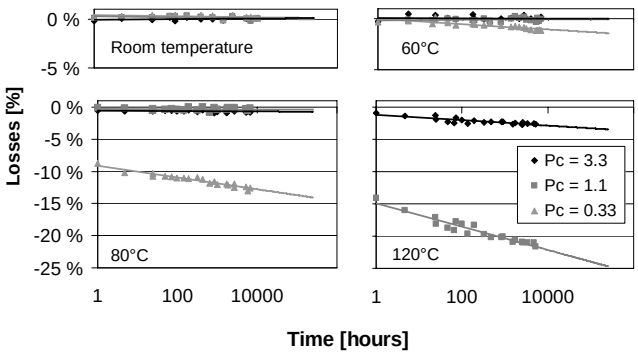

Fig. 1. Flux losses as a function of time at room temperature, 60°C, 80°C and 120°C for material 1 with room temperature coercivity of 1240 kA/m.

B. Effect of Temperature

Fig. 2 shows the magnetization losses for material 2 (see Table I) samples with three different Pc values at three different temperatures. When Pc = 3.3, time dependent losses are very small even at 150°C. No significant differences between samples in different temperatures. The total loss after 30 years is expected to be less than 3 %. When Pc = 1.1, clear losses start to occur at 150°C. However, at 120°C and 80°C, losses stay under 3 % in 30 years' time. When Pc = 0.33, clear losses occur at as low as 120°C.

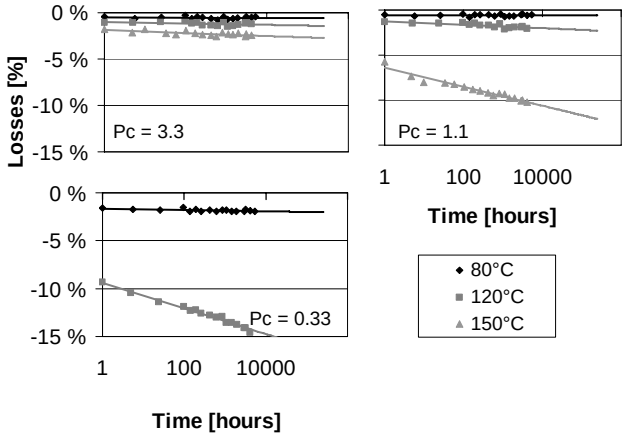

Fig. 2. Flux losses as a function of time for material 2 with room temperature coercivity of 1600 kA/m when Pc = 3.3, 1.1 and 0.33.

C. Effect of Coercivity

Fig. 3 compares the losses of different materials at 150°C. When the Pc = 3.3 all three materials are fairly stable. Losses in 30 years are less than 3 % for all these materials. When the Pc = 1.1, losses in material 2 increase to about 12 % in 30 years. The two other materials show very small losses. When the Pc = 0.33, the total loss after 30 years in material 2 drops to about 32 % and it falls outside the scale. The initial loss in the other two materials is minor. In any event, losses over time in material 3, increases the total loss to approximately 6 %.

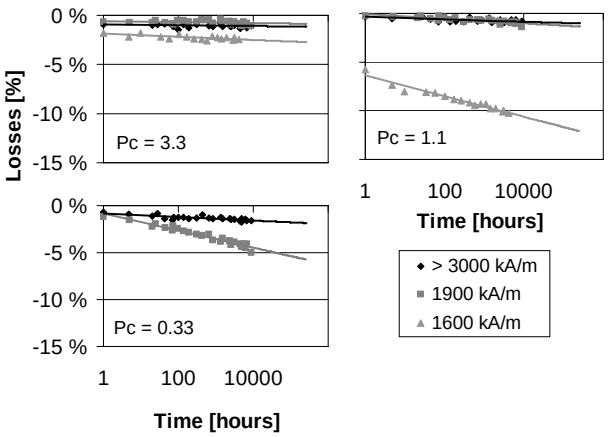

Fig. 3. Flux losses at 150°C as a function of time for materials 2-4 with different room temperature coercivities when Pc = 3.3, 1.1 and 0.33.

D. Effect of Stabilization Heat Treatment

Fig. 4 compares the loss behavior of stabilized and unstabilized samples at 80°C. The Pc of the samples was 0.33. The trend curve for losses in stabilized samples is more horizontal, but the difference between these curves is very small. Losses over 2 % for both stabilized and unstabilized samples measured after 9 000 hours of exposure indicates, however, that horizontal loss trend of stabilized samples will change in some point to the downward trend.

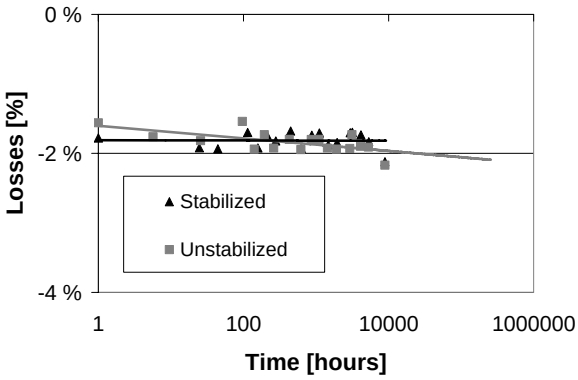

Fig. 4. Loss trends for unstabilized and stabilized samples of material 2 at 80°C when Pc = 0.33.

IV. Discussion

The obtained trend curves for flux losses show clearly the division of the irreversible losses into two categories. The intersection point of the trend curve with the loss axis represents the loss occurring immediately at a certain temperature, term $M(t_0)$ in (1). The following trend curve defines the losses over time, $S*ln(t/\ t_0)$ in (1). Both terms depend on the coercivity of the material, the permeance coefficient of the magnetic circuit and the temperature. The results also show that when an immediate loss occurs, there will also be losses over time. However, if the immediate loss is negligible, the following losses with time are not necessarily negligible: for example, in fig. 3 the losses with time in material 3 (at 150°C when Pc = 0.33) will exceed 5 % in 30 years time.

A dramatic difference in the loss behavior of different sized magnets (i.e. different Pc values) can be detected. Near the closed circuit condition (Pc = 3.3), losses stay within 3 % in material 1 (Hci = 1240 kA/m at room temperature) until 120°C and in other materials until 150°C. When the Pc is reduced to 1.1, materials with lower coercivities start to show severe losses at temperatures over 120°C. With a Pc = 0.33, losses occur at as low as 80°C.

Trout [16] has pointed out that there is a lack of clear definition of the term "maximum operating temperature" for permanent magnets at the moment. Maximum working temperature values given for different materials might be misleading, since the amount of flux loss also depends strongly on the permeance coefficient of the circuit. One expects no losses at the given maximum working temperature. For example, for Chinese magnet grade M, with a minimum coercivity of about 1200 kA/m, the maximum working

temperature is defined as 100°C. However, Fig. 1 shows that already at 80°C there occur severe losses in such a material if the Pc is small. For the SH grade, with a minimum room temperature coercivity of about 1600 kA/m, the maximum working temperature is defined as 150°C. However, Fig. 2 shows that at 150°C, severe losses occur in this kind of material in magnetic circuits with a Pc = 1.1 or less.

However, the room temperature coercivity value is not enough to specify the behavior of a permanent magnet material at elevated temperatures. The coercivity also needs to be defined at the application temperature. The temperature dependence of the coercivity of a permanent magnet material varies for example with grain size [17]. The shape of the BH curve also affects the loss behavior.

Losses over time seem to be reduced with the stabilization heat treatment. The magnetization of the stabilized samples in Fig. 4 can be considered as stable within the first 5000 hours. How is the trend curve going to continue after that, is not clear. Fig. 4 also leaves the question of how to define a sufficient stabilization temperature. It is reasonable to expect a stable behavior for the stabilized magnets at shorter exposures than the time at the intersection point of the two trend curves. Thus, the intersection point of these curves should be shifted more to the right to ensure the stability of the magnets for the whole lifetime of the application. This means a higher stabilization temperature and greater initial loss.

V. Conclusion

Temperature stability of a magnet is demonstrated to be strongly dependent on the coercivity of the permanent magnet material but also on the permeance coefficient of the magnetic circuit.

Flux losses are negligible at low temperatures, where there is no knee in the BH curve or when the operating point is clearly above such knee. When the Pc approaches the knee, time-dependent losses start to occur. Below the knee, the total flux loss increases with a decreasing Pc. However, the proportion of time-dependent losses in the total loss decreases.

According to this study the maximum amount of time-dependent losses expected to occur in commercial sintered Nd-Fe-B magnets in a 30-year period is about 10 %. This requires temperatures above the critical temperature and initial losses greater than 10 %. However, without exceeding the critical temperature the losses over time can still in some cases be about 6 %.

Losses over time during the application could be avoided with proper stabilization heat treatment. The temperature of the heat treatment has to be high enough to ensure the stability of the magnet for the whole life time of the application.

With appropriate design of the circuit and proper selection of the magnet material, the irreversible flux losses in Nd-Fe-B magnets can be minimized down almost to zero. Careful engineering can guarantee the required lifetime for industrial applications in most cases.

Acknowledgment

This work was supported by the European Regional Development Fund. Samples were provided by Neorem Magnets Ltd.

References

[1] T. Haring, K. Forsman, T. Huhtanen and M. Zawadzki, “Direct drive-opening a new era in many applications,” *IEEE Pulp and Paper Industry Technical Conference,* 16- 20, pp. 171 –179, June 2003..

[2] k. Yamazaki, M. Shina, M. Miwa and J. Hagiwara, “Investigation of Eddy Current Loss in Divided Nd-Fe-B Sintered Magnets for Synchronous Motors Due to Insulation Resistance and Frequency,” *IEEE Trans. Magn.*, vol. 44, no. 11, p. 4269-4272, Nov. 2008.

[3] M. Markovic and Y. Perriard, “An Analytical Determination of Eddy-Current Losses in a Configuration With a Rotating Permanent Magnet,” *IEEE Trans. Magn.*, vol. 43, no. 8, pp. 3380-3386, Aug. 2007.

[4] S. Ruoho, E. Dlala, and A. Arkkio, “Comparison of Demagnetization Models for Finite-Element Analysis of Permanent-Magnet Synchronous Machines,” *IEEE Trans. Magn.*, vol. 43, no. 11, pp. 3964-3968, Nov. 2007.

[5] D. Li, H.F. Mildrum and K.J. Strnat, “Permanent magnet properties of sintered Nd-Fe-B between -40 and +200°C” *J. Appl. Phys.*, vol. 57, no. 8, pp. 4140-4142, 1985.

[6] Y. Kato, “Thermal stability of sintered and bonded rare-earth magnets,” *J. Appl. Phys.*, vol. 85, no. 8, pp. 4868-4870, 1999.

[7] P. Tenaud, F. Vial, and M. Sagawa, “Improved corrosion and temperature behaviour of modified Nd-Fe-B magnets,” *IEEE Trans. Magn.*, vol. 26, no. 5, p. 1930-1932, Sept. 1990.

[8] P. Campbell, *Permanent Magnet Materials and Their Applications*, Cambridge University Press, 1994.

[9] Y. Yang, X. Wang, W. Song and R. Tang, ”Study on the performance sensitivity to ambient temperature for permanent magnet synchronous motor used in pump jack,” *Sixth International Conference on Electrical Machines and Systems, 2003.*

[10] M. Negrea and M. Rosu, ”Thermal analysis of a large permanent magnet synchronous motor for different permanent magnet rotor configurations,” *IEEE International Electric Machines and Drives Conference, 2001.*

[11] C.C. Hwang, S.B. John and S.S. Bor ”The analysis and design of a NdFeB permanent-magnet spindle motor for CD-ROM drive,” *IEEE Trans. Energy Conv*., vol. 14, no. 4, pp. 1259-1264, 1999.

[12] A.G. Clegg, I.M. Coulson, G. Hilton and H.Y. Wong, “The temperature stability of NdFeB and NdFeBCo magnets,” *IEEE Trans. Magn.*, vol. 26, no. 5, pp. 1942-1944, Sept. 1990.

[13] H.F. Mildrum, and G.M. Umana, “Elevated temperature behavior of sintered Nd-Fe-B type magnets,” *IEEE Trans. Magn.*, vol. 24, no. 2, pp. 1623-1625, March 1988.

[14] R. Skomski, and J.M.D. Coey, *Permanent Magnetism. Studies in Condensed Matter Physics,* J.M.D. Coey and D.R. Tilley eds., London: Institute of Physics Publishing 1999, pp. 191-204.

[15] E.P. Wohlfarth,, “The coefficient of magnetic viscosity,” *J. Phys. F: Metal Physics*, 1984. 14: p. L155.

[16] S.R. Trout, “Material selection of permanent magnets, considering thermal properties correctly,” *Electrical Insulation Conference and Electrical Manufacturing & Coil Winding Conference.* 2001. Cincinnati, USA.

[17] K. Uestuener, M. Katter and W. Rodewald, “Dependence of the mean grain size and coercivity of sintered Nd-Fe-B magnets on the initial powder particle size,” *IEEE Trans. Magn.*, vol. 42, no. 10, pp. 2897-2899, Oct. 2006.

Publication II

Haavisto, M., Tuominen, S., Kankaanpää H. and Paju, M.

Time Dependence of Demagnetization and Flux Losses Occurring in Sintered Nd-Fe-B Permanent Magnets

IEEE Transactions on Magnetics, **46** (2010) pp. 3582 – 3584

Time Dependence of Demagnetization and Flux Losses Occurring in Sintered Nd-Fe-B Permanent Magnets

Minna Haavisto[1], Sampo Tuominen[1], Harri Kankaanpää[2], Martti Paju[1], *Member, IEEE*

[1]Magnet Technology Centre, Prizztech Ltd., Pori, Finland
[2]Neorem Magnets Oy, Ulvila, Finland

It is a common impression that the measured B(H) curves of permanent magnet materials indicate the temperature and the operating point at which flux losses start to occur. As long as the operating point stays above the knee of the B(H) curve, no losses will be expected. The demagnetization process is, however, a time dependent process and losses occurring immediately are followed by a thermal aftereffect. In this work, the time dependence of flux losses in commercial permanent Nd-Fe-B magnets was studied. Flux losses are presented as a function of temperature for different exposure times. The measured B(H) curves of the Nd-Fe-B material studied were then compared to the results of loss measurements. It was found that B(H) curves will not always indicate the overall losses well. The measured B(H) curve was found to represent the demagnetization state of the tested magnet more or less after only ten milliseconds of exposure to the elevated temperature. When the operating point of the magnet is approaching the B(H) curve knee, the time dependent losses will become significant. To control the time dependent losses in sintered Nd-Fe-B magnets the operating point needs to be sufficiently far away from the knee of the B(H) curve.

***Index Terms*— Permanent magnets, Losses, Neodymium compounds, Stability**

I. Introduction

THE magnetization and demagnetization of permanent magnets are always time dependent processes [1]. Magnetic viscosity will delay the process in the material. The magnetization of a permanent magnet as a function of time can be expressed as:

$$M(t,H) = M(t_0,H) - S(H)\ln\frac{t}{t_0}\ , \qquad (1)$$

where the first term on the right hand side represents the change occurring initially and the second term the time dependent after-effect also known as a thermal after-effect, since it is a thermally activated process. *S(H)* is the viscosity coefficient of the magnet, which is not only a characteristic of a material but also dependent on the geometry of the magnetic circuit and the temperature [2]. The reference time t_0 can be considered as a starting time in which the initial change has already occurred.

Eq. (1) is determined experimentally and it is necessarily an approximation. It fails when $t \rightarrow 0$ or $t \rightarrow \infty$ and thus it is applicable only to a limited time interval. Applicable time range is not clear and it is difficult to study very short or very long time scales experimentally. Our earlier studies [3] have shown that (1) describes well the demagnetization behavior of sintered NdFeB magnets at least within the time range from 1 hour to 10 000 hours.

The utilization of permanent magnets in high technology applications, like motors and generators, requires strict control of the demagnetization process. A method for considering the demagnetization behavior of Nd-Fe-B magnets in the application design has been studied recently [4,5]. This demagnetization model considers only the initial demagnetization of a magnet, the first term in (1). This initial loss can be determined by the B(H) curves of the material.

Measured B(H) curves are broadly used when estimating the behavior of a magnet in different temperatures. The demagnetizing field caused to the magnet by the magnetic circuit is illustrated by a load line $-B/\mu_0 H$ [6]. The slope of the load line is also called the permeance coefficient (P_c) of the magnet. The intersection point of the load line with the B(H) curve is called the operating point. It is generally assumed that when the operating point of a Nd-Fe-B magnet falls on the linear region of its B(H) curve, no losses will occur. However, B(H) curves are measured very quickly, in just a few seconds and so they represent the state of the magnetization at t_0, which is a very short time. The following time dependent after-effect is typically not taken into account, since it is assumed to be negligible.

This work studies this thermal aftereffect of a sintered Nd-Fe-B magnet.

II. Method

Rectangular shaped, fully magnetized, sintered NdFeB samples were kept in different temperatures for at least 2 000 hours and their residual inductions were measured at logarithmic time intervals. The method is described in more detail in [3]. Corrosion protection of the samples was provided by wrapping them in aluminum foil.

The material chosen for this study has a room temperature coercivity of 1240 kA/m and a remanent induction of 1.26 T. Magnetic properties of the studied material were determined by B(H) curve measurements in three different temperatures: at 22°C, 80°C and 100°C. Magnet Physik Permagraph C-300 was used in these measurements.

Tests were carried out in open circuit conditions. The sample size used in this study was 10 x 10 x 4.6 mm leading to P_c (or $-B/\mu_0 H$) value of 1.1. This is, however, some kind of average value for the sample Pc. In reality, the Pc varies inside the

Digital Object Identifier inserted by IEEE

magnet and there will be areas with lower and higher Pcs as well.

III. Results and Discussion

A. BH curves

The measured B(H) curves of the material are presented in Fig.1. The load line representing the P_c value 1.1 is also plotted. At room temperature, the B(H) curve in the second quadrant is linear, but even at 80°C a knee occurs. The load line of the samples, however, stays above the knee at least at a temperature of 100°C and below.

B. Viscosity coefficient S

The results of the residual induction measurements can be plotted as a function of time and according to these measurement points, trend curves in the form of (1) can be drawn. Measured flux losses at different temperatures with corresponding trend curves are shown in Fig.2. At 80°C the losses are very small and the corresponding trend curve is horizontal, but at 90°C the angular coefficient of the trend curve becomes negative. At 100°C there is already a loss of almost 5 % after one hour and the angular coefficient of the trend curve have decreased.

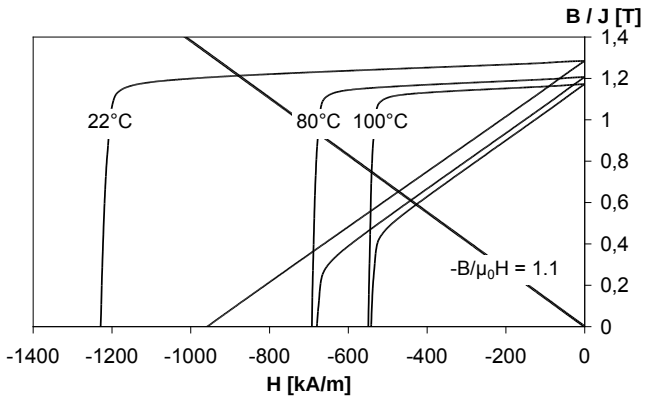

Fig. 1. Measured B(H) curves of the studied material at 22°C, 80°C and 100°C with a load line $B/\mu_0 H = 1.1$.

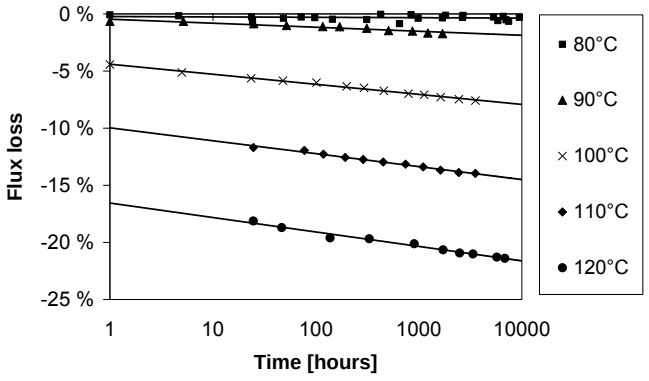

Fig. 2. Flux losses as a function of time at different temperatures. Room temperature coercivity of the material is 1240 kA/m and the Pc of the samples is 1.1.

From these curves the initial loss, in this case a loss after one hour, *M (1h)*, and the viscosity constant *S* can be determined for each temperature. In Fig.3 these are plotted as a function of temperature. After the immediate loss starts to occur it grows in a linear fashion with temperature, but the growth of the viscosity coefficient *S* more or less follows an s-type curve. The growth of the viscosity coefficient starts at a lower temperature than the growth of the initial loss. Below a certain temperature both of them are very close to zero. According to Trout [7], a suitable determination for the expression "maximum operating temperature" would be the maximum temperature where both of these terms could be considered as zero. According to this suggestion, the maximum operating temperature of the test material would be 80°C when Pc of the circuit ≥ 1.1.

Magnetic viscosity as a phenomenon has been studied in many papers [8-10]. Analysis of the phenomenon allows a better understanding of the coercivity mechanisms in magnetic materials. The viscosity coefficient *S(H)* is found to be proportional to the irreversible susceptibility χ^{irr} [10], which means that when the change of magnetization is the greatest, the viscosity coefficient will also reach its maximum. This will occur at the coercive field.

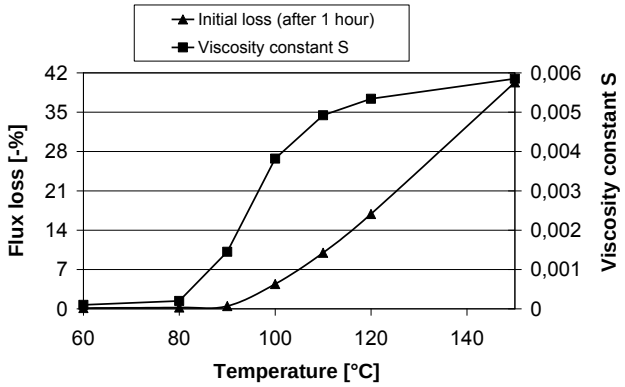

Fig. 3. Comparison of the changes in the immediate loss and the viscosity coefficient S as a function of temperature.

The demagnetizing field in this study is caused only by the self-field of the magnet. It means that the demagnetizing field (H) and thus also the Pc ($=-B/\mu_0 H$) is not uniform across the volume of the magnet. The field will be the strongest (meaning the lowest Pc) at the middle of the top and bottom surfaces of the magnet. In these regions the working point will drop below the knee even though the average Pc stays above it as the temperature is raised. Those areas will be demagnetized first.

The partial demagnetization of the magnets will naturally change the self-field and also the operating point. The decrease in self-field also affects the viscosity coefficient S, which will also decrease. This means that trend curves assumed as straight lines in Fig.2 will actually curve slightly towards a horizontal equilibrium. So the logarithmic trend curves shown can be considered to describe the worst scenario type of loss behavior of a single magnet, with an original average P_c of 1.1.

C. Flux losses as a function of temperature

The comparison of the B(H) curves in Fig.1 and the measured loss behavior of the same material (Fig. 3) reveal that, although the load line is above the knee at 100°C, both initial losses and the subsequent time-dependent losses occur. In Figs.2 and 3 the initial loss is considered as a flux loss after 1 hour. One hour was chosen as t_0, since the time measurement accuracy would not support shorter measurement periods.

However, using resulting loss curve equations, shorter time scales can be generated by expecting that the losses will follow the same logarithmic law of (1) also in the time range of seconds. The initial loss after one second can be approximated by changing the time scale of Fig. 2 to seconds. The losses after a lifetime of 30 years can be approximated as well based on the trend curve equations. These approximations are presented in Fig. 4 as a function of temperature. It can be seen that after one second at 100°C the loss is calculated to be less than 2 %, while after 30 years it would be over 9 %.

During the B(H) curve measurement, the field changes, dynamically sweeping the whole second quadrant of the demagnetization curve in just a few seconds. By also approximating losses after 10 ms (Fig. 4), a loss curve with almost zero losses at 100°C can be generated. This curve matches the measured B(H) curve better (Fig.1) and this loss curve could be considered to represent the demagnetization state during the B(H) curve measurement. However, the actual loss after 10 ms is not known, since the validity of (1) is uncertain in this time range. The presented value is only a calculated fictitious value to propose a way to connect the time scales of the B(H) curves and the conditions in the application. The real loss behavior in the ms time range is almost impossible to measure and for the machine application point of view it is also irrelevant. The loss after 1 hour and the loss after 30 years are the most important.

If one compares the calculated flux loss values after 10 ms and that after 30 years, a difference of 13 percentage units at 110°C and above can be seen. The difference between the curves "after 10 ms" and "after 1 hour," is almost the same as the difference between the curves "after 1 hour" and "after 30 years." Thus, almost half of the expected time-dependent losses due to the thermal aftereffect will occur within the first hour.

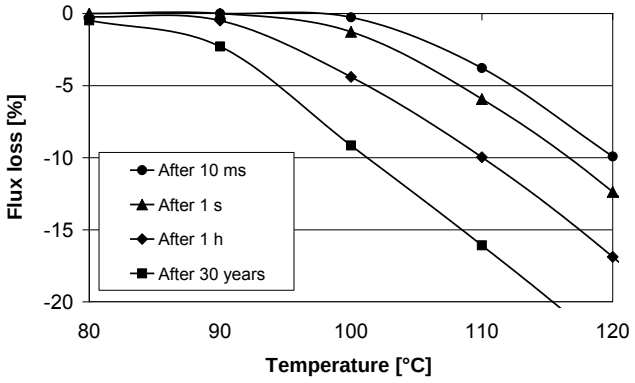

Fig. 4. Flux losses as a function of temperature in magnets with room temperature coercivity of 1240 kA/m and permeance coefficient of 1.1.

Flux losses as a function of temperature (like in Fig. 4) are in many cases presented with only one curve. An example of this is found in [11]. According to this study, it seems to be relevant to mention the measurement method and especially the time the samples have been exposed to the temperature before measuring the loss. If the losses are only calculated utilizing the measured B(H) curves, the curves will represent only the loss after a very short time.

A sudden uncontrolled temperature rise in an application is mostly due to some kind of fault condition. In application design it is important to take into consideration all possible conditions and make sure that even the fault condition will not destroy the magnets. Even though the fault condition of the device with a temporary temperature rise will not last for years, the error could in some cases be significant if only the losses "after 10 ms" are considered. After one hour, the losses might be 6 % units bigger than the losses after 10 ms. In any event, the temperature in the application will not cool down within milliseconds.

IV. Conclusion

In sintered Nd-Fe-B magnets applied in an open circuit, flux losses start to occur at a lower temperature than the B(H) curves of the material might indicate. The time-dependent thermal aftereffect will dominate when the operating point of the magnet is close to the knee of the B(H) curve. In the commercial sintered Nd-Fe-B magnets studied, the total flux loss was approximately 4.5 % after one hour and was estimated to be 9 % after 30 years at 100°C. However, the operating point of the magnets at 100°C is clearly above the knee of the B(H) curve and the loss after 10 ms is approximated to be zero.

When the operating point of the sintered Nd-Fe-B magnet is far from the knee, the time-dependent losses will also be zero. In the case of the magnets tested here, this temperature was 80°C. It is ca. 20°C lower than the maximum operating temperature determined according to the B(H) curves.

Acknowledgment

This work was supported by the Finnish Cultural Fund, Emil Aaltonen Foundation, and Ulla Tuominen Foundation.

References

[1] R. Skomski, and J.M.D. Coey, *Permanent Magnetism. Studies in Condensed Matter Physics*, J.M.D. Coey and D.R. Tilley eds., London: Institute of Physics Publishing 1999, pp. 191-204.

[2] E.P. Wohlfarth,, "The coefficient of magnetic viscosity," *J. Phys. F: Metal Physics*, 1984. 14: p. L155.

[3] M. Haavisto and M. Paju, " Temperature Stability and Flux Losses Over Time in Sintered Nd-Fe-B Permanent Magnet," *IEEE Trans. Magn.*, vol. 45, no. 12, pp. 5277-5280, Dec. 2009.

[4] S. Ruoho, E. Dlala, and A. Arkkio, "Comparison of Demagnetization Models for Finite-Element Analysis of Permanent-Magnet Synchronous Machines," *IEEE Trans. Magn.*, vol. 43, no. 11, pp. 3964-3968, Nov. 2007.

[5] S. Ruoho and A. Arkkio, "Partial Demagnetization of Permanent Magnets in Electrical Machines by an Inclined Field," *IEEE Trans. Magn.*, vol. 44, no. 7, pp. 1773-1778, July 2008.

[6] P. Campbell, *Permanent Magnet Materials and Their Applications*, Cambridge University Press, 1994.
[7] S.R. Trout, "Material selection of permanent magnets, considering thermal properties correctly," *Electrical Insulation Conference and Electrical Manufacturing & Coil Winding Conference.* 2001. Cincinnati, USA.
[8] R. Street and J. C. Woolley, "A study of Magnetic Viscosity," *Proc.Phys.Soc.*, vol. 62A, pp. 562-572, 1949.
[9] P. Gaunt, "Magnetic viscosity and thermal activation energy," *J. Appl. Phys.*, vol.59, no. 12, pp. 4128-4132, June 1986.
[10] D. Givord, A. Lienard, P. Tenaud and T. Viadieu, "Magnetic viscosity in Nd-Fe-B sintered magnets," *J. Magn. Magn. Mat..*, vol. 67, no. 3, pp. L281-L285, 1987.
[11] S. Ruoho, J. Kolehmainen, J. Ikäheimo and A. Arkkio, "Demagnetization Testing for a Mixed-Grade Dovetail Permanent-Magnet Machine," *IEEE Trans. Magn.*, vol. 45, no. 9, pp. 3284-3289, Sept. 2009.

Publication III

Haavisto, M. and Paju, M.,

Time-dependent demagnetization in sintered NdFeB magnets

Proceedings of 20th International Workshop on Rare Earth Permanent Magnets and Their Applications, Bled (2010) pp. 224-226

Time-Dependent Demagnetization in Sintered NdFeB Magnets

MINNA HAAVISTO, MARTTI PAJU
Magnet Technology Centre, Prizztech Ltd., Tiedepuisto 4, 28600 Pori, Finland

Abstract: *In the design of permanent magnet devices it is important to ensure that no demagnetization will occur under operating conditions. BH curves, measured or calculated, are typically used in the selection of a suitable magnet material. The measured BH curves of the selected magnet material are expected to reveal the conditions, i.e. temperature and working point, at which demagnetization starts to occur. However, demagnetization is a time-dependent process and the measured BH curve shows only an image of the magnetization state of the material after a fairly short exposure time. Long-term irreversible flux losses detected in sintered NdFeB magnets cannot be deduced from the BH curves of the material. Loss measurements for at least 1000 hours are needed to give a reliable picture of the long-term loss behaviour of the magnet. For an industrial NdFeB magnet of 38SH grade with a permeance coefficient of 0.5, the maximum working temperature was found to be 110 °C.*

Key words: *demagnetization, flux loss, NdFeB, stability*

Address: Minna Haavisto, Martti Paju, Tel: +358447105339, Fax +3582605399

1. Introduction

Permanent magnet technology has great potential in the modern motor and generator industry. There are, however, some doubts about the stability of the magnetic properties in the long term. The time dependence of magnetization and demagnetization has been studied extensively, but mostly on the time-scale of seconds [1-4]. The information obtained may be useful in the design of magnetic data storage devices, but is not relevant for motor designers, who need stability information on the scale of years. There is no evidence that results obtained in measurements within a few seconds or minutes would be applicable on a wider timescale.

The long-term stability of rare earth permanent magnets is discussed in one technical report by IEC [5]. The report presents measured irreversible losses as a function of time between 1 and 1 000 hours. However, the corrosion protection of the samples was not mentioned. In the long term, corrosion would cause permanent losses in addition to demagnetization. Corrosion can be considered as the main reason for long-term instabilities after the plateau of constant flux loss per logarithmic time cycle, as described in {IEC/TR62518, 2009 #1305}. Our previous studies have demonstrated that irreversible flux losses in sintered NdFeB magnets kept at a stable elevated temperature obey the logarithmic time dependence at least in the timescale of 1 to 10 000 hours (over 1 year), if sufficient corrosion protection is applied [6]. In this work we compared the long-term flux loss behaviour of a sintered industrial NdFeB magnet with its measured BH curve data.

2. Method

Samples were prepared by water cutting from a larger block of industrial 38SH material. The sample size was 10x10 mm and the height varied between 2.3 and 5.2 mm, leading to permeance coefficients (load lines/ working points) ranging from 0.5 to 1.3. The BH curves of the material were measured with a HymPulse magnetic properties tester at Metis Instruments&Equipment Nv. The samples were fully magnetized in a 3.5 T pulsed field. The reference value of the flux of each sample was measured with a Helmholtz coil immediately after magnetization. The samples were then placed into ovens with stable elevated temperatures. Corrosion protection was performed by wrapping the samples in aluminium foil. The samples were taken out of the ovens at logarithmic time intervals. The samples were cooled down to room temperature and remeasured with a Helmholtz coil. A minimum of 10 measurements were performed within a time period of 1000 hours. Based on the measurements, logarithmic trend curves were determined to describe the loss behaviour of each magnet.

3. Results and Discussion

3.1. BH Curves

The BH curves of the studied material measured at 20 °C, 100 °C and 140 °C are presented in Fig.1. At room temperature the BH curve is linear, but at 100 °C a small knee occurs. At 140 °C the knee is even clearer. The load lines representing the permeance coefficients of 0.5, 0.8 and 1.3 are also shown. At 100 °C all the working points are far away from the knee. At 140 °C some of the working points have already fallen off the linear part, while some of them remain on the linear part of the curve.

3.2. Losses at 140°C

Based on the BH curves one would expect some losses in samples with Pc = 0.5 at 140 °C, but samples with Pc = 1.3 are expected to be stable. Figure 2, however, also shows

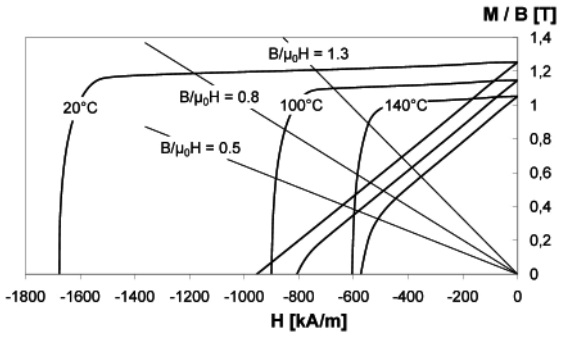

Fig. 1. Measured BH curves for the 38SH material studied. Sample sizes represent the load lines ($B/\mu_0 H = Pc$) between 0.5 and 1.3.

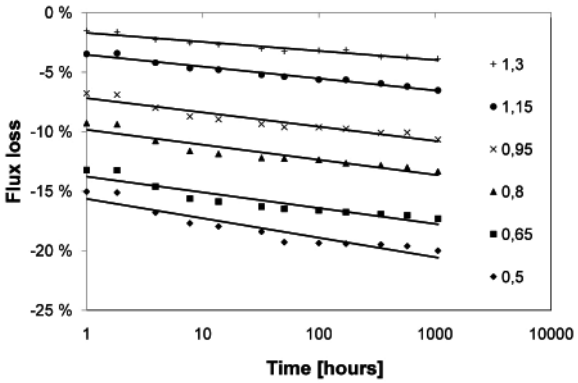

Fig. 2. Flux losses as a function of time in 38SH samples with different Pcs. Losses will occur even in samples with Pc = 1.3.

losses in those samples. The initial loss after one hour increases with a decreasing Pc, and for samples with Pc = 0.5 it is as much as 15 %. The slope of the trend line also increases with a decreasing Pc. As the Pc decreases the deviation of the measurement points from the trend line also increases. It can be seen that the measurement points take a more curve-like form, saturating towards a fixed loss level. The reason for this might be the changes in self-fields of the magnets as demagnetization proceeds.

The total loss expected after 30 years can be estimated from the trend lines in Fig. 2. Correspondingly, the loss after 1 second can be calculated, if the logarithmic trend is assumed to continue from the second scale onwards. Calculated losses after 1 second, after 1 hour, and after 30 years are plotted as a function of permeance coefficient in Figure 3. The flux losses decrease smoothly as the permeance coefficient increases. The curve for loss after 1 second, however, crosses the zero line at Pc = 1.15, and at Pc = 1.3 the calculated loss after 1 second is positive, which is physically impossible. This raises the question whether logarithmic loss behaviour is valid across the timescales of seconds and hours. Similar results were obtained with other materials as well and the effect was more pronounced in materials with higher H_{ci}. No clear explanation for this was found.

3.3. Maximum Working Temperature

The magnet producer reports the maximum working temperature for this type of magnet to be 150 °C. According to the measurement data presented in Fig. 2, even 140 °C would be too high a temperature at least for magnets with a Pc < 1.3. For the smallest sample (Pc = 0.5) at 140 °C, the initial loss after 1 second is estimated to be 8 % and the total loss after 30 years will increase to 26 %. These losses are far too high to be accepted in applications. To find a more suitable operating temperature, we repeated the test for the magnets with Pc = 0.5 at temperatures of 130 °C, 120 °C, 110 °C and 100 °C.

The detected flux losses are presented in Fig. 4 as a function of time. Trend curves are extended to reach 30 years time. The curves clearly show that below 110 °C the magnet is stable and that above 110 °C losses start to occur. So the maximum working temperature for this kind of magnet could be taken as 110 °C.

At 130 °C (also at 140 °C to some extent) the loss behaviour seems to be step-like rather than a continuous line. This is probably due to some instabilities of temperature. After the first loss measurement, the samples were exposed to a temperature a few degrees higher than the 130 °C that was set. This caused asubstantial flux loss,

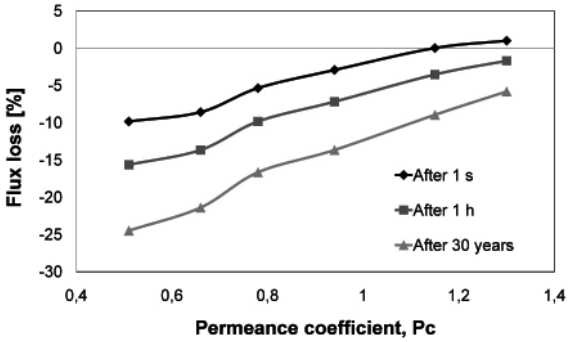

Fig. 3. Estimated flux loss as a function of the permeance coefficient of the magnet after 1 second, after 1 hour, and after 30 years exposure to the temperature of 140 °C. Flux loss values are calculated according to the trend lines presented in Fig. 2.

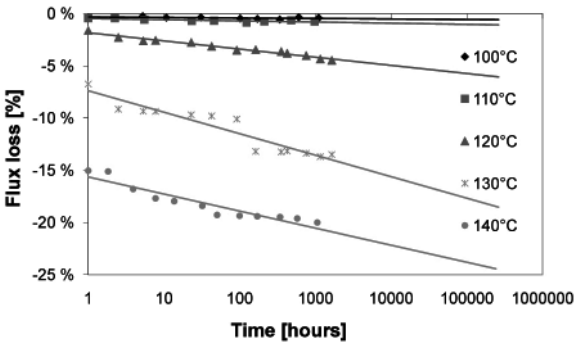

Fig. 4. Flux losses as a function of time for 38SH samples with Pc = 0.5 in different temperatures.

which gave rise to a stabilizing effect. Thus, further losses follow a more or less horizontal line until demagnetization starts again with a sudden drop in magnetization. In the long run, the effect of this event is of no significance, but it does affect the accuracy of the estimated losses after 30 years. In this case, measurement points up to 10 000 h would be preferred to achieve more accurate estimates.

Flux losses can also be presented as a function of temperature for different exposure times, as shown in Fig. 5. This figure indicates that after a very short period of time, such as 1 second, no losses are expected even at 130 °C, but time-dependent losses will be almost 20 % in 30 years. Rapid BH curve measurement cannot detect this time-dependent demagnetization. Again, the calculated losses after 1 second at 120 °C and 130 °C, are unrealistically slightly positive.

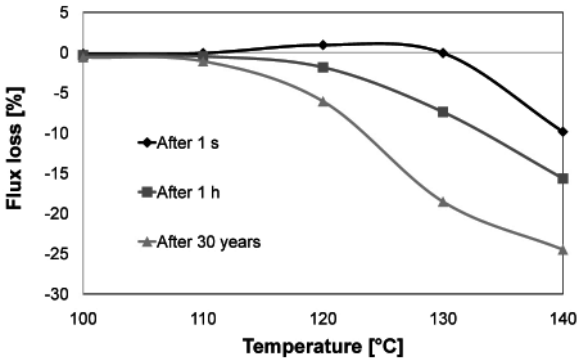

Fig. 5. Estimated flux losses as a function of temperature for a 38SH magnet with Pc = 0.5. Curves represent losses after 1 second, after 1 hour, and after 30 years exposure to the temperature. Flux loss values are calculated according to the trend lines presented in Fig. 4.

4. Conclusions

Long-term irreversible flux losses in sintered NdFeB magnets were the focus of study here. No simple connection between the measured BH curves and the detected open circuit flux losses were found. Time dependent demagnetization starts at a lower temperature and a higher Pc than the BH curves would indicate.

Based on long-term flux loss measurements, the maximum working temperature for a magnet with a certain Pc can be determined. The maximum working temperature determined by this method will assure that no demagnetization will occur even after many years, as long as the temperature is kept below the maximum and the opposite magnetic field is kept below the self-field of the tested magnet. Losses due to oxidation are not taken into consideration and sufficient corrosion protection is needed to avoid permanent losses.

The maximum working temperature for the NdFeB material of 38SH grade with Pc = 0.5 studied here was determined to be 110 °C.

Acknowledgments
This work was supported by the Finnish Cultural Fund, the Emil Aaltonen Foundation, the Ulla Tuominen Foundation and the High Technology Foundation of Satakunta.

References

[1] G. Bottoni, D. Candolfo, A. Cecchetti, J. Magn. Magn. Mater. 2004, 272-276(Part 3), 2271-2273.
[2] H. Sun, W. Pang, R. Street, IEEE Trans. Magn. 2000, 36, 3360-3362.
[3] A. Lyberatos, J. Magn. Magn. Mater. 1999, 202, 239-250.
[4] D. C. Crew, G. McCormick, R. Street, IEEE Trans. Magn. 1996, 32, 4356-4358.
[5] IEC/TR 62518, Technical report, 2009.
[6] M. Haavisto, M. Paju, IEEE Trans. Magn. 2009, 45, 5277-5280.

Publication IV

Haavisto, M., Tuominen, S., Kankaanpää, H. and Paju, M.,

Estimation of Time-Dependent Polarization Losses in Sintered Nd-Fe-B Permanent Magnets

IEEE Transactions on Magnetics, **47** (2011) pp. 170 – 174

Estimation of Time-Dependent Polarization Losses in Sintered Nd-Fe-B Permanent Magnets

Minna Haavisto[1], Harri Kankaanpää[2], Martti Paju[1], *Member, IEEE*

[1]Magnet Technology Centre, Prizztech Ltd., Pori, Finland
[2]Neorem Magnets Oy, Ulvila, Finland

The thermal stability of sintered NdFeB magnets can be described by the temperature coefficient of remanent flux density α only on condition that demagnetization due to rising temperature or field and oxidation of the magnets are totally avoided. This also requires the control of time-dependent demagnetization at elevated temperatures. We have studied the time dependent polarization losses in sintered NdFeB magnets with different coercivities by determining temperature T_0 for each magnet (Pc = 1.1). T_0 is the maximum temperature at which the total polarization loss even after 30 years of exposure is estimated to be less than 2 %. Temperature T_0 for four magnets produced from different materials are presented in this work. Flux losses at temperatures higher than T_0 after different exposure times are also described. The estimated flux loss after 30 years is found to be roughly twice the loss after 1 hour, except in the vicinity of T_0. At temperature T_0 + 10°C it could be as high as four times the loss after 1 hour.

***Index Terms*— Permanent magnets, Losses, Neodymium compounds, Stability**

I. Introduction

THERMAL stability is a very important characteristic for the usability of NdFeB magnets in motor and generator applications. It is crusial that the variation in remanent flux density is kept as low as possible.

From the application point of view, thermal stability can be understood as the changes in remanent polarization as the temperature changes. These changes, mainly polarization losses with increasing temperature, can be divided into reversible and irreversible changes according to whether the original polarization is recovered or not as the temperature is returned to the original state. A reversible decrease in polarization with increasing temperature is always present, and cannot be eliminated. However, it can be reduced by modifying the material composition. Irreversible polarization losses in sintered NdFeB magnets result from demagnetization or oxidation and can be avoided by means of proper design, material selection and corrosion protection.

There are various material characteristics as well as environmental factors that affect the thermal stability of sintered NdFeB magnets. Therefore a wide range of different kinds of thermal stability studies can be found in the literature. Some of the studies report material characteristics like intrinsic coercivity, H_{ci} [1-4] or temperature coefficients of remanence, α [1,2,5,6] or coercivity, β [1,2,7,8] as measures for thermal stability. There are also studies reporting detected irreversible flux losses [1,3-5,8-11] in magnets tested after a certain temperature exposure.

Fundamental material characteristics, like H_{ci}, α, and β, are quite easy to measure and are typically given by the magnet manufacturer. Temperature coefficients give a good picture of the materials temperature behavior, but are not sufficient when considering the thermal stability of a magnet in an application. One also needs data about the shape of the B(H) curves and magnetic circuit information [12]. With all this information, initially occurring polarization losses due to a sudden temperature rise, can be estimated. To be able to estimate long-term losses, more information would be needed about the long-term environmental conditions and long-term demagnetization characteristics of the material [13-14].

There is no consistent way to express or even measure the long-term behavior of magnetic materials. The irreversible flux losses measured after temperature exposure of one or two hours tells us something about the long-term effects. However, these represent only one condition with one exposure time. Therefore this information is difficult to utilize in machine design.

Long-term demagnetization in permanent magnets is due to so-called magnetic viscosity effect. Based on experimental data, the decay in polarization is found to obey a logarithmic law [15]:

$$M(t) = M(t_0) - S \ln \frac{t}{t_0} \quad (1)$$

Where M is the remanent magnetization, S is the magnetic viscosity coefficient and t_0 is the reference time. The viscosity coefficient S is constant only at a constant demagnetizing field and constant temperature. To get the material characteristic, independent of the field, this magnetic viscosity coefficient S is divided by the irreversible susceptibility χ_{irr} of the material [16]:

$$S_v = \frac{S}{\chi_{irr}} \quad (2)$$

S_v has been found to be constant at a constant temperature and values for NdFeB magnets have been measured by Givord et al. [16-17]. In these tests S and χ_{irr} are measured within a time scale of seconds. The measurement equipment does not allow accurate measurements over longer periods. However, on a time scale of hours or years, the time dependence of χ_{irr} [18] can no longer be neglected. S_v necessarily becomes time-

Digital Object Identifier inserted by IEEE

dependent.

It is very difficult to provide constant field conditions with a constant elevated temperature for a period of years. We have studied commercial NdFeB magnets in open circuit conditions, and followed the demagnetization process for more than 10 000 hours [14]. Unfortunately in this type of measurement the field condition is not constant across the sample and not even independent of time. As the demagnetization proceeds, the field condition will also change. However, the changes measured in magnetization were found to follow the logarithmic decay law (1) well, leading to the assumption that the field changes were negligible in size. This test method was considered to serve practical needs better than traditional viscosity measurements.

This work continues the previous studies [13-14] by comparing the time-dependent demagnetization behavior of commercial NdFeB magnets with different coercivities. The effect of the B(H) curve shape is also considered.

II. Method

The samples were commercial sintered NdFeB magnets produced by Neorem Magnets Oy. The materials contained varying amounts of Dy resulting in varying coercivities. Material properties of the samples are listed in Table I (intrinsic coercivities at room temperature are listed in Table II). The size of the rectangular-shaped samples was 10 x 10 mm with a height of 4.6 mm resulting in a permeance coefficient (P_c) value of 1.1.

The magnetic properties of the samples were determined using a Magnet Physik Permagraph C-300. The B(H) curves were measured only at room temperature (22°C), 80°C, 100°C, and 150°C. For material 3, a curve was also measured at 180°C, and for material 4, only curves at 100°C, 150°C and 180°C were measurable. Coercivities at other temperatures were calculated assuming a linear decrease between the measured temperatures.

The samples were kept at constant temperatures (80°C, 90°C, 100°C and so on) for at least 500 hours, and their residual inductions were measured at logarithmic time intervals: the first measurement was performed after 1 hour, the second after 2 hours, the third after 4 hours, the fourth after 8 hours, and so on. A minimum of 10 measurements within a 500-hour period were carried out. For each temperature, six identical samples were tested and the result is taken as an average loss of these six samples. The method is also described in [14]. Corrosion protection was provided by wrapping the samples in aluminum foil.

TABLE I
PROPERTIES OF THE MATERIALS STUDIED

Material	Dy content	Room temperature remanence B_r [T]	Temp. coeff. α of B_r (20-100°C) [%/°C]	Temp. coeff. β of H_{ci} (20-100°C) [%/°C]
1	1 %	1.28	0.11	0.71
2	4 %	1.23	0.10	0.59
3	7.5 %	1.15	0.09	0.54
4	11.5 %	1.02		

The measured flux loss values were converted into percentage values, since they equal with the percentage polarization and magnetization loss values. Furthermore, percentage losses enable a comparison of magnet materials with different remanent polarizations and are more useful for engineers than absolute loss values in Teslas.

According to the measured losses, the trend curves of the form of (1) were determined for each material at each temperature. The intersection of the trend curve with the vertical axis gives the estimated loss after 1 hour $M(t_0)$, when the unit of time is an hour. Additionally, the estimated losses after 30 years are calculated according to the trend curve equations.

To facilitate the comparison of the time-dependent demagnetization behavior of materials with different coercivities, the maximum temperature at which the losses in the magnets studied were estimated to remain below 2 % even after 30 years was termed T_0. Based on the estimation of the measurement accuracy, conditions where losses stay below 2 % can be considered stable. Note, that T_0 is not a material parameter, but depends also on the dimensions of the magnet. Thus, it will be also a function of P_c.

III. Results and Discussion

A. Polarization losses in magnets with different coercivities

Table II lists the temperatures T_0 determined for the samples with a P_c of 1.1. The intrinsic coercivities both at room temperature and at T_0 are also listed. As expected increase in room temperature coercivity leads to a clear increase in T_0. At the same time the intrinsic coercivity at T_0 seems to decrease. The coercivity of material 3 at T_0 deviates from the regularity, which suggests that the T_0 for that material has not been chosen correctly. The loss behavior curves in Fig.2 reveal that a more suitable T_0 for material 3 would have been somewhere between 160°C and 170°C, closer to 170°C, but unfortunately the temperatures were studied only at 10°C intervals.

TABLE II
COERCIVITIES OF THE SAMPLES

Material	Maximum temperature (T_0) at which total loss < 2% (P_c = 1.1)	Intrinsic coercivity [kA/m]	
		At room temperature	At T_0
1	80°C	1240	690
2	130°C	1540	620
3	160°C	2000	630
4	220°C	>2500	560

The polarization losses measured at temperatures T_0, T_0+10°C, T_0+20°C and T_0+30°C are presented in Fig. 1 for materials 2, 3 and 4 (only T_0, T_0+10°C and T_0+20°C). Measurement data for material 1 can be found in [13]. Trend lines are extended to reach an expected lifetime of 30 years.

The estimated polarization losses as a function of temperature for these magnets are presented in Fig. 2. For clarity, the curves in Fig. 2 are presented only starting from T_0.

Below T_0, no losses were detected. For low coercivity materials, losses start to occur at fairly low temperatures, but the progress of demagnetization with rising temperature is moderate. High coercive materials show a more intense loss behavior. In addition, the time dependence of the losses increases with increasing T_0.

The curves in Fig. 2 show clearly the temperature T_0 below which the losses are negligible for each magnet. Coercivities at T_0 (listed in Table II) could be considered as the minimum permissible coercivities for magnets with a permeance coefficient of 1.1. The required minimum coercivity for a low coercivity material seems to be higher.

Squareness factors (SF) for the measured B(H) curves of these materials are all above 0.9, mainly around 0.94. The squareness of the B(H) curve is typically considered to be one type of quality measure for magnet material. An example of the effect of a lower SF is presented in section B.

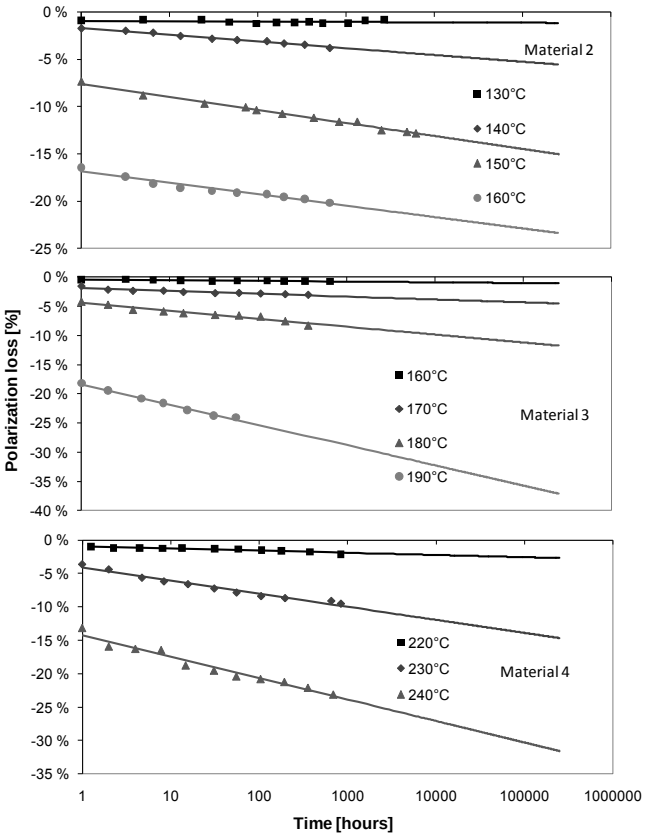

Fig. 1. Polarization losses measured as a function of time in magnets with a permeance coefficient of 1.1 produced from materials 2, 3, and 4.

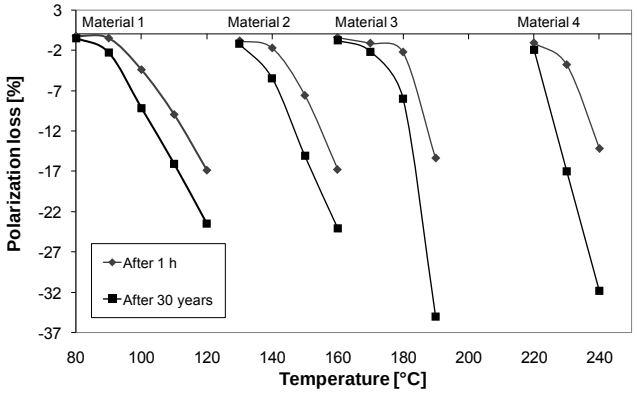

Fig. 2. Estimated polarization losses as a function of temperature in four different magnets with a permeance coefficient of 1.1. The material coercivities are listed in Table II.

Viscosity coefficients S, as defined in (1), for materials 1-4 are listed in Table III. At temperatures T_0 the viscosity coefficients are smaller than 10^{-3}. At temperatures above T_0, viscosity coefficients increase gradually as the temperature increases. At higher temperatures they could reach as high as $15x10^{-3}$. The regularity is again broken in the case of material 3 due to the inaccuracy of the determination of T_0.

Estimated loss values after 1 hour and after 30 years for the magnets are listed in Table IV. It can be seen that the losses after 30 years are mostly twice the losses after 1 hour except at the temperature T_0 + 10°C. For material 3, this is the temperature T_0 + 20°C due to the choice of T_0.

At the vicinity of T_0 the loss after 30 years can be as high as four times that after 1 hour. This has to be taken into account, when choosing a temperature test for magnets. Instead of measuring the irreversible polarization loss after 1 or 2 hours, it would be better to measure the loss both after 1 and after 2 hours, and perhaps also after 4 and 8 hours as well. It would give more realistic information about the time dependence of irreversible polarization losses.

Fig. 3 shows the estimated polarization losses after 30 years as a function of the number of measurement points for material 3. The estimate seems to reach fairly good accuracy after the first four measurement points. It is somewhat difficult to determine the time and temperature precisely, since the temperature inside the samples is not monitored and this causes inaccuracy especially in the first measurements. With a lengthening exposure time at a constant temperature, however, the accuracy of the results improves.

TABLE III
VISCOSITY COEFFICIENTS OF THE SAMPLES (P_C = 1.1) AT DIFFERENT TEMPERATURES

Material	T_0 [°C]	Viscosity coefficient S at temperature T [10^{-3}]				
		$T = T_0$	$T = T_0$ + 10°C	$T = T_0$ + 20°C	$T = T_0$ + 30°C	$T = T_0$ + 40°C
1	80	0.2	1.5	3.8	4.9	5.3
2	130	0.3	3.0	6.1	5.9	
3	160	0.3	0.8	4.6	15.8	
4	220	0.7	10.6	14.2		

TABLE IV
ESTIMATED LOSSES OF THE SAMPLES (P_c = 1.1) AT DIFFERENT TEMPERATURES

Material	T_0 [°C]	Estimated polarization loss after 1 h at temperature T [%]					Estimated polarization loss after 30 years at temperature T [%]				
		$T = T_0$	$T = T_0$ + 10°C	$T = T_0$ + 20°C	$T = T_0$ + 30°C	$T = T_0$ + 40°C	$T = T_0$	$T = T_0$ + 10°C	$T = T_0$ + 20°C	$T = T_0$ + 30°C	$T = T_0$ + 40°C
1	80	-0.2	-0.5	-4.4	-10	-17	-0.5	-2.3	-9.2	-16	-24
2	130	-0.8	-1.7	-7.6	-17		-1.2	-5.4	-15	-24	
3	160	-0.4	-1.1	-2.2	-15		-0.8	-2.2	-8.0	-35	
4	220	-1.1	-3.8	-14			-1.9	-17	-32		

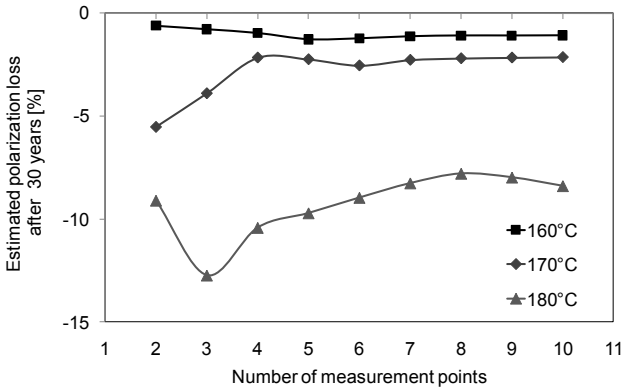

Fig. 3. Estimated polarization loss after 30 years as the number of measurement points increases. Magnets made of material 3.

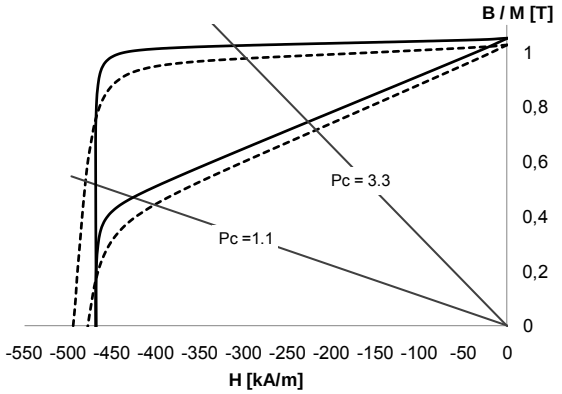

Fig. 4. B(H) curves for two different materials: A (solid line) and B (dashed line). The losses measured for magnets made of these materials are listed in Table IV. Also the corresponding load lines of the samples are shown.

B. Polarization losses in samples with different B(H) curve squareness factors

Two previously tested NdFeB materials, material 2 in this paper and material 2 in [14] were found to have similar coercivity at 150°C, but the shape of the B(H) curve differs. Fig. 4 shows the B(H) curves of these materials at 150°C. The working point corresponding to P_c = 1.1 is very close to the knee and therefore samples with P_c = 3.3 were also studied. Materials were labeled A and B. The squareness factors for the curves of materials A and B were 0.98 and 0.87, respectively.

The estimated polarization losses based on the measured loss trends are listed in Table IV. In samples with P_c = 3.3, the losses in material A are clearly smaller than in material B. In contrast, in samples with P_c = 1.1 material B shows smaller losses than material A. Again, the estimated loss after 30 years is approximately twice that of after 1 hour.

Based on the B(H) curves shown in Fig. 4, it is impossible to deduce the long-term loss behavior of these materials.

TABLE V
ESTIMATED LOSSES OF THE SAMPLES

Pc	Material	Irreversible polarization loss [%]	
		After 1 hour	After 30 years
1.1	A	7.6	15
	B	6.4	12
3.3	A	0.5	1
	B	1.9	2.7

IV. CONCLUSIONS

The time dependent polarization losses in sintered NdFeB magnets with different intrinsic coercivities were investigated. For magnets with P_c = 1.1 made of four different materials, a determination was made of the maximum temperature T_0 at which the total polarization loss even after 30 years is estimated to be less than 2%. Temperatures T_0 varied between 80°C and 220°C. The intrinsic coercivity at T_0 varied between 560 kA/m and 690 kA/m, and it was found to decrease with increasing T_0.

The estimated polarization loss after 30 years was found to be roughly twice the loss after 1 hour, except at temperature T_0 + 10°C. At that temperature the loss after 30 years can be as high as four times that after 1 hour. The time-dependent demagnetization was more pronounced in materials with higher room temperature coercivity as the temperature rose above T_0. In addition, the squareness of the B(H) curve was found to affect the long-term demagnetization behavior.

Time-dependent demagnetization should be taken into account when determining the thermal stability of magnets. Instead of measuring the irreversible polarization losses only after 1 hour, further measurements at least after 2, 4 and 8 hours exposure should be carried out. Based on the resulting logarithmic loss trends, the losses after longer and more useful exposure times could also be estimated.

ACKNOWLEDGMENT

This work was supported by the Finnish Cultural Fund, the Emil Aaltonen Foundation, the Ulla Tuominen Foundation,

and the High Technology Foundation of Satakunta.

REFERENCES

[1] B.M. Ma, W. L. Liu, Y. L. Liang, D. W. Scott and C. O. Bounds, "Comparison of the improvement of thermal stability of NdFeB sintered magnets: Intrinsic and/or microstructural," *J. Appl. Phys.*, vol. 75, no. 10, pp. 6628-6630, May 1994.

[2] Z. Chen, A. Yan and X. Wang, "Effects of intergranular additions of oxides on the coercivity, thermal stability and microstructure of Nd---Fe---B magnets," *J. Magn. Magn. Mater.*, vol. 162, no. 2-3, pp. 307-313, 1996.

[3] T. S. Chin, C. H. Lin, Y. H. Huang, J. M. Yau, S. J. Heh, and F. D. King, "Enhanced thermal stability of sintered (Nd,Dy)(Fe,Co)B magnets by the addition of Ta or Ti," *IEEE Trans. Magn.*, vol. 29, no. 6, pp. 2788-2790, Nov. 1993.

[4] Y. Kato, "Thermal stability of sintered and bonded rare-earth magnets," *J. Appl. Phys.*, vol. 85, no. 8, pp. 4868-4870, 1999.

[5] A. Yan, Z. Chen, X. Song and X. Wang, "Effect of MgO additive on coercivity, thermal stability and microstructure of Nd---Fe---B magnets," *J. Alloys Compd.*, vol. 239, no. 2, pp. 172-174, 1996.

[6] L.Q. Yu, J. Zhang, S.Q. Hu, Z.D. Han and M. Yan, "Production for high thermal stability NdFeB magnets," *J. Magn. Magn. Mater.*, vol. 320, no. 8, pp. 1427-1430, 2008.

[7] L. Li, J, Yi, Y. Peng and B. Huang, "The effect of compound addition Dy2O3 and Sn on the structure and properties of NdFeNbB magnets," *J. Magn. Magn. Mater.*, vol. 308, no. 1, pp. 80-84, 2007.

[8] A.S. Kim and F.E. Camp, "The role of oxygen for improving magnetic properties and thermal stability of sintered (Nd,Dy)(Fe,Co)B magnets," *IEEE Trans. Magn.*, vol. 31, no. 6, pp. 3656-3658, Nov. 1995.

[9] R. Zhang, Y. Liu, J. Ye, W. Yang, Y. Ma and S. Gao, "Effect of Nb substitution on the temperature characteristics and microstructures of rapid-quenched NdFeB alloy," *J. Alloys Compd.*, vol. 427, no. 1-2, pp. 78-81, 2007.

[10] R. Zhang, Y. Liu, J. Li, S. Gao and M. Tu, "Effect of Ti&C substitution on the magnetic properties and microstructures of rapidly-quenched NdFeB alloy," *Mater. Charact.*, vol. 59, no. 5, pp. 642-646, 2008.

[11] W-H. Cheng, W. Li, C-J. Li and S-Z. Dong, " The magnetic properties, thermal stability and microstructure of Nd-Fe-B/Ga sintered magnets prepared by blending method," *J. Magn. Magn. Mater.*, vol. 334, no. 2, pp. 274-278, 2001.

[12] M. T. Thompson, "Practical Issues in the Use of NdFeB Permanent Magnets in Maglev, Motors, Bearings, and Eddy Current Brakes," *Proceedings of the IEEE*, vol. 97, no. 11, pp. 1758-1767, Nov. 2009.

[13] M. Haavisto and M. Paju " Time Dependence of Demagnetization and Flux Losses Occurring in Sintered Nd-Fe-B Permanent Magnets," *IEEE Trans. Magn.*, to be published

[14] M. Haavisto and M. Paju " Temperature Stability and Flux Losses Over Time in Sintered Nd-Fe-B Permanent Magnets," *IEEE Trans. Magn.*, vol. 45, no. 12, p. 5277-5280, Dec. 2009.

[15] R. Skomski, and J.M.D. Coey, *Permanent Magnetism. Studies in Condensed Matter Physics*, J.M.D. Coey and D.R. Tilley eds., London: Institute of Physics Publishing 1999, pp. 191-204.

[16] D. Givord, A. Lienard, P. Tenaud and T. Viadieu, "Magnetic viscosity in Nd-Fe-B sintered magnets," *J. Magn. Magn. Mat..*, vol. 67, no. 3, pp. L281-L285, 1987.

[17] D. Givord, P. Tenaud, T. Viadieu and G. Hadjipanayis, "Magnetic viscosity in different Nd-Fe-B magnets *J. Appl. Phys.*, vol. 61, no. 8, pp. 3454-3456, April 1987.

[18] A. Lyberatos and R. W. Chantrell, " The fluctuation field of ferromagnetic materials," *J. Phys.: Condens. Matter.*, vol. 9, no. 12, pp. 2623–2643, 1997.

Publication V

Haavisto, M., Kankaanpää, H., Santa-Nokki, T., Tuominen, S. and Paju, M.

Effect of Stabilization Heat Treatment on Time-Dependent Polarization Losses in Sintered Nd-Fe-B Permanent Magnets

EPJ Web of Conferences, **40** (2013) article no. 06001

EPJ Web of Conferences **40**, 06001 (2013)
DOI: 10.1051/epjconf/20134006001

Effect of Stabilization Heat Treatment on Time-Dependent Polarization Losses in Sintered Nd-Fe-B Permanent Magnets

M. Haavisto[1], H. Kankaanpää[2], T. Santa-Nokki[1], S. Tuominen[1] and M. Paju[1]

[1]Magnet Technology Centre, Prizztech Ltd., Pori, Finland
[2]Neorem Magnets Oy, Ulvila, Finland

Abstract. Some companies in the motor and generator industry utilizing sintered NdFeB magnets have adopted pre-ageing heat treatment in order to improve the stability of the magnets. The parameters of this stabilization heat treatment are based mainly on assumptions rather than on any published research results. In this work, the effects of pre-ageing treatment on the time-dependent polarization losses of two different types of commercial sintered NdFeB magnets were studied. The material showing the squarer J(H) curve did not benefit from the pre-ageing treatment, since it seems to be stable under a certain critical temperature. In contrast, a stabilizing effect was observed in the material showing rounder J(H) curve. After the stabilization heat treatment, the polarization of the magnets was found to be at lower level, but unchanged over a certain period of time. The length of this period depends on the temperature and the duration of the pre-ageing treatment. In addition, our analysis reveals that the stabilization heat treatment performed in an open circuit condition does not stabilize the magnet uniformly.

1 Introduction

Stabilizing heat treatment also known as pre-aging heat treatment is a method used in order to improve the thermal stability of permanent magnets. This means that the magnets are exposed to a higher temperature than their maximum operating temperature before being installed to the application. However, there are not many published papers about the effects of such heat treatment on the subsequent loss behaviour of sintered NdFeB magnets. Radiation-induced demagnetization is claimed to decrease due to this kind of thermal stabilization [1]. The pre-ageing heat treatment that caused -0.69 % decrease to the polarization was found to be sufficient to decrease the subsequent demagnetization in the electron beam exposure close to zero.

The effects of stabilization heat treatment on SmCo based magnets have been studied previously [2-3]. As long as the stabilization treatment is performed at moderate temperatures, the effects are purely due to domain wall motion and a stabilizing effect is attained [2]. The remanence of the magnets was reduced proportionally during the stabilization treatment. In [3], the time-dependent demagnetization of SmCo magnets within a three-year measurement period was found to decrease to about 0.3 % due the two-hour pre-ageing treatment.

The principal idea of thermal stabilization is that the magnetization of the weakest domains in the magnet is flipped due to thermal activation. The domains that maintain their original magnetization state, despite thermal exposure, are assumed to be stable at temperatures below the stabilization temperature. Based on this assumption, stabilization heat treatment is introduced as a part of the production process in some companies utilizing sintered NdFeB magnets. The exposure temperature and the duration of the heat treatment are more or less chosen on the basis of rough estimates.

In this work we studied the effect of the pre-ageing heat treatment on the time-dependent polarization losses in sintered NdFeB permanent magnets. The effect of the J(H) curve squareness of the material on the thermal stabilization was also studied.

2 Method

Test materials were commercial sintered NdFeB magnets produced by Neorem Magnets Oy. Materials were specified according to their measured B(H) curves.

Two different materials were chosen from previously tested materials [4-6]. The criteria of the selection was that the coercivities of the materials were close to each other at a certain elevated temperature at which a small knee also appeared in the second quadrant of the B(H) curves. Additionally, the shape of the J(H) curves was expected to be different. Material 2 in [4] was

chosen as material A in this research and material 2 in [5] as material B. At 120°C the difference in the coercivities of these materials is less than 3 %.

The magnetic properties of the samples were determined by the B(H) curve measurements carried out with Magnet Physik Permagraph C-300. The properties of the studied materials at room temperature are presented in Table 1 and at 120°C in Table 2. The B(H) and J(H) curves measured at 120°C and 130°C are presented in figure 1.

The squareness factor (SF) is used as a measure for the squareness of the J(H) curve.

$$SF = \frac{H_k}{H_{Ci}} \quad (1)$$

where H_{ci} is the intrinsic coercivity of the material and H_k refers to the field at which 10 % of the remanence is lost (= field at 90 % of B_r) [6].

The rectangular-shaped samples were 10 x 10 mm in size, with varying heights (the direction of magnetization). The heights of material B samples were 4.1, 4.9 and 5.6 mm. These correspond to permeance coefficient (P_c) values of 1.0, 1.2 and 1.4 when determined from the dimensions of the samples [7]. The height of material A samples was 4.6 mm leading to a P_c of 1.1.

The testing method for studying the time-dependent demagnetization is described in detail in [4]. The ageing temperature in this study was 120°C. Polarization loss measurements were performed with a Helmholtz coil at room temperature. Losses are presented as a percentage of the original polarization values measured straight after magnetization. Each loss value is an average of the measured losses of five identical samples.

The stabilization heat treatment prior to ageing was performed at 130°C for a duration of one hour.

Table 1. Properties of studied materials.

Material	Room temp. coercivity H_{ci} [kA/m]	Room temp. remanence B_r [T]	Temp. coeff. α of B_r (20-100°C) [%/°C]	Temp. coeff. β of H_{ci} (20-100°C) [%/°C]
A	1540	1.24	-0.13	-0.59
B	1680	1.21	-0.09	-0.62

Table 2. Properties of the materials at 120°C.

Material	Coercivity H_{ci} [kA/m]	Remanence B_r [T]	H_k [kA/m]	Squareness factor SF
A	677	1.08	656	0.97
B	658	1.07	658	0.89

The demagnetizing field inside the samples was calculated using FEM. The software used was Opera by Vector Fields. One eighth of the samples were modelled with magnetic properties: B_r = 1.2134 T, H_{cb} = 924 kA/m and recoil permeability of 1.045. Values are determined from the B(H) curve of material B at room temperature. B(H) curve was assumed to be linear. The analysis with non-linear B(H) curve measured at 120°C failed.

In order to study the distribution of the demagnetization, the magnetic flux density near the sample surface was scanned along the center line of the sample before and after the stabilization heat treatment. The measurements were performed with a Lakeshore gaussmeter, model 450 and Lakeshore MNA-1904-VH hall probe fixed perpendicular to the sample surface. The magnetic flux density was scanned across the sample at a distance of 0.2 mm.

3 Results and discussion

3.1 Polarization losses in stabilized and non-stabilized samples

The polarization loss measurements were carried out for 10 000 hours to be able to predict the long-term behaviour of the stabilized magnets. Figure 2 shows the detected losses as a function of time for the samples with an average P_c = 1.1 and 1.2 for materials A and B respectively. The logarithmic trend lines [8] for losses are also plotted in figure 2. The trend lines are lengthened to reach 260 000 hours, which corresponds to an expected life-time of 30 years.

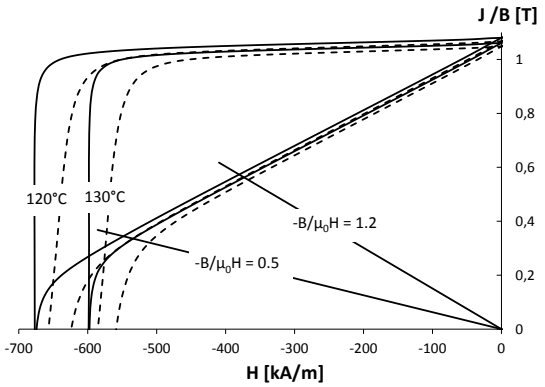

Fig. 1. B(H) and J(H) curves at 120°C and 130°C for materials A (solid line) and for material B (dashed line). Load lines 0.5 and 1.2 are also included.

The loss behaviour of material A magnets is similar in stabilized and non-stabilized samples. These two trend lines overlap and the estimate of the total loss after 30 years is less than 1 % in both cases. This indicates that this type of magnet does not benefit from stabilization treatment. The loss behaviour of material B magnets, however, differs clearly depending on whether the samples were stabilized or not. Non-stabilized samples exhibit a decreasing loss trend, starting from a 1.7 % loss after one hour's exposure and resulting in a loss estimate of 4.5 % in 30 years. In contrast, stabilization treatment at 130°C causes a loss of approx. 3 % and this state of magnetization remains until about 1 000 hours when the samples are kept at 120°C. At this point the decreasing loss trend of the non-stabilized samples is obtained and it

seems that the subsequent loss trends overlap. Further measurement points would ensure this behaviour, but it is inconvenient to implement the measurements, since it requires years of exposure.

The effect of sample height on the loss behaviour of stabilized and non-stabilized samples produced from material B is presented in figure 3. All the samples exhibit similar loss trends, only the magnitudes of the initial as well as the subsequent time-dependent losses are different. The slope of the trend line and the initial loss in non-stabilized samples increases as the thickness of the sample decreases (figure 3 a). The stabilization treatment also causes increasing losses with decreasing magnet thickness (figure 3 b). Subsequent exposure at a lower temperature does not cause any further loss until 1 000 hours of exposure is reached. As the exposure is extended from 1 000 to 10 000 hours the losses turn to follow the trends of the non-stabilized samples (figure 3c). This is logical, since the stabilization heat treatment only partly demagnetizes the samples and does not affect the microstructure of the magnets. The same partial demagnetization occurs in the non-stabilized samples due to thermal activation over time. As the same demagnetized state is achieved regardless of the thermal history, the subsequent demagnetization behaviour is expected to be identical.

This shows that insufficient stabilization heat treatment will make the magnets stable only for part of the lifetime of the application. The usage of magnets exhibiting squarer J(H) curves would be more practical. According to this study, a squareness factor of 0.97 is sufficient to ensure stability over time and thus, pre-ageing treatment is unnecessary. Our previous study [5] supports this conclusion.

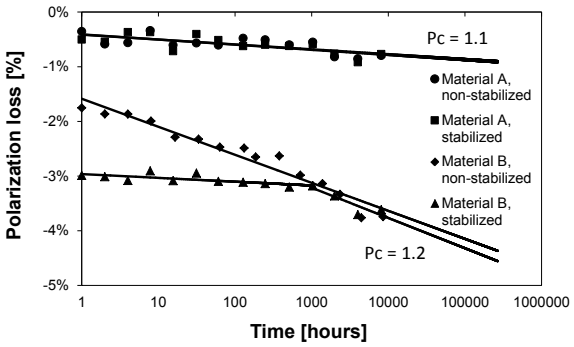

Fig. 2. Polarization losses as a function of time for stabilized and non-stabilized magnets produced from materials A and B. The dimensions of the samples were 10 x 10 x 4.6 mm in material A samples and 10 x 10 x 4.9 mm in material B samples.

3.2 Partial demagnetization of stabilized magnets

FEM models of the material B samples were generated in order to understand the partial demagnetization process occurring during the stabilization heat treatment. The variations of $-B_z/\mu_0 H_z$ (often considered to be the same as P_c) in the samples before treatment are presented in figure 4. This figure reveals that $-B_z/\mu_0 H_z$ or P_c in actual fact varies dramatically inside the sample. The P_c reaches its minimum at the centre of top and bottom surfaces of the samples and falls to as low as approx. 0.5 in our samples. Figure 1 b shows that the working point of 0.5 is already slightly below the B(H) curve knee at 130°C. Some initial loss in the samples from material B is thus expected.

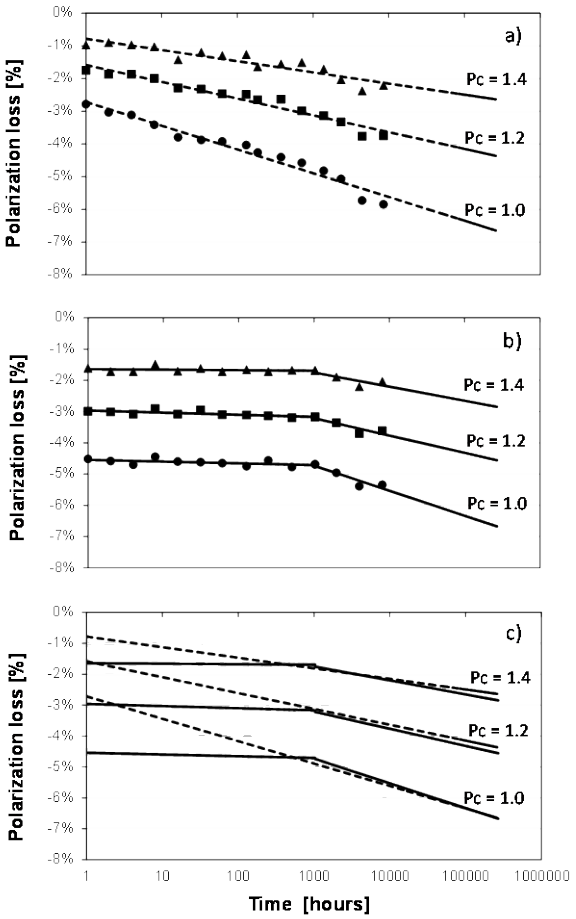

Fig. 3. Polarization losses in non-stabilized samples (a) and stabilized samples (b) (material B at 120°C) and the combined trends of the two (c).

The partial demagnetization is concentrated to the areas where $-B_z/\mu_0 H_z$ is below about 0.55 i.e. close to the centres of the surfaces that are perpendicular to the magnetization direction. Figure 5 shows the magnetic flux density profiles measured on the top of this surface (P_c of the sample = 1.0) before and after the stabilization treatment. The flux density is lower at the centre of the surface than at the edges.

The area falling below the knee point of B(H) curve is much larger in the case of the magnets of 4.1 mm in height (figure 4 a) than in the magnets of 5.6 mm in height (figure 4 c). Besides this, the difference in the minimum of $-B_z/\mu_0 H_z$ explains the difference in the demagnetization states of different sized magnets after pre-ageing at 130°C.

Correspondingly, the time-dependent demagnetization occurring in the non-stabilized samples is most likely to occur in the areas where P_c is close to the B(H) curve knee. This area is the largest in the lowest samples in height even after the initial demagnetization. This could also explain the greater demagnetization occurring over time.

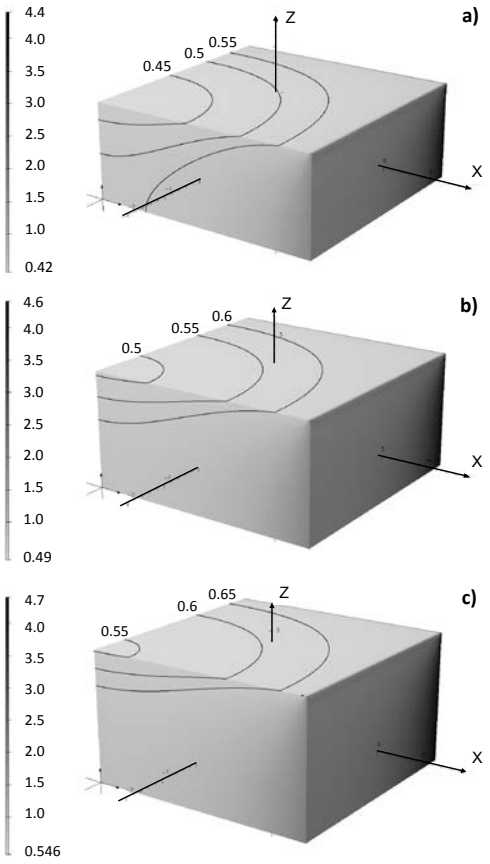

Fig. 4. Variations of $-B_z/\mu_0 H_z$ inside the studied samples at room temperature, before the exposure to elevated temperature. The heights of the modelled magnets are 4.1 mm (a), 4.9 mm (b) and 5.6 mm (c) corresponding to an average P_c of 1.0 (a), 1.2 (b) and 1.4 (c). Models include one eighth of the samples. The upper corners on the right-hand side are the actual corners of the magnet and the lower corners on the left-hand side are the centres of the magnets. The models describe the samples produced from material B.

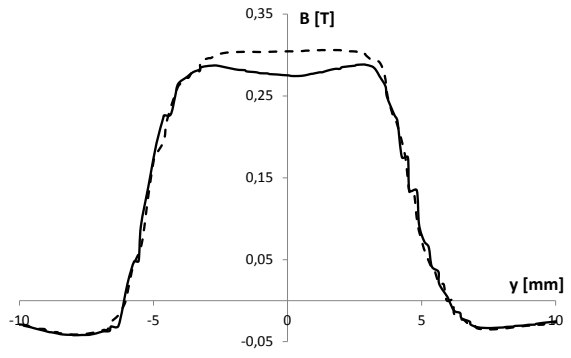

Fig. 5. Scanned magnetic flux density on the surface perpendicular to the magnetization direction (Z) of a sample from material B (P_c = 1.0): before the stabilization heat treatment (dashed line) and after the treatment (solid line). Scanning was performed about 0.2 mm from the magnet surface.

As the partial demagnetization of the permanent magnets thermally stabilized in open circuit condition occurs at a certain location of the magnet, the stabilization does not necessarily cover the whole magnet volume. This might cause problems if the magnetic circuit is different in the application.

4 Conclusions

The effects of stabilization heat treatment on the time-dependent demagnetization of sintered NdFeB magnets were studied. According to the results, the following five conclusions can be drawn:

1) Sintered NdFeB magnet materials showing a square J(H) curve (SF > 0.97) do not need any stabilization treatment.

2) NdFeB material following rounder J(H) curve shows a stabilization effect. The polarization is found to be at lower level, but stable in pre-aged magnets over a certain period of time. The principle is that the same partial demagnetization that occurs over time in non-stabilized magnets, is induced in the magnets by the pre-ageing treatment.

3) The temperature and duration of the pre-ageing treatment can be optimized so that the partial demagnetization is sufficient, ensuring stability over the required time, but not too heavy to cause any excess losses.

4) The pre-ageing treatment should be performed in similar magnetic conditions to those the magnets will face in the application. Stabilization treatment performed in open circuit condition does not stabilize magnets uniformly.

5) The P_c calculated from the dimensions of the magnet is only an average value for the sample. In fact, the P_c varies significantly inside the magnet.

Acknowledgements

This work was supported by the Finnish Cultural Fund, the Emil Aaltonen Foundation, the Ulla Tuominen Foundation, the High Technology Foundation of Satakunta, and the European Regional Development Fund.

References

1. T. Bizen, Y. Asano, T. Hara, X. Marechal, T. Seike, T. Tanaka, H. Lee, D. Kim, C. Chung, H. Kitamura, Nucl. Instr. and Meth. A **515**, 850–852 (2003)
2. H. Mildrum, M. Hartings, K. Wong, K. Strnat, IEEE Trans. Magn. **10**, 723-725 (1974)
3. J. Liu, M. Walmer, IEEE Trans. Electron Dev. **52**, 899-901 (2005)
4. M. Haavisto, H. Kankaanpää, M. Paju, IEEE Trans. Magn., **47**, 170-174 (2011)
5. M. Haavisto, H. Kankaanpää, T. Santa-Nokki, S. Tuominen, M. Paju, (to be published)
6. D. Branagan, M. Kramer, Y. Tang, R. McCallum, J. Appl. Phys. **85**, 5923-5925 (1995)
7. R.J. Parker, *Advances in Permanent Magnetism*, (John Wiley & Sons, 1990)
8. M. Haavisto, M. Paju, IEEE Trans. Magn. **45**, 5277-5280 (2009)

Tampereen teknillinen yliopisto
PL 527
33101 Tampere

Tampere University of Technology
P.O.B. 527
FI-33101 Tampere, Finland

ISBN 978-952-15-3191-0
ISSN 1459-2045